

TECHNISCHE UNIVERSITÄT MÜNCHEN

Lehrstuhl für Strahlenbiologie

Fakultät für Medizin

**The effect of low-dose ionising radiation on the proteome of
the murine hippocampus**

Daniela Hladik

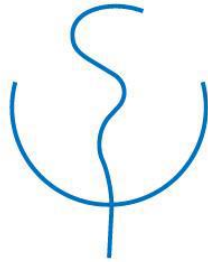
Vollständiger Abdruck der von der Fakultät für Medizin der Technischen Universität München zur Erlangung des akademischen Grades eines Doktors der Naturwissenschaften genehmigten Dissertation.

Vorsitzende: Prof. Dr. Stephanie E. Combs

Prüfende der Dissertation:

1. Prof. Dr. Michael J. Atkinson
2. Prof. Dr. Gabriele Multhoff

Die Dissertation wurde am 25.08.2020 bei der Technischen Universität München eingereicht und durch die Fakultät für Medizin am 29.12.2020 angenommen.



Doctoral thesis

TECHNISCHE UNIVERSITÄT MÜNCHEN

Chair of Radiation Biology

Faculty of Medicine

**The effect of low-dose ionising radiation on the proteome of
the murine hippocampus**

Daniela Hladik



Table of content

Table of content	3
Summary.....	5
Zusammenfassung.....	7
1 Introduction	9
1.1 Ionising radiation in modern society	9
1.2 The direct and indirect effects of IR.....	9
1.3 Vulnerability of the brain.....	10
1.4 The effects of IR on the brain	11
1.4.1 Evidence of health effects from epidemiology	11
1.4.2 Impairment of cognitive function in animal models	13
1.4.3 The effect of radiation on neurogenesis	13
1.4.4 Radiation effects on neuronal morphology	15
1.4.5 Inflammation, oxidative stress and activation of glia cells.....	16
1.5 Ketamine and the brain	17
1.6 Aim of the thesis.....	18
2 Methodology to analyse the effects of low-dose radiation on the hippocampus.....	20
2.1 Treatment of mice	20
2.2 Analysis of the proteome.....	21
2.2.1 Sample preparation	21
2.2.2 LC-MS/MS.....	22
2.2.3 Label-free peptide quantifications and identification	23
2.2.4 Pathway analysis.....	24
2.2.5 Validation of the LC-MS/MS	24
2.3 Measurement of free radicals.....	25
2.4 Structural analysis of CA1 neurons	26
3 Results and Discussion.....	28
3.1 CREB signaling mediates a dose-dependent radiation response in the murine hippocampus evident two years after total body exposure	28

3.1.1	Aim and summary of the study	28
3.1.2	Contribution	29
3.1.3	Publication	29
3.2	Combined treatment with low-dose ionizing radiation and ketamine induces adverse changes in CA1 neuronal structure in murine hippocampus	39
3.2.1	Aim and summary of the study	39
3.2.2	Contribution	40
3.2.3	Publication	40
3.3	DNA damage accumulation during fractionated low-dose radiation compromises hippocampal neurogenesis	56
3.3.1	Aim and summary of the study	56
3.3.2	Contribution	57
3.3.3	Publication	57
4	Conclusions	68
4.1	Effect of low-dose IR on the murine hippocampus	68
4.1.1	Low-dose exposure leads to a long-term increase in oxidative stress and inflammation.....	68
4.1.2	Effect on neuronal structures.....	70
4.1.3	Effect on the hippocampal cell composition.....	72
4.2	The effect of low-dose irradiation on the hippocampal proteome	73
4.2.1	The central role of the CREB pathway	74
4.3	Final Conclusion.....	76
	References.....	77
	List of figures and table	88
	Abbreviations	90
	Acknowledgement.....	92

Summary

Ionising radiation has a wide variety of applications in the clinic. Different types of ionising radiation, delivered as an external beam or as internally applied radioactive substances, are indispensable tools in the detection and treatment of malignant diseases and in diagnostic imaging procedures. The benefits of these practices for patients are indisputable, but nevertheless several deleterious side effects are incurred by the radiation exposures, although these are constantly being reduced as a result of new research knowledge and improved protective measures. However, there is still a lack of knowledge and awareness of possible long-term consequences in the area of low-dose radiation exposures, such as those used in computer tomography.

The aim of this doctoral thesis is to investigate the effects of low-dose radiation in clinically relevant situations on the brain, an organ that was long considered as relatively resistant to radiation. Today, radiation-induced neurocognitive dysfunction is known to be a side effect of repeated diagnostic procedures or radiation therapy. The underlying molecular mechanisms were studied in this thesis.

Experimental evidence shows that a single low-dose exposure induces changes in the cellular proteome indicating damage that increases in intensity over time, but with significant differences depending on the dose. A dose of 0.5 Gy led to enhanced expression of marker proteins of apoptosis, oxidative stress and inflammation, while a lower dose of 0.063 Gy led to activation of the neuroprotective CREB signalling pathway. In paediatric medicine sedatives are often given during computer tomography and X-ray imaging procedures to reduce motion and improve image quality. A recent behavioural study suggests that the deleterious effect of radiation on the brain may be increased by simultaneous administration of the commonly used sedative ketamine. Co-treatment of irradiation and ketamine resulted in the appearance of increasingly complex dendrite branching and a reduced synapse density. These structural changes could ultimately lead to a limitation of the neuronal signalling and thus to changes in behaviour observed.

In the third part of this thesis, the effects of repeated low-dose radiation treatment, corresponding to the exposure of the normal tissue during radiotherapy, were studied. An accumulation of persistent DNA double strand breaks was observed in line with a decline

in adult neurogenesis and reduced numbers of dividing precursor cells. Proteome alterations were specifically pronounced in the neurotrophic signalling, with a strong suppression directly after exposure and a compensatory upregulation after three months. In summary, the effects of low doses of ionising radiation showed a strong effect on the brain of mice, both in combination with ketamine and alone. It is therefore necessary to raise awareness of the effects of low doses in order to reconsider the current dose limits set in the radiation protection recommendations for brain exposure. New knowledge on radiation-related effects will not only help to improve radiation protection strategies but also to better assess the side effects versus benefits of clinical radiation, particularly in children.

In addition, the observed activation of neuroprotective mechanisms by very low doses indicates a possible therapeutic strategy to adapt cells and tissues prior to high-dose exposure.

Zusammenfassung

Ionisierende Strahlung findet aktuell vielseitig Anwendung im klinischen Alltag und ist ein unverzichtbares Hilfsmittel in der Diagnostik und der Therapie maligner Tumorerkrankungen. Obwohl der Nutzen von Strahlung für die Patienten hierbei unumstritten ist, zeigen sich eine Reihe von Nebenwirkungen, die es durch neue Schutzmaßnahmen zu reduzieren gilt. Um dies zu gewährleisten fehlt es derzeit jedoch an Wissen über und am Bewusstsein für mögliche Langzeitfolgen niedrig dosierter Strahlung, wie sie beispielsweise in der Computertomographie eingesetzt wird.

Das Ziel dieser Doktorarbeit ist es, die Auswirkungen von niedrigen Strahlendosen in klinisch relevanten Situationen auf das Gehirn, das lange Zeit als relativ strahlenresistent galt, zu untersuchen. Heutzutage sind strahleninduzierte neurokognitive Funktionsstörungen als eine Nebenwirkung von wiederholten diagnostischen Verfahren oder Strahlentherapie bekannt. Die Arbeit fokussiert sich auf die zugrunde liegenden molekularen Mechanismen im Hippocampus, ein Gehirnareal, das auf Grund adulter Neurogenese verhältnismäßig strahlen-sensitiv ist.

Die Ergebnisse dieser Arbeit zeigen, dass eine einmalige Bestrahlung zu einer Veränderung des Proteoms führt, die im Laufe der Zeit an Intensität zunimmt. 0.5 Gy haben eine erhöhte Expression von Markerproteinen für Apoptose, oxidativen Stress und Entzündung zur Folge, wohingegen eine sehr niedrige Dosis von 0.063 Gy zur Aktivierung des neuroprotektiven CREB-Signalwegs führte.

In der pädiatrischen Medizin werden bei bildgebenden Verfahren, wie zum Beispiel der Computertomographie, häufig Beruhigungsmittel verabreicht, um Bewegungen zu reduzieren und die Bildqualität zu verbessern. Eine kürzlich durchgeführte Verhaltensstudie an Mäusen deutet darauf hin, dass die schädliche Wirkung der Strahlung auf das Gehirn durch die gleichzeitige Verabreichung des häufig verwendeten Beruhigungsmittels Ketamin verstärkt werden könnte. Die Kombination von Bestrahlung mit Ketamin führte zum Auftreten zunehmend komplexer Dendritenverzweigungen und einer verringerten Synapsendichte. Diese strukturellen Veränderungen könnten letztlich zu einer Einschränkung der neuronalen Signalübertragung und damit zu den beobachteten Verhaltensänderungen führen.

Im dritten Teil dieser Arbeit wurden die Auswirkungen wiederholter Niedrigdosisbestrahlung, die der Exposition des gesunden Gewebes während der Strahlentherapie entspricht, auf dem Hippocampus untersucht. Es wurde eine Anhäufung von persistenten DNA-Doppelstrangbrüchen beobachtet, die mit einem Rückgang der adulten Neurogenese und einer verringerten Anzahl sich teilender Vorläuferzellen einherging. Auf Proteomebene zeigten sich besonders ausgeprägte Effekte auf die Gruppe der Neurotrophine, welche direkt nach der Exposition stark verringert und nach drei Monaten kompensatorischen hochreguliert detektierbar war.

Zusammenfassend lässt sich sagen, dass ionisierende Strahlung im niedrigen Dosisbereich, wie sie häufig im klinischen Alltag Einsatz findet, im Mausmodell eine starke Auswirkung auf den Hippocampus hat. Dies gilt sowohl für die Kombination mit Ketamin als auch für die alleinige Nutzung von niedrigen Strahlendosen. Es ist daher notwendig, das Bewusstsein für die Folgen niedrig dosierter Bestrahlung zu stärken, die aktuellen Dosisgrenzwerte für die Gehirnexposition zu überdenken und Nebenwirkungen gegenüber dem Nutzen der klinischen Bestrahlung, besonders bei Kindern, besser einzuschätzen. Darüber hinaus weist die Aktivierung neuroprotektiver Mechanismen durch niedrige Strahlendosen auf eine neue therapeutische Strategie hin, gesundes Hirngewebe vor den schädlichen Effekten hoch dosierter Bestrahlung zu schützen.

1 Introduction

1.1 Ionising radiation in modern society

Radiation has become an integral part of our society, not only because of the unavoidable exposure to natural radiation sources, but especially through exposures from artificial radiation sources. The average annual dose in western countries has almost doubled over the last two decades to 4 mSv per year, mainly due to the rapid growth in the use of ionising radiation (IR) in medicine. IR has great potential in medical imaging and oncology and has supported medical progress since its introduction in the early 20th century. However, the same effects of radiation that are exploited in the short-term for cancer therapy also pose a long-term threat to healthy cells, tissues, organs and ultimately the whole organism. Omics technologies including genomics, transcriptomics, proteomics and metabolomics have demonstrated the complexity with which biological systems respond to different radiation exposure events (Azimzadeh et al., 2014; L. Huang et al., 2016; Leszczynski, 2014). The adverse effects range from primary effects on genetic stability, cell fate and survival to secondary effects such as oxidative stress and inflammation (Chen et al., 2011; Chiang et al., 1997; Fike et al., 2007; Fike et al., 2009; McBride et al., 2002; Parihar et al., 2014; Tseng et al., 2014).

1.2 The direct and indirect effects of IR

High-energy IR, such as gamma and X-rays are electromagnetic, i.e. they are a stream of photons, massless particles that move as waves. Gamma radiation is released by the radioactive decay of elements such as ⁶⁰Co and ¹³⁷Cs while X-rays are generated by the capture of accelerated charged particles, mainly electrons, hitting a metal target which results in the release of thermal energy and X-ray photons. (Figure 1)

Both types of photon radiation damage cells through their ability to transfer their energy and consequently to eject electrons from atomic orbitals. This leads to the creation of charged molecules with free electrons. The ionising effect in tissues can be divided into direct and indirect ionisations. Biomolecules such as deoxyribonucleic acid (DNA) can be directly hit by incident photons, causing energy deposition and ionisation of the biomolecule itself. As the major component of living cells is water, radiolysis to produce

free water radicals is the main cause of indirect effects. This creates reactive oxygen species (ROS) such as hydroxyl (HO⁻) and alkoxy (RO₂⁻) ions along the radiation track (Figure 1). These reactive molecules then react with adjacent biomolecules that are components of DNA, cytosolic proteins, membranes and organelles (Wardman, 2009). It has been shown that most radiation-induced damage is due to the indirect effect (Desouky et al., 2019; Saha, 2013).

DNA damage, particularly in the form of DNA double-strand breaks (DSBs), represents the greatest long-term risk to health as this may provoke genetic instability by the generation of mutations and chromosome aberrations that ultimately lead to changes in cell function, carcinogenesis and other pathological endpoints (Chang et al., 2017; Lieber, 2010).

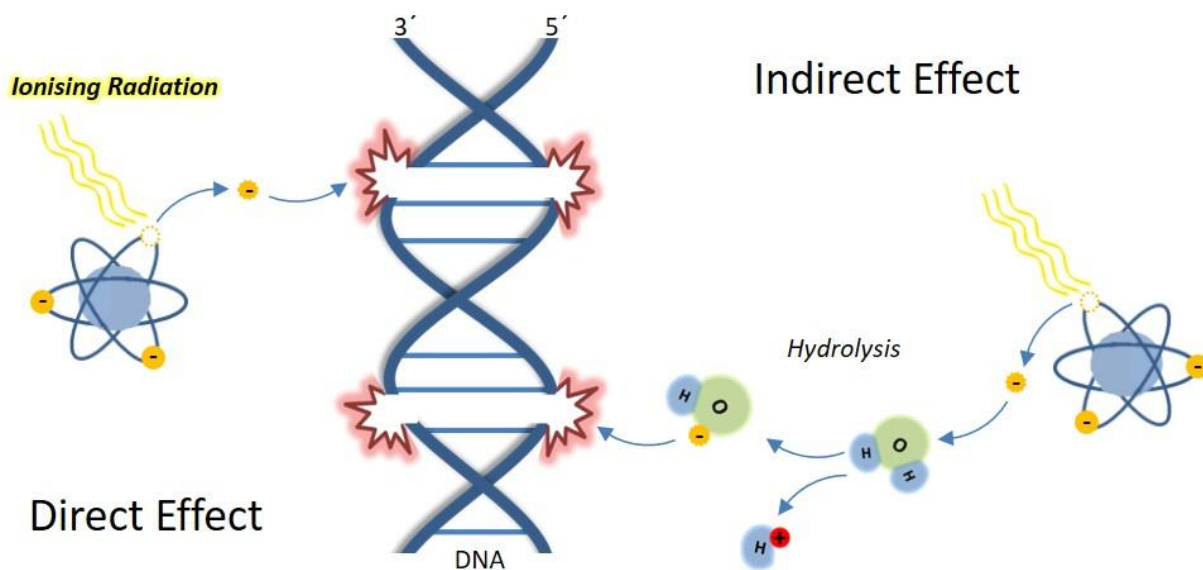


Figure 1: The direct and indirect effect of IR. IR produces free electrons that either hit DNA molecules directly disrupting their molecular structure or the water molecules generating free radicals that then may further damage DNA molecules.

1.3 Vulnerability of the brain

Whether a tissue or organ is sensitive to radiation depends in part on the proliferation status of the constituent cells. The greater the rate of cell division the higher the relative sensitivity to radiation and the probability of damage being passed on to daughter cells. It

was assumed for many decades that the adult brain was relatively radiation resistant because the proliferation of neuronal cells after maturation is limited to the very early stages of life. However, there are regions in the brain where neurogenesis occurs even in the adults: The sub ventricular zone of the lateral ventricles, the sub granular zone of the dental gyrus of the hippocampus and the olfactory bulbs all show continual cell proliferation (Eriksson et al., 1998). These areas are therefore more sensitive to radiation, as evidenced by radiation-induced alterations in neurogenesis, neuronal morphology and synaptic plasticity due to direct DNA damage, increased ROS and the associated response of the brain's immune system. Ultimately, these molecular changes can lead to neuronal deficits and neurodegenerative diseases (Hladik et al., 2016).

1.4 The effects of IR on the brain

1.4.1 Evidence of health effects from epidemiology

Epidemiological studies are an important source of quantitative information on the risks of radiation on the brain. Cohort studies dealing with radiation risk assessment include survivors of the 1945 atomic bombing in Japan (Hiroshima and Nagasaki), patients who have received radiotherapy against malignant and non-malignant diseases (tinea capitis, haemangioma, cancer treatment), individuals who have been exposed for diagnostic purposes (repeated computer tomography (CT) scans), and nuclear workers.

The Life Span Study (LSS) of Japanese atomic bomb survivors provides the best quantitative estimates of the cancer risk of low linear energy transfer (LET) radiation exposure in humans. The importance of this cohort is based on the fact that it consists of a fundamentally healthy population exposed to a variety of radiation doses at any age (Preston et al., 2007). First reports concerning cancer incidence were published in 1994 (Mabuchi et al., 1994; Preston et al., 1994; Ron et al., 1994; Thompson et al., 1994). Over the years, brain cancer occurrence in the LSS cohort was assessed several times (Ozasa et al., 2012; Preston et al., 2003). In summary, the LSS studies highlight the fact that the age at exposure is positively correlated with the brain cancer risk. Children exposed to radiation suffer from more serious consequences than adults. (Smoll et al., 2016)

The occurrence of brain tumours, both malignant and benign, has been also reported as a long-term consequence in children following radiation exposure of the head for the treatment of tinea capitis, a dermatophytosis in the area of the hair crown, and for treatment of haemangioma. In these cases, the underlying brain tissue received exposures ranging from 0.1 to 1.5 Gray (Gy). Studies have found a strong dose-effect and similar to the results of the LSS studies, an increasing brain cancer risk with decreasing age at exposure (Karlsson et al., 1998; Ron et al., 1988; Sadetzki et al., 2005). The intensity of the radiation-related consequences became stronger with time (Kleinerman, 2006). In addition to an increased tumour risk, exposed children developed more psychiatric diseases than non-exposed (Omran et al., 1978) and had a slightly higher incidence of mental retardation (Ron et al., 1982). A large portion of childhood cancer patients who received radiation treatment suffer from a significant, long-lasting decline in cognition and visual memory (Karen E. Hoffman, 2009; Spiegler et al., 2004).

Recently, several studies of brain cancer risk in patients undergoing CT scans have been published. The relative low-energy X-rays in CT imaging could be biologically twice as effective per dose unit as the mainly high-energy γ -rays that were the predominant source of exposure in the atomic bomb attack (Pearce et al., 2012). The doses applied in a repeated head CT range from 40 to 50 mGy (K. P. Kim et al., 2012; C. Lee et al., 2012). The evaluation of a British retrospective cohort study that included data from nearly 180,000 patients showed that the increase in brain tumour incidence increased significantly at a cumulative dose of at least 50 mGy. The researchers assume that a few CT images of the head triples the risk of brain tumours in children younger than 15 years (Pearce et al., 2012). The coincidence of CT scans and brain tumours was also found in other studies (W. Y. Huang et al., 2014; Mathews et al., 2013). It is difficult to draw a clear conclusion from these studies as radiation-based diagnostics is always performed on the basis of other medical indications (Otake et al., 1984). Therefore, it cannot be excluded that the observed side effects come from the causative disease. For this reason, it is essential to further investigate the effects of low-dose radiation on the healthy organism. (Hladik et al., 2016)

1.4.2 Impairment of cognitive function in animal models

In accordance with the findings from human cohort studies (see section 1.4.1), an impairment of cognitive function and memory has also been reported in animal experiments. Radiation-related cognitive dysfunction has been measured in several studies with rats. A significant disorientation of memory function was observed up to twelve months after fractionated brain irradiation (cumulative dose 30 Gy - 40 Gy) (Lamproglou et al., 1995; Yoneoka et al., 1999). A significant increase in working memory errors was measured six to nine months after fractionated (8 x 5 Gy) γ -irradiation, using a partially-baited radial arm maze test (Brown et al., 2007). In addition, Shi et al. demonstrated that clinically relevant doses of fractional irradiation of the brain led to an impairment of spatial learning capacity and reference memory that was assessed by the performance in the Morris Water Maze test (Shi et al., 2006). The same evidence was also provided by Warrington et al. who found that comparable treatment caused a transient deficit in contextual learning, a disturbance of working memory and a progressive impairment of learning in mice (Warrington et al., 2012).

In order to better imitate the anatomical and physiological properties of humans, Robbins et al. focussed on the radiation effect on the brain using non-human primates (NHP). They reported a significant reduction in higher order cognitive function in NHPs exposed to a fractionated whole-brain radiation dose that is expected to be biologically similar to that delivered to non-tumorous brain regions in glioma patients (Robbins et al., 2011).

These studies give a good insight into the potentially harmful effects of radiation on cognitive processes and neuronal function. Nevertheless, the cellular and molecular mechanisms underlying radiation-induced cognitive impairment are still not completely understood (Y. W. Lee et al., 2012). The conventional model of radiation-induced cancer clearly is not applicable to a tissue where mutated cells do not undergo clonal expansion, and where mutation is not known to underlie cognitive changes. Suggested mechanisms include impaired neurogenesis, altered neuronal morphology, and neuroinflammatory processes that are next described in more detail (Greene-Schloesser et al., 2013).

1.4.3 The effect of radiation on neurogenesis

Many studies have demonstrated that radiation-induced cognitive defects are the result of an inhibition of neurogenesis, especially when exposed early in life (J. S. Kim et al.,

2008; Madsen et al., 2003; Raber et al., 2004; Rola, Raber, et al., 2004; Snyder et al., 2005; Yang et al., 2012). Neurogenesis is the process of generating functional mature neurons from neuronal stem cells. This is most active during brain development before birth and in early childhood, whilst neurogenesis in adults is restricted to the dentate gyrus (DG) of the hippocampus, the sub ventricular zone (SVZ) of the lateral ventricle and the olfactory bulbs (OB) (Eriksson et al., 1998) (see Figure 2)

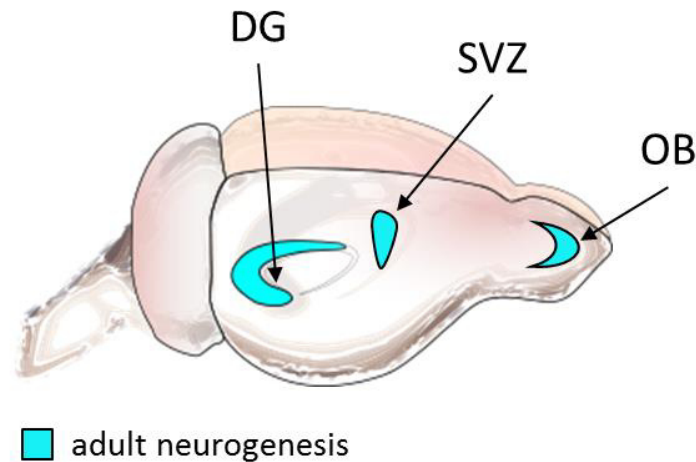


Figure 2: Adult neurogenesis in the mouse brain. Mid-sagittal view of the mouse brain with the three main regions of adult neurogenesis: dentate gyrus (DG) of the hippocampus, sub ventricular zone (SVZ) and the olfactory bulb (OB).

The hippocampus is the part of the brain where processes associated with the consolidation of memory, learning, and spatial orientation occur (Eichenbaum, 2001). Therefore, based on the observations of radiation-induced behavioural changes, this region is of interest in the radiation response. Radiation influences neurogenesis by inducing apoptosis in dividing cells, leading to a reduction of mitotic neuronal stem cells (NSC) and thus reducing the number of differentiated neurons (Lazarini et al., 2009). Additionally, the decrease in neuronal stem cell numbers reduced the proliferation capacity of the remaining NSCs, resulting in a decrease in differentiation capacity into mature neurons (Bellinzona et al., 1996; Mizumatsu et al., 2003; Monje et al., 2002). The radio-sensitivity of NSCs has been demonstrated in several studies after exposure to doses of 1 Gy and higher (Peissner et al., 1999; Verheyde et al., 2007). The increased radio-sensitivity of NSC compared to mature neurons was also noted after a single exposure to 5 or 10 Gy, where only stem cells underwent apoptosis while the non-proliferating mature neurons in the hippocampus were not affected (Parent et al., 1997;

Peissner et al., 1999). Rola et al. showed a significant reduction in the number of immature neurons after irradiation, the decrease ranging from 34 % at 1 Gy to 71 % at 3 Gy (Rola, Otsuka, et al., 2004). Rola et al. studied the acute effects of whole brain x-radiation and were able to show a dose-dependent decrease in proliferating NSCs, immature neurons and neurons 48 hours after doses of 2-10 Gy in young adult mice. To determine long-term effects on neurogenesis, the same mice were exposed to a single dose of 5 Gy and analysed 3 months after exposure, including behavioural tests. A direct correlation between the reduced number of proliferating cells and the increased cognitive impairment was demonstrated (Rola, Raber, et al., 2004). Similar results, namely reduction of neurogenesis and cognitive decline has been observed after fractionated whole brain radiation in several other studies (W. H. Lee et al., 2012; Shi et al., 2006; Yoneoka et al., 1999).

In the study by Casciati et al., the radiation effect on neurogenesis after birth and in adults was compared. It was shown that the brain of newborn mice had a significantly higher sensitivity than the adult brain. The rate of apoptosis was measured one day after 2 Gy X-ray irradiation in the hippocampus of mice treated 10 days or 10 weeks after birth. Only the mice exposed at the age of 10 days showed increased apoptosis (Casciati et al., 2016).

1.4.4 Radiation effects on neuronal morphology

In contrast to the evidence of radiation-induced effects on NSCs, much less is known about the effects of irradiation on more mature neurons. The individual cellular morphology and structure that is required to form neuronal networks is crucial for learning and memory processes and thus also a potential target for radiation-induced impairment. Indeed, radiation-associated neuronal damage ultimately leads to disruption of synaptic plasticity and thus to a restriction of cognitive performance (Parihar et al., 2013).

Especially the neuronal dendrites, the site of synaptic contacts, are important structures involved in synaptic plasticity (Shen et al., 2010). Accordingly, appropriate dendritic morphology is required for many aspects of neuronal function, including signal transduction and information processing. Structural damage is associated with severe cognitive disorders and mental retardation (Huttenlocher, 1991; Kaufmann et al., 2000; Terry et al., 1981; Tronel et al., 2010). Parihar et al. found dose-dependent (1-10 Gy) and

a sustained reduction of dendritic complexity of hippocampal neurons in mice 10 and 30 days after exposure. The branching, length and area of the dendrites were reduced by more than 50% compared to non-irradiated controls (Parihar et al., 2013). Comparable results were also found in a study limited to the dental gyrus and cornu Ammonis 1 (CA1) part of the hippocampus (Chakraborti et al., 2012) and also as a result of proton irradiation (Parihar et al., 2015; Tseng et al., 2014).

Neurotransmission requires the formation of specific types of dendritic spines that act as integrative units in the synaptic circuit. It has been shown that a single radiation exposure reduces the number and density of dendritic spines, depending on the dose. Particularly immature filopodia, a subtype of dendritic spines, showed a high sensitivity to γ -ray exposure (1 and 10 Gy) compared to more mature spine morphologies, such as fungal subtypes (Parihar et al., 2013). In another study, young adult mice were exposed to 10 Gy skull irradiation and the spines of the hippocampus were quantified one week and one month after the irradiation. One month after the irradiation, a reduction in spine density of almost 30% was observed. The analysis of spine morphology showed that irradiation led to a significant reduction in the proportion of fungal spines in the DG and CA1 dendrites at both time points (Chakraborti et al., 2012).

In conclusion, it is known that changes in cognition are associated with altered neuronal morphology and structure and that these changes are actively induced by radiation in a dose-dependent manner and by different radiation types (γ and X-rays and protons).

1.4.5 Inflammation, oxidative stress and activation of glia cells

As described in 1.2 most of the radiation induced damage on neurons and their structures are caused by the generation of free radicals. Oxidative stress in the brain is generally regarded as one of the causes of neuropathological processes such as Alzheimer's and Parkinson's disease (Markesbery, 1997; McGeer et al., 1991; Zhou et al., 2008), and is also associated with normal brain aging (Sohal et al., 1994; Talamini et al., 2012). A sustained increase in oxidative stress leads to cellular damage that triggers the acute inflammatory response in brain that is manifested by the activation of microglia and astrocytes. These cells respond to oxidative damage in their environment with the release of pro-inflammatory mediators via redox-responsive transcription factor-mediated molecular signalling pathways (Conner et al., 2011; Greene-Schloesser et al., 2012; W.

H. Lee et al., 2010). Several studies in rodents have documented the increased levels of interleukins, chemokines, metalloproteinases, adhesion molecules, and the necrosis factor- α (TNF- α) in response to radiation. This response, in turn, leads to overactivation of the immune system (Baluna et al., 2006; Chiang et al., 1997; Chiang et al., 1993; Denham et al., 2002; Gaber et al., 2003; Hong et al., 1995; Hwang et al., 2006; Kempf et al., 2014; S. H. Kim et al., 2002; Kyrkanides et al., 1999; Olschowka et al., 1997; Spleiss et al., 1998).

The inflammatory environments contributes not only to neurodegenerative diseases but also to cognitive impairment as well as neurovascular and certain psychiatric disorders (Anderson et al., 2017; Fike et al., 2009; Limoli et al., 2007; Mizumatsu et al., 2003).

Mice exposed to a single cranial dose of ≥ 15 Gy showed radiation-induced activation of glia cells that, in turn, resulted in an immediate increase in the number of neutrophils and a delayed increase in the number of T-cells, major histocompatibility complex (MHC) II-positive cells and clusters of differentiation 11 (CD11) positive cells in the brain (Moravan et al., 2011). The abovementioned cell types are capable of producing reactive oxygen species that then activate more microglia and immune cells leading to a further increase in the level of oxidative stress (Greene-Schloesser et al., 2012). The local release of pro-inflammatory mediators, the additional production of ROS and the radiation-activated microglia, can combine to inhibit neurogenesis by reducing the maturation of neural precursor cells in the hippocampus (Blomstrand et al., 2014; Jenrow et al., 2013; Prise et al., 2011).

These studies provide evidence that oxidative stress-mediated inflammation is involved in the pathophysiological process of brain injury after irradiation.

1.5 Ketamine and the brain

Sedation is often administered to ensure immobility during the treatment of children with position-dependent radiological procedures such as cancer therapy or imaging techniques (Green et al., 2011; McMullen et al., 2015). Since 1970, the anaesthetic drug ketamine has been used in paediatric medicine for this purpose (James et al., 2010). It exerts its sedative properties via selective blockage of the N-methyl-d-aspartate (NMDA) receptors that are ionotropic glutamate receptors. These, in turn, respond with enhanced

glutamatergic firing. Extracellular glutamate itself then activates post-synaptic α -amino-3-hydroxy-5-methyl-4-isoxazolepropionic acid receptors (AMPA receptors) that are upstream regulators of pathways important for synaptic plasticity, learning and memory. (Duchen et al., 1985; Furukawa et al., 2005; Li et al., 2009)

A chronic increase in extracellular glutamate is thought to play a role in many neurodegenerative diseases, including Alzheimer's disease. During early brain development high-dose ketamine exposure has been shown to induce neurodegeneration followed by cognitive impairment (Fredriksson et al., 2003; Fredriksson et al., 2004; Viberg et al., 2008). Importantly, a study using a mouse model showed an impairment of cognitive function after exposure to a combination of ketamine and radiation even at low clinically relevant doses that, if administered alone, neither influenced cognition. Behavioural tests showed a reduction in habituation, hyperactivity, and reduced learning and memory skills three and six months after a single combination exposure (Buratovic et al., 2018).

1.6 Aim of the thesis

The negative impact of high-dose radiation on the brain is well understood on cognitive processes in the developing brain. These long-term effects are associated with impaired neurogenesis and a reduction of neuronal network complexity driven by cell killing and an oxidative stress-induced inflammatory response (Hladik et al., 2016).

In contrast, knowledge about the health effects of low-dose IR in the brain is still very limited and controversial. In particular, the possible negative alterations of low doses from medical procedures are currently cause for public concern. It is therefore important to understand the possible consequences of low-dose radiation in order to improve protective measures.

The work presented here was conducted in order to investigate how low, clinically relevant, doses of IR affect the brain in the long-term. The studies were focussed on the effects on the hippocampus to identify relevant signalling pathways related to behavioural changes, neurological impairment and progression of normal brain aging.

We hypothesized that the use of low-dose radiation in medicine has the potential for side effects that are more serious than previously assumed. The studies have been designed

to investigate the low-dose radiation effect in combination with the natural aging of the brain to see whether irradiation may promote aging and the development of neurodegenerative diseases.

2 Methodology to analyse the effects of low-dose radiation on the hippocampus

The effects of low-dose radiation alone, or in combination with the sedative ketamine, were investigated in this doctoral thesis. The focus of the study was the hippocampus, the area of the brain that is believed to be relatively sensitive to radiation in adults due to the continued neurogenesis occurring in this area. The experiments are focussed on the proteome changes at different time points after exposure of young or adult mice, accompanied by bioinformatic analysis, validation experiments, and structural investigations.

The following chapters describe the treatment procedure, the proteomics workflow, the validation strategies for the proteomic data and the additional cellular assays that were performed. The results of these studies have been published in three peer-reviewed research articles.





2.1 Treatment of mice

Female F1 hybrids (B6C3F1) of C57BL/6J male and C3HeB/FeJ females were used in the first study (3.1, overview Table 1). The mice were exposed to whole body gamma-irradiation using doses of 0 (control), 0.063, 0.125 and 0.5 Gy delivered at a dose-rate of 0.063 Gy/min (^{60}Co , Eldorado 78 Teletherapy irradiator) at the age of 10 weeks. The mice were sacrificed with CO_2 24 months post-exposure and the hippocampi were micro dissected from the right hemisphere and stored at $-80\text{ }^\circ\text{C}$.

For the ketamine-study (3.2, overview Table 1), male neonatal (post-natal day (PND)10) Naval Medical Research Institute (NMRI) mice were gamma-irradiated using total body doses of either 100 mGy or 200 mGy with a dose rate of 0.2 Gy/min (^{137}Cs , Gammacell 40 Exactor, MDS Nordion) or exposed to a single subcutaneous injection of ketamine (7.5 mg/kg body weight) or treated with ketamine followed by irradiation (100 mGy or 200 mGy) one hour later. After six months, the mice were sacrificed with CO_2 and both hippocampi were dissected. The right hemispheres were stored at $-80\text{ }^\circ\text{C}$ for proteome analysis, and the left hemisphere used for morphological studies after further processing as described in 2.4.

In the third study (3.3, overview Table 1) male C57BL/6 mice (Charles River Laboratories) were exposed to repeated doses of 0.1 Gy by a linear accelerator (Artiste™). Mice were exposed at postnatal day (PND) 11 (juvenile) or PND56 (adult) with either 5, 10, 15 or 20 fractions delivered 5 days a week. The hippocampi of juvenile and adult mice that received a total dose of 2Gy (20 x 0.1 Gy) were analysed after 72h, 1 month, 3 months and 6 months.

Table 1: Summary of the experimental designs

		Study 1	Study 2	Study 3
Study design	Strain 	F1 C3HeB/FeJ and C57BL/6J	NMRI	C57BL/6
	Sex 	female	male	male
	Irradiation 	0.063 Gy, 0.125 Gy, 0.5 Gy	0.1 Gy, 0.2 Gy, Ket, 0.1 Gy Ket, 0.2 Gy Ket	5x, 10x, 15x, 20x 0.1 Gy
		¹³⁷ Cs 0.063 Gy/min	¹³⁷ Cs 0.2 Gy/min	beam energy, 6-MV photons
	Treatment 	PNW10	PND10	PND11
	Analysis	24 months	6 months	72 hours, 1, 3, 6 months
Methods	Proteomics	x	x	x
	Bioinformatical analysis	x	x	x
	Western blotting	x	x	X
	Carbonylation	x		
	Golgi staining		x	

2.2 Analysis of the proteome

2.2.1 Sample preparation

Frozen hippocampi were submerged in liquid nitrogen and pulverized using a mortar and pestle. The resulting tissue powder was suspended in RIPA cell lysis buffer (Thermo Fisher) enriched with phosphatase and protease inhibitors (Roche). After a short sonication, the lysates were incubated under shaking conditions at 4°C for 20 min followed by centrifugation at 13,000 g at 4°C for 15 min. Protein concentrations of the supernatants were determined using the bicinchoninic acid (BCA) method according to manufacturer's instructions (Thermo Fisher) and measured at 595 nm on an Infinite M200 (Tecan GmbH).

Figure 3 illustrates the label-free liquid chromatography-tandem mass spectrometry (LC-MS/MS) workflow performed in this work.

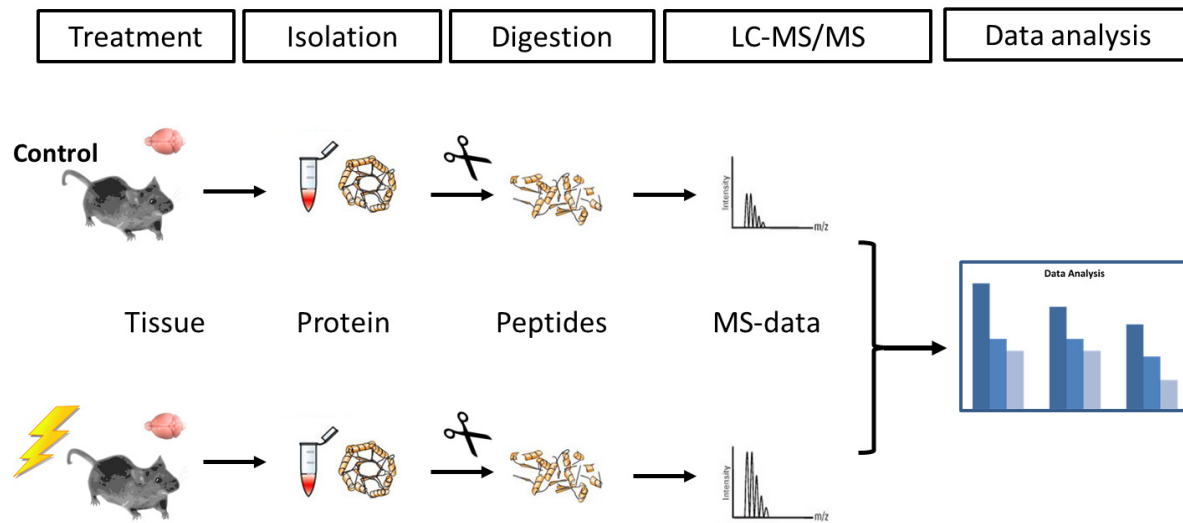


Figure 3: Overview of label-free proteomics workflow. Mice were either irradiated or sham-irradiated and the proteins were isolated from the areas of interest after harvesting the brains. The protein solutions were digested and run on a QExactive. The acquired MS-spectra were analysed for label-free quantification and pathway analysis.

2.2.2 LC-MS/MS

In all three studies the proteomes were analysed using label-free quantification. This method determines the relative amount of each measured peptide without the need for stable isotope, dye or mass tag labelling as used in other mass spectrometry methods (Asara et al., 2008; Bantscheff et al., 2007). This allows the measurement of alterations across the entire proteome. The spectral counting methodology provides a higher dynamic range of quantification but with less accuracy compared to other labelling methods (Patel et al., 2009).

Ten μg of protein lysate was digested using a modified filter-aided sample preparation (FASP) protocol (Wisniewski, Zougman et al. 2009). The digested samples were stored at $-20\text{ }^{\circ}\text{C}$ until further processing. Mass spectrometry (MS) measurement was performed in a data-dependent acquisition (DDA) mode on a QExactive (QE9 high field (HF) mass spectrometer (Thermo Fisher Scientific Inc.) coupled to an Ultimate 3000 nano-RSLC pre-separation reverse phase liquid chromatography column (Thermo Fisher Scientific Inc.). Approximately $0.5\text{ }\mu\text{g}$ of each digested sample was automatically loaded onto a nanotrap

column (300 μm inner diameter (ID) \times 5 mm, packed with Acclaim PepMap100 C18, 5 μm , 100 \AA ; LC Packings) before separation by reversed-phase chromatography (Acquity UPLC M-Class HSS T3 Column 75 μm ID \times 250mm, 1.8 μm) at 40°C. The MS-data was acquired at a resolution of 60,000 full widths at half-maximum with automatic gain control target set of 3×10^6 and maximal 50 ms injection time. The MS data was recorded with a mass range from 300 to 500 m/z. The 10 top abundant peptides in the pre-scan were chosen for fragmentation (MS/MS) if they were at least 2-fold charged with a dynamic exclusion of 30 s. MS/MS spectra were recorded at a resolution of 15,000 with an automatic gain control (AGC) target set to 10^5 and a maximum injection time of 100 ms. Normalized collision energy was defined to 28 and all spectra were recorded in profile type.

2.2.3 Label-free peptide quantifications and identification

To analyse the LC/MS data obtained for the quantification and identification of proteins, the acquired MS spectra were analysed with Progenesis Q1 software (Version 3.0, Nonlinear Dynamics) for label-free quantification. The profile data of the MS runs were converted to peak lists including m/z values, intensities, abundances, and m/z width. MS/MS spectra were transformed similarly and then stored in peak lists comprising m/z and abundance. The retention times of all samples were aligned to one reference sample automatically, allocated to the corresponding treatment groups and the raw abundances were normalized. All MS/MS spectra were exported from the Progenesis Q1 software as Mascot generic files and used for peptide identification with Mascot (version 2.5) using the Ensemble mouse database (Release 80, 54,197 sequences). The search parameters were peptide mass tolerance of 10 ppm, fragment mass tolerance of 20 mmu, one allowed missed cleavage; carbamidomethylation of cysteine was set as a fixed modification, oxidation of methionine and deamination of asparagine and glutamine as variable modifications. A Mascot-integrated decoy database search was set to a false discovery rate (FDR) of 1%. The resulting mean values of normalized abundances of unique peptides were calculated for every protein separately and then used for the calculation of abundance ratios, comparing the data between exposed samples and controls. Following filtering criteria were used: Proteins were identified and quantified with a minimum of two

unique peptides (UP) and fold-changes of ≤ 0.7 or ≥ 1.3 ($q \leq 0.05$) were considered as significantly differentially expressed.

2.2.4 Pathway analysis

The significant deregulated proteins were analysed using Ingenuity Pathway Analysis (IPA, QIAGEN, www.qiagen.com/ingenuity), a literature based program that allows analysis, integration, and interpretation of omics data. It provides predictions about possible upstream and downstream targets and associated mechanism based on the observed deregulation of the proteome. Additionally, the program associates the proteome changes with known biological processes and diseases.

For the analysis of the canonical pathways predicted to be involved in the radiation response, the list of significant deregulated proteins including accession numbers, fold changes and p-values were uploaded and analysed.

In a bottom-up proteomics approach such as the one used in this thesis, proteins are digested into peptides prior to analysis and more than one unique peptide is required to identify a protein of interest. However, the component peptides themselves must be within the detectable size range and be able to form a sufficiently ionised molecule. Additionally, only relatively high abundant proteins are quantifiable with the label-free MS-approach. Therefore, proteins that do not fulfil these criteria do not appear in the MS runs.

2.2.5 Validation of the LC-MS/MS

Through bioinformatics analysis central regulators can be indicated based on the deregulation of a network of identified proteins and further validated. For Western blot analysis, samples (15 μg) were dissolved in Lämmli buffer, separated using a 4-12 % gradient gel and transferred to a nitrocellulose membrane by overnight electroblotting at 17 V. Membranes were then blocked using 8% non-fat dry milk powder (NFDM) dissolved in tris-buffered saline with tween20 (TBST) and incubated with a primary antibody overnight at 4°C. After three washing steps in TBST, the membrane was incubated for at least 1 h with the horseradish peroxidase (HRP)-coupled secondary antibody (either anti-mouse or anti-rabbit) and visualised with chemiluminescence detection. Protein bands were quantified with the ImageJ software. A Ponceau staining of the membrane was used

to visualize all transferred proteins and to compensate for variation in loading, and transfer and to exclude technical errors.

2.3 Measurement of free radicals

As described in chapter 1.1.1 radiation leads to production of ROS that can promote protein oxidation, leading to the formation of carbonyl groups on protein side chains. Therefore, the amount of carbonylated protein is an important biomarker for the level of oxidative stress, allowing a quantitative estimation of the ROS production. However, caution is needed as, in addition to radiation-induced ROS, an increased carbonyl content may occur during normal brain aging and in neurodegenerative diseases (Levine, 2002). In this study, the carbonylated proteins were quantified using the Protein Carbonyl Content Assay Kit (Biovision). This assay is based on 2, 4- Dinitrophenylhydrazine (DNPH) targeting the protein carbonyl-associated aldehyde and ketone-groups. The resulting reaction products are stable 2,4-DNPhydrazone derivatives that are quantifiable at 375 nm (Levine et al., 1994) (see Figure 4).

500 µg protein was mixed with 100 µl DNPH, vortexed and incubated under shaking conditions. After 15 min 30 µl trichloroacetic acid (TCA) was added to precipitate proteins and the mixture vortexed and placed on ice for 10 min followed by a 2 min centrifugation step at maximum speed. The supernatant was discarded, and the pellet was washed with ice-cold acetone twice, including 30 seconds in a sonicating bath to effectively disperse the pellet. After satisfactory removal of free DNPH, samples were incubated for 10 min at -20° and labelled proteins again pelleted via centrifugation. Finally, the pellets were dissolved in 200 µl guanidine and 100 µl of the solution was transferred into a 96-well plate. The absorbance was measured at 375 nm. To exclude falsification due to protein loss during the procedure, a BSA assay was performed on the final solution. The measured OD values were adjusted to the BSA assay results.

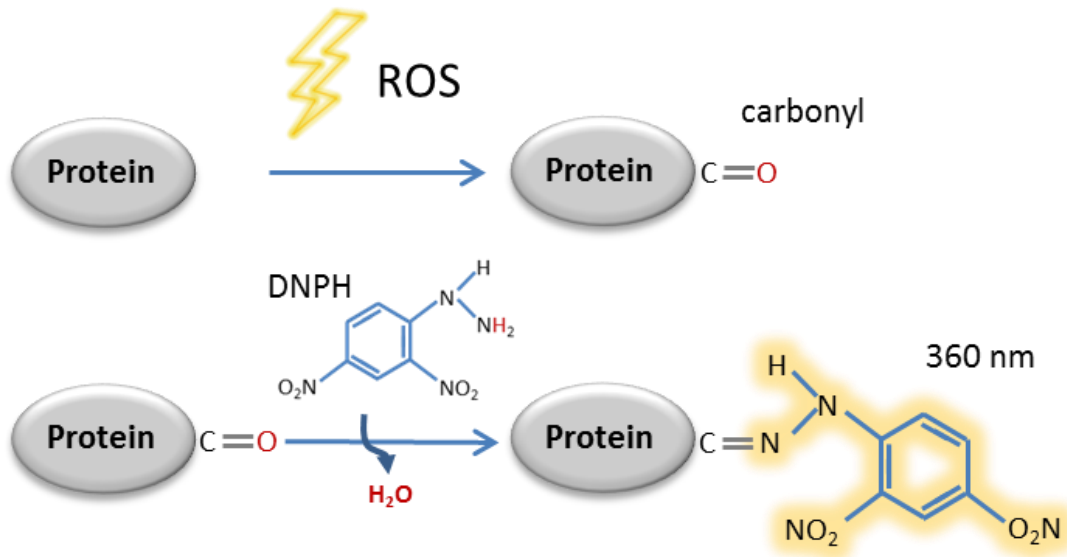


Figure 4: Detection of radiation-induced free carbonyl groups representative for oxidative stress. Reactive oxygen species (ROS) generate persistent carbonyl groups on proteins by oxidation. The reactive agent DNPH is tagged on the carbonyl groups forming DNP hydrazones that are detectably at 375 nm.

2.4 Structural analysis of CA1 neurons

Golgi staining was developed in 1873 by Camillo Golgi to visualize nerve tissue (Grant, 2007). This assay is still a reliable method to study the architecture of neurons. Golgi staining is based on the precipitation of reduced metallic silver granules onto the oligosaccharide coating on the surface of neural cells. The tissue is treated with chromium salts followed by an application of silver nitrate. Only some of the neurons present are stained, which makes it possible to study individual neurons in detail. The reason why only some neurons are stainable is still unknown.

Golgi staining was performed with the FD Rapid GolgiStain Kit (FD NeuroTechnologies) according to manufacturer specifications. The dissected left hemispheres were briefly rinsed with phosphate-buffered saline (PBS) and incubated for 1 week in 5 ml Golgi-Cox solution (A-B) for fixation and impregnation at room temperature (RT). The tissue was then incubated for at least 48 hours at 4°C in solution C containing silver nitrate, protected from light, before freezing for tissue sectioning. 100 µm coronal sections were prepared with a cryostat at -20 °C, mounted on gelatine-coated microscope slides and stained for 10 min in Solution D/E. The sections were then washed twice with H₂O for 4 min,

dehydrated in an ascending alcohol series (50%, 75%, 95% ethanol for 4 min each), incubated 3 times in xylene for 4 min and covered by coverslips.

The stained CA1 neurons of the hippocampus were identified and their structure reconstructed under 40 x magnification (Zeiss AxioPlan 2 microscope) using the Neurolucida software (MBF Bioscience, Williston, USA). Acquired images were further analysed with the Neurolucida Explorer software (MBF Bioscience). Apical and basal dendrites were analysed separately. The number of dendrites, total length and branching was quantified. Density of spines was calculated by dividing the total number of spines by the total length of all dendrites. The Sholl analysis is a tool to analyse the complexity of neurons and is based on counting the number of dendritic branches at given distances from the soma. The radius interval was set to 10 μm starting from 10 μm to an end at 200 μm distance from the centre. Figure 5 illustrates the whole workflow applied in this experiment.

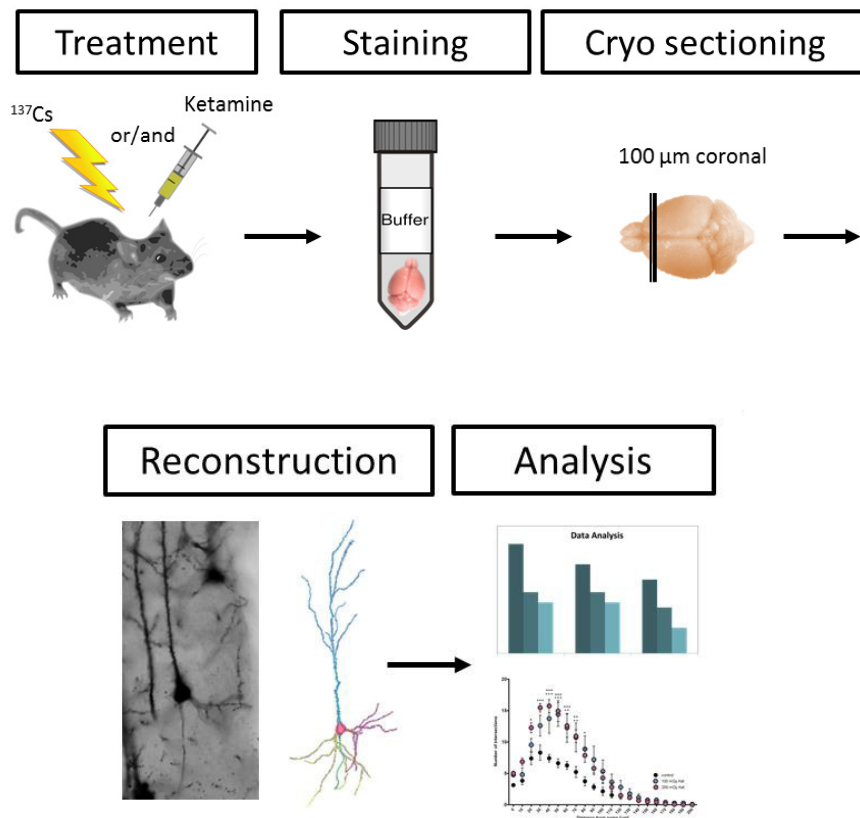


Figure 5: Experimental schedule of the structural analysis of CA1 neurons. Mice were treated or sham-treated and the harvested brains were stained, cut and analysed using microscopy. The neurons in the CA1 area of the hippocampus were reconstructed with the Neurolucida software and analysed with the Neurolucida Explorer software.

3 Results and Discussion

3.1 CREB signaling mediates a dose-dependent radiation response in the murine hippocampus evident two years after total body exposure

3.1.1 Aim and summary of the study

The risks of low-dose radiation from natural sources or medical applications are not yet well understood. Although the health benefits of radiation-based imaging and cancer treatment are undeniable, legitimate concerns have been expressed about the adverse health effects that may occur later in life. It is already known that radiation doses of 0.5 Gy and above have harmful pathological effects (Hladik et al., 2016). Knowledge of lower doses is very limited, as are the nature of any effects that occur long after exposure. The aim of this study was to investigate the low-dose radiation response in the hippocampus. Female B6C3F1 mice were exposed to 0, 0.063, 0.125 or 0.5 Gy (^{60}Co , dose rate 0.063 Gy/min) at an age of 10 weeks. This corresponds to a young adult age in humans when only adult neurogenesis remains active. The hippocampi were collected 24 months after the exposure and analysed using quantitative label-free LC-MS/MS analysis. The bioinformatics analysis of protein changes (IPA analysis) revealed that the most affected canonical pathway was cAMP response element-binding protein (CREB) signalling, and the associated pathways upstream and downstream of CREB. A positive z-score indicating activation of the pathway was seen after the doses of 0.063 and 0.125 Gy, while the higher 0.5 Gy dose led to a deactivation (negative z-score). The CREB protein, CREB protein phosphorylated on Serine 133 (Ser133), and the expression of upstream and downstream targets all showed the same pattern of deregulation, supporting the IPA analysis. Since CREB has been shown to promote neuroprotection in response to several external stimuli, markers for inflammation and cell death were also tested. The dose of 0.063 Gy resulted in a decrease in proteins indicative of inflammation, namely ionized calcium-binding adapter molecule 1 (IBA-1) (activated microglia) and glial fibrillary acidic protein (GFAP) (reactive astrocytes), while the 0.5 Gy dose had a pro-inflammatory effect in the hippocampus. Here bcl-2-associated x protein (BAX) and caspase-3 (CASP-3), two proteins involved in the apoptotic process, as well as total carbonylated proteins (markers

of oxidative stress) were increased only after the 0.5 Gy exposure. These data show that very low doses (0.063 Gy) elicit a different response two years after exposure than the higher dose of 0.5 Gy. The lowest dose is postulated to have a protective effect while the highest dose tested in this study had a harmful effect. The adverse effects at the higher dose tested are similar to the changes seen during normal brain aging, leading us to make the new hypothesis that radiation induced an accelerated rate of normal brain aging.

3.1.2 Contribution

This study was a part of the INSTRA project initiated and mainly designed by Prof. Dr. Jochen Graw and Dr. Claudia Dalke of the Institute of Developmental Genetics, HMGU. The radiation treatment was carried out by Dr. Helmut Schlattl and his team, the sacrificing of the mice and the tissue sampling were performed by Dr. Lillian Garrett, Dr. Stefan Kempf and Dr. Ute Rößler who were supported by other members of the INSTRA consortium. I performed the protein lysis, concentration measurements and preparation for the LC-MS/MS runs that were performed by Dr. Christine von Törne under the direction of Prof. Dr. Stefanie Hauck. The bioinformatics analyses of the proteomic data, all Western blots and the carbonylation assay were performed by me. Mr. Jos Philipp created the volcano blots. I designed all the other figures, performed the statistical analysis and wrote the manuscript. Dr. Omid Azimzadeh, Prof. Dr. Michael J. Atkinson and Dr. Soile Tapio supported me throughout the study with advice, scientific discussion and proofreading of the manuscript.

3.1.3 Publication

The data were presented in an original research paper published on November 28th, 2019 in the Journal of Proteome Research:

CREB Signalling Mediates Dose-Dependent Radiation Response in the Murine Hippocampus Two Years after Total Body Exposure.

Daniela Hladik, Claudia Dalke, Christine von Toerne, Stefanie M. Hauck, Omid Azimzadeh, Jos Philipp, Marie-Claire Ung, Helmut Schlattl, Ute Rößler, Jochen Graw, Michael J. Atkinson and Soile Tapio

J Proteome Res. 2019 Nov 8. doi: 10.1021/acs.jproteome.9b00552 (Hladik et al., 2020)

CREB Signaling Mediates Dose-Dependent Radiation Response in the Murine Hippocampus Two Years after Total Body Exposure

Daniela Hladik,^{†,#} Claudia Dalke,[‡] Christine von Toerne,[§] Stefanie M. Hauck,[§] Omid Azimzadeh,^{†,‡} Jos Philipp,[†] Marie-Claire Ung,[‡] Helmut Schlattl,^{||} Ute Rößler,[⊥] Jochen Graw,[‡] Michael J. Atkinson,^{†,#} and Soile Tapio^{*,†,‡}

[†]Institute of Radiation Biology, Helmholtz Zentrum München GmbH, German Research Center for Environmental Health GmbH (HMGU), 85764 Neuherberg, Germany

[‡]Institute of Developmental Genetics, HMGU, 85764 Neuherberg, Germany

[§]Research Unit Protein Science, HMGU, 80939 Munich, Germany

^{||}Research Unit Medical Radiation Physics and Diagnostics, HMGU, 85764 Neuherberg, Germany

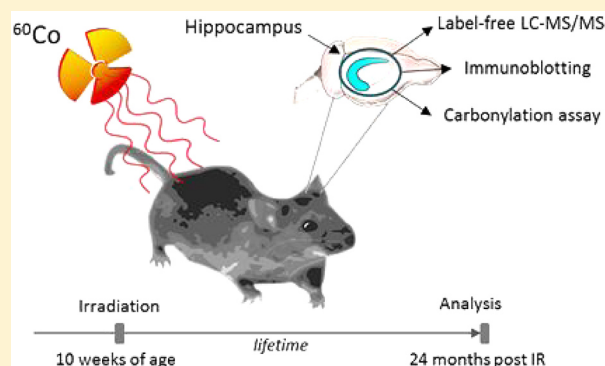
[⊥]Federal Office for Radiation Protection, Department SG Radiation Protection and Health, 85764 Oberschleißheim, Germany

[#]Technical University Munich (TUM), 80333 Munich, Germany

S Supporting Information

ABSTRACT: The impact of low-dose ionizing radiation (IR) on the human brain has recently attracted attention due to the increased use of IR for diagnostic purposes. The aim of this study was to investigate low-dose radiation response in the hippocampus. Female B6C3F1 mice were exposed to total body irradiation with 0 (control), 0.063, 0.125, or 0.5 Gy. Quantitative label-free proteomic analysis of the hippocampus was performed after 24 months. CREB signaling and CREB-associated pathways were affected at all doses. The lower doses (0.063 and 0.125 Gy) induced the CREB pathway, whereas the exposure to 0.5 Gy deactivated CREB. Similarly, the lowest dose (0.063 Gy) was anti-inflammatory, reducing the number of activated microglia. In contrast, induction of activated microglia and reactive astroglia was found at 0.5 Gy, suggesting increased inflammation and astrogliosis, respectively. The apoptotic markers BAX and cleaved CASP-3 and oxidative stress markers were increased only at the highest dose. Since the activated CREB pathway plays a central role in learning and memory, these data suggest neuroprotection at the lowest dose (0.063 Gy) but neurodegeneration at 0.5 Gy. The response to 0.5 Gy resembles alterations found in healthy aging and thus may represent radiation-induced accelerated aging of the brain.

KEYWORDS: ionizing radiation, label-free proteomics, hippocampus, CREB signaling, brain, aging



INTRODUCTION

Technologies using low-dose ionizing radiation (IR) have become frequent and indispensable in medical diagnostics. In addition, during conventional radiation therapy regimens, large volumes of healthy tissue are exposed to low-dose IR exposures. Although the health benefits of radiation-based imaging and therapy are indisputable, the rising and repetitive use of computed tomography (CT) scanning may result in cumulative radiation doses well beyond 0.1 Gy.^{1,2} Justifiable concerns have been raised about adverse long-term health consequences, especially for exposures involving the brain.³ Radiation doses of 0.5 Gy and higher may induce harmful pathological effects in the central nervous system.⁴ In mice, cognitive impairment has been reported after total body irradiation already at 0.5 Gy.^{5,6}

Several studies have investigated radiation effects in the hippocampus as this brain area plays a central role in learning

and memory.⁷ In the murine hippocampus, permanently increased inflammation, astrogliosis, enhanced oxidative stress, and mitochondrial dysfunction were shown at doses around 1 Gy.^{5,8} Impaired neurogenesis, due to a depletion of neuronal stem and progenitor cell pools in the *dentate gyrus*, was observed 6 months after a single cranial 2 Gy dose and after a fractionated total body dose (20 × 0.1 Gy), especially if given to juvenile C57BL/6 mice.^{9,10}

The response to low doses of IR may differ substantially from that observed at high doses.¹¹ Some studies suggest that very low doses may induce even protective, adaptive, or anti-inflammatory mechanisms.^{12–16} All in all, there is great uncertainty about

Received: August 14, 2019

Published: October 28, 2019

the molecular processes underlying biological responses to low-dose exposure.

The aim of this study was to investigate potential long-term effects of a single total body exposure in the hippocampus. Female B6C3F1 mice were irradiated at the age of 10 weeks using doses of 0 (“control”), 0.063 (“low”), 0.125 (“medium”), or 0.5 Gy (“high”). Radiation-induced changes in the hippocampal proteome were measured 4, 12, 18, and 24 months after the exposure, but significant alterations were only seen in the old mice 24 months postexposure. At this time point, the two lower doses led to an activation of neuroprotective pathways, whereas the higher dose (0.5 Gy) resulted in an inactivation of the memory-related CREB pathway and an increase of pro-inflammatory and apoptotic markers.

■ EXPERIMENTAL SECTION

Animal Treatment

This study was approved by the Government of Upper Bavaria (Az. 55.2-1-54-2532-161-12). All experiments were done in strict accordance with the German Law of Animal Protection, the Declaration of Helsinki, and the ARRIVE guidelines. The breeding schedule to produce female F1 B6C3F1 hybrids (C57BL/6JG x C3HeB/FeJ)F1 has been described before.¹⁷ All mice were kept under specific pathogen-free conditions. At the age of 10 weeks, groups of mice were exposed to a single total body radiation at 0 (sham-irradiated control), 0.063, 0.125, or 0.5 Gy (⁶⁰Co gamma-radiation, dose rate 0.063 Gy/min) (Eldorado 78 Teletherapy irradiator, AECL, Canada). Groups of mice were killed with CO₂ 4, 12, 18, or 24 months after the exposure.

Tissue Collection

Four mice per dose group and time point were used for isolation of hippocampi. All dissections were performed in the morning between 8:00 and 11:30 am. The mice were killed with CO₂, and the head was detached from the rest of the body with scissors. The scalp skin was cut between the eyes down the middle line using a scalpel to remove the skin. The skull was cut laterally at the foramen magnum on both sides with fine scissors up to the middle line. The skull flaps were detached with forceps, the brain gently removed and cut into both hemispheres; the hippocampus of the right hemisphere was removed carefully with a scalpel, gently rinsed in cold PBS and snap frozen with liquid nitrogen. All samples were stored at −80 °C.

Protein Lysis and Measurement of Protein Concentration

Frozen tissues were pulverized and suspended in RIPA buffer (Thermo Fisher, Darmstadt, Germany) containing phosphatase and protease inhibitors (Sigma-Aldrich, Taufkirchen, Germany). After sonication, lysis, and centrifugation, protein concentrations were measured using BCA Protein Assay Kit (Thermo Fisher) according to the manufacturer's instructions. The protein lysates were stored at −20 °C.

Mass Spectrometry

Ten μg of each protein lysate was digested enzymatically with a modified filter-aided sample preparation (FASP) protocol.¹⁸ The digests were stored at −20 °C until MS measurement. This was performed in data-dependent acquisition (DDA) mode using a Q Exactive high field mass spectrometer (Thermo Fisher, Darmstadt, Germany). The digested lysates (0.5 μg) were injected automatically and loaded to the online-coupled RSLC (Ultimate 3000, Thermo Fisher) HPLC system including a nano trap column (300 μm inner diameter ×5 mm, packed

with Acclaim PepMap100 C18, 5 μm, 100 Å; LC Packings, Sunnyvale, CA). The sample mixtures were resolved by reversed phase chromatography (Acquity UPLC M-Class HSS T3 Column 75 μm ID × 250 mm, 1.8 μm; Waters, Eschborn, Germany) at 40 °C using a 3–41% acetonitrile gradient with 0.1% formic acid at 250 nL/min for 105 min. The high-resolution (60 000 full width at half-maximum) MS spectra were recorded with a maximum injection time of 50 ms from 300 to 1500 *m/z* with automatic gain control target set to 3 × 10⁶. The 10 most abundant peptide ions from the MS prescan were selected for fragmentation (MS-MS) if they were at least doubly charged, with a dynamic exclusion of 30 s. MS-MS spectra were recorded at 15 000 resolution with automatic gain control target set to 1 × 10⁵ and a maximum of 100 ms injection time. Normalized collision energy was set to 28, and all spectra were recorded in profile type.

Protein Identification and Quantification

The acquired spectra were evaluated using Progenesis Q1 software (Version 3.0, Nonlinear Dynamics) for label-free quantification as previously described¹⁹ with the following changes: Spectra were searched against the Ensembl mouse database (Release 80, 54 197 sequences). The search parameters used were a 10 ppm peptide mass tolerance and a 20 mmu fragment mass tolerance. Carbamidomethylation of cysteine was set as the fixed modification, and the oxidation of methionine and deamidation of asparagine and glutamine were allowed as variable modifications, allowing only one missed cleavage site. Mascot integrated decoy database search was set to a false discovery rate (FDR) of 1%. The resulting mean values of normalized abundances of unique peptides (UP) were calculated for every protein separately and used for the calculation of abundance ratios and statistical analysis, comparing the data between exposed samples and controls.

Pathway Analysis

For the analysis of the canonical pathways predicted to be responding to irradiation, the list of significantly deregulated proteins with their accession numbers, fold changes and *q*-values were imported into Ingenuity Pathway Analysis (IPA) (QIAGEN Redwood City, www.qiagen.com/ingenuity).

Immunoblot Analysis

For validation of key protein changes immunoblotting was performed as described previously.¹⁰ Band intensities were normalized to the Ponceau staining (Figure S1). The following antibodies were applied in this study. From Cell Signaling (Cell Signaling Technology Europe B.V., Frankfurt am Main, Germany): ERK1/2 (#9102), Thr202/Tyr204 ERK1/2 (#9101), p38 (#3810), Thr180/Tyr182 p38 (#9211), cleaved CASP3 (#9661), BCL-XL (#2762); from Abcam (Abcam plc, Cambridge, UK): CREB (ab31387), Ser133 CREB (ab32096), ARC (ab118929), PSD-95 (ab18258), IBA1 (ab5076), GFAP (ab7260), NRF2 (ab31163); from Santa Cruz (Santa Cruz Biotechnology, Inc., Heidelberg, Germany): c-FOS (sc-47724), BAX (sc-7480). Protein bands were quantified with ImageJ 1.50f3.²⁰

Protein Carbonyl Content

Quantification of protein carbonyl content was done according to the manufacturer's instructions using the Protein Carbonyl Content Assay Kit from Biovision (Milpitas, CA, USA).

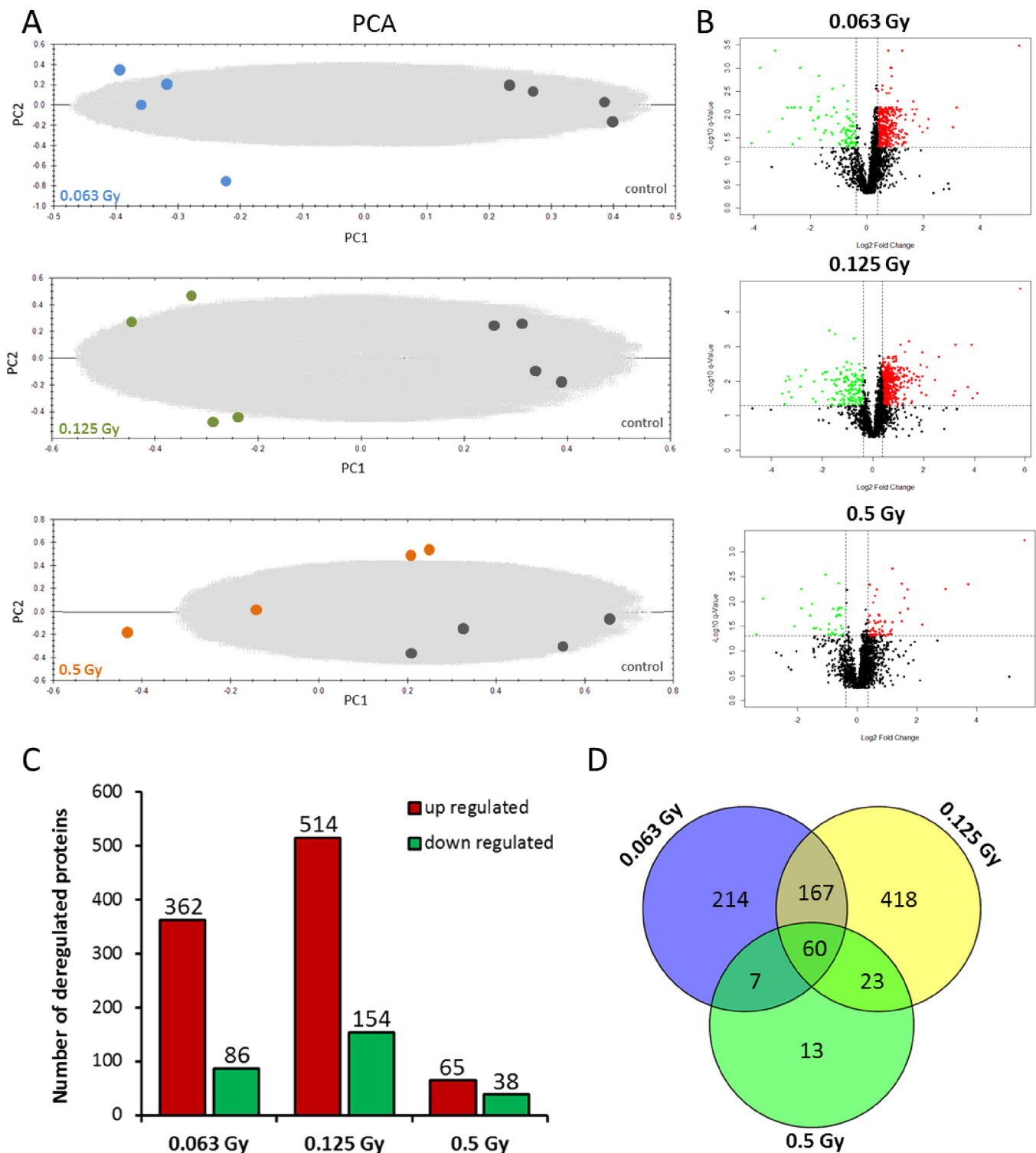


Figure 1. Radiation effects on the hippocampal proteome 24 m postexposure. (A) A principal component analysis (PCA) of hippocampal proteomes exposed to 0.063, 0.125, or 0.5 Gy in comparison with the sham-irradiated control group. (B) Volcano plots representing the distribution of all quantified proteins (identification with at least 2 UP) in hippocampus exposed to a single radiation dose (0.063, 0.125, 0.5 Gy) in comparison to sham-irradiated controls. Upregulated proteins are shown in red and downregulated in green, fold change ± 1.3 . (C) Total numbers of significantly upregulated (red) and downregulated (green) proteins are shown for all dose groups ($q \leq 0.05$, fold change ± 1.3). (D) The Venn diagram showing the numbers of shared deregulated proteins between the three experimental groups and the proteins exclusively deregulated in only one dose. $n = 4$.

Statistical Analysis

For proteomic analysis, the following filtering criteria were used: Proteins identified and quantified with 2 UP, had a q -value of ≤ 0.05 , and fold-changes of ≤ 0.77 or ≥ 1.3 were considered as

significantly differentially expressed. For other experiments, statistical analysis was performed with GraphPad Prism software (GraphPad Software, San Diego, USA) using an unpaired Student's t test. The data are presented as standard error of the

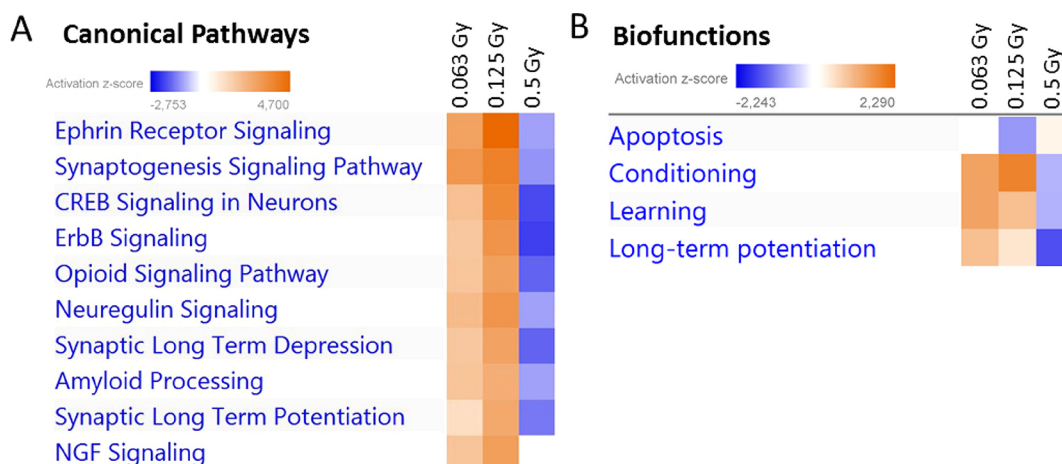


Figure 2. Radiation-induced changes in biological pathways related to normal neuronal functioning two years postexposure. (A) The IPA analysis of associated signaling pathways based on all significantly deregulated hippocampal proteins for all three dose groups is shown. The canonical pathways are ranked by their z-score. The orange color represents a positive z-score indicating an activation of the pathway; the blue color represents a negative z-score predicting a deactivation. (B) Affected neuronal biofunctions for all three dose groups ranked by the z-score (IPA) are shown. The orange color represents a positive z-score indicating an activation of the pathway; the blue color represents a negative z-score predicting a deactivation.

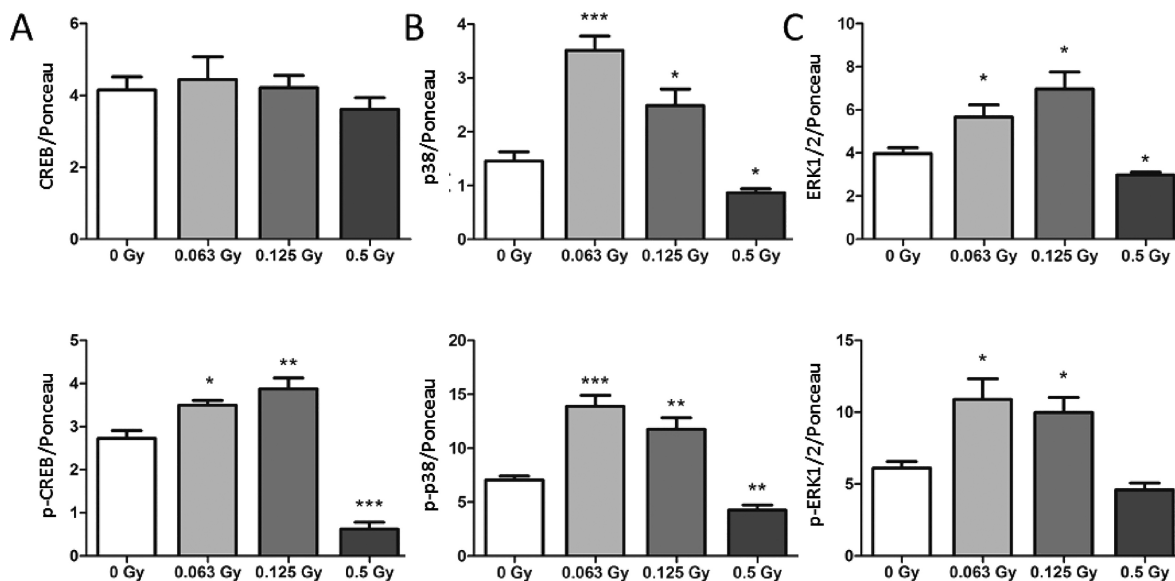


Figure 3. Deregulation of the CREB signaling in hippocampus 24 m after radiation exposure. Immunoblot analysis of the relative expression of CREB and phospho-(Ser133) CREB (A), p38 and phospho-(Thr180/Tyr182) p38 (B) and ERK1/2 and phospho-(Thr202/Tyr204) ERK1/2 (C) for the four treatment groups normalized to the total amount of proteins is shown. Error bars represent the SEM, $n = 4$, * $p < 0.05$, ** $p < 0.01$, *** $p < 0.001$ (Student's t test).

mean (SEM); p -values ≤ 0.05 were defined as significant. Four biological replicates were included in all experiments. Each treatment group was compared individually to the sham-irradiated control group.

Data Availability

The mass spectrometry proteomics data have been deposited to the ProteomeXchange Consortium via the PRIDE²¹ partner repository with the data set identifier PXD015729.

RESULTS

The Hippocampal Proteome Shows Changes Two Years after a Single Radiation Exposure

The hippocampal proteome was analyzed at different time points (4, 12, 18, 24 months) after total body doses of either 0, 0.063, 0.125, or 0.05 Gy. Interestingly, when the mice were at a

younger age (4, 12, 18 months), very few radiation-induced changes in the hippocampal proteome were found (Table S1; <http://dx.doi.org/doi:10.20348/STOREDB/1153/1213>). In contrast, with the progressing age, the radiation effect became noticeable. Therefore, we investigated the 24-month time point in more detail.

In the hippocampus of aged mice (24 months after the irradiation) 3588 proteins were identified in total, of which 2336 were quantified with 2 UP. All identified proteins are listed in Table S2. All quantified proteins for each radiation dose group are shown in Tables S3–S5. Principal component analysis (PCA) established that clusters of each biological replicate were separated depending on the radiation dose (Figure 1A). The corresponding Volcano plots of all quantified proteins are shown in Figure 1B. Applying the proteomics filtering criteria, the analysis showed the following numbers of significantly

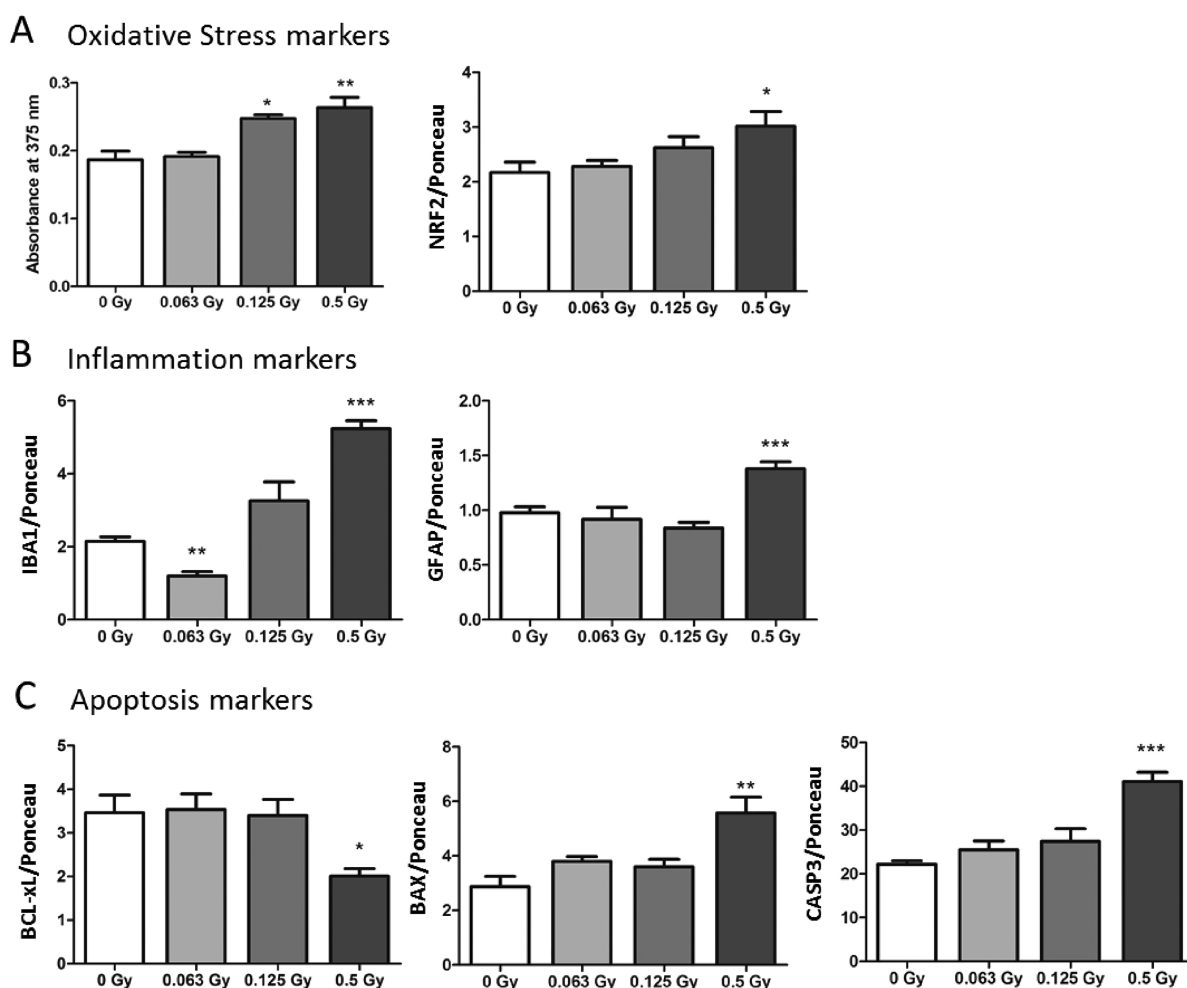


Figure 4. Radiation-induced changes in oxidative stress, inflammation, and apoptosis in the hippocampus. (A) The levels of carbonylated (oxidized) proteins (colorimetric assay) and NRF2 (immunoblotting) assessed in the hippocampus of control and irradiated mice are shown. (B) The levels of activated microglia (IBA1) and reactive astrocytes (GFAP) using immunoblotting are shown. (C) The levels of BCL-xL (antiapoptotic), BAX (proapoptotic), and cleaved CASP3 (proapoptotic) analyzed using immunoblotting are shown. Error bars represent the SEM, $n = 4$, * $p < 0.05$, ** $p < 0.01$, *** $p < 0.001$ (Student's t test).

deregulated proteins in comparison to the control group: 448 in the 0.063 Gy group, 668 in the 0.125 Gy group, and 103 in the 0.5 Gy group (Tables S6–S8). The total numbers of up- and down-regulated proteins for each experimental group are presented in Figure 1C. Shared deregulated proteins between all experimental groups are shown in the Venn diagram in Figure 1D.

Irradiation Affects Biological Pathways Related to Synaptic Plasticity and Neuroprotection

The pathway analysis showed that irradiation affected CREB signaling and the pathways upstream or downstream of CREB (Figure 2A). The ephrin receptor, opioid, neuregulin, and NGF signaling are all upstream regulators of CREB, each involving ligands that bind to corresponding receptors (ErbB, TRK, and G-coupled receptors) activating kinase cascades.^{22–24} These kinases phosphorylate CREB inducing the transcription of target genes, which in turn are involved in the affected downstream pathways: long-term potentiation (LTP), long-term depression (LTD), synaptogenesis, and amyloid processing. All affected canonical pathways are essential for synaptic plasticity and neuroprotection. The two lowest dose groups showed positive z -scores for all these pathways (orange color), indicating radiation-induced activation. In contrast, the high-dose group

showed negative z -scores for nine of the most important pathways, indicating deactivation (blue color) (Figure 2A).

Similarly, to investigate which biofunctions are affected by irradiation, all deregulated proteins were analyzed for neuronal functions and apoptosis using IPA (Figure 2B). An inhibition of apoptosis was predicted especially for the medium-dose group, in contrast to moderate activation in the high-dose group. In line with the canonical pathway analysis, LTP and related functions such as learning, conditioning, and cognition were activated by the two lowest dose groups but inhibited by the high-dose group.

Immunoblotting Confirms Long-Term Changes of the CREB Pathway

The levels of total and phosphorylated forms of CREB and its upstream regulators p38 and ERK1/2 were measured (Figure 3, Figure S1). The CREB phosphorylation (Ser133) was increased at the two lowest doses but markedly decreased at the highest dose (Figure 3A). No difference was seen in the total protein amount of CREB (Figure 3A).

In the case of the upstream kinase p38, both the levels of total and the phosphorylated form (Thr180/Tyr182) were increased at the lowest doses but decreased at 0.5 Gy (Figure 3B). Similarly, the total and the phosphorylated levels of ERK1/2

(Thr202/Tyr204) were increased at 0.063 Gy and at 0.125 Gy but decreased at 0.5 Gy (Figure 3C).

The expression of three target proteins of CREB, c-FOS, ARC, and PSD-95, were also measured to investigate the transcriptional activity of CREB (Figure S1, Figure S2). All three proteins showed significant upregulation at the medium dose, and c-FOS also at the lowest dose. No changes were seen at the highest dose.

Oxidative Stress, Inflammation, and Apoptosis Show Dose-Dependent Alteration

High-dose radiation as well as normal aging process lead to increase in oxidative stress in the brain.^{25,26} Protein carbonyl modifications, a major hallmark of oxidative stress, were measured in different dose groups to elucidate alterations in reactive oxygen species (ROS) levels. A dose-dependent increase in carbonylated proteins was observed in the medium- (0.125 Gy) and high-dose (0.5 Gy) group (Figure 4A, Table S9). The expression of nuclear factor erythroid 2-related factor 2 (NRF2), a central regulator of cellular antioxidant capacity, showed a significant 1.4-fold increase in the highest dose group (Figure 4A, Figure S1).

Chronic increase in oxidative stress is associated with activation of the innate immune system of the brain.²⁷ To investigate this, we measured the level of activated microglia as a marker of pro-inflammatory response using IBA1 staining (Figure 4B, Figure S1). Interestingly, the number of activated microglia was reduced at the lowest dose suggesting an anti-inflammatory effect. In contrast, the number of activated microglia was markedly enhanced at the highest dose indicating increased inflammation. Similarly, the number of reactive astroglia (GFAP) was increased at the highest dose suggesting astrogliosis (Figure 4B, Figure S1).

Since the dose of 0.5 Gy was predicted by the proteomics data to induce apoptosis (Figure 2B), we next measured changes in the expression of apoptotic markers. BCL-xL protein, a target of the transcription factor CREB, is an antiapoptotic factor that is able to suppress pro-apoptotic proteins such as BAX and cleaved caspase 3 (CASP3). Immunoblot analysis showed that the dose of 0.5 Gy, but not the lower doses, had a significant effect on the expression of apoptotic markers (Figure 4C, Figure S1). The level of BCL-xL was decreased by 1.7-fold, while the expression of pro-apoptotic BAX and CASP3 was markedly increased, indicating the presence of cells undergoing apoptosis.

Taken together, these results show that a single total body dose of 0.5 Gy is able to induce oxidative stress, inflammation, and apoptosis in the hippocampus two years after the exposure, possibly due to inactivation of the CREB pathway.

DISCUSSION

In this study, we have shown that relatively low exposures to IR, comparable to those received by clinical diagnostics and therapy, have a marked impact on the murine hippocampal proteome two years later. In general, the two most common cell types in the brain, and probably also in the hippocampus, are neurons and different glial cells.²⁸ The ratio of neurons to glial cells in the hippocampus is approximately 1:2, while the volumetric ratio is around 1:1.²⁹ The observed alterations in the proteome profiles could arise from either one, or both, of these cell populations.

Radiation-induced proteome changes indicated alterations especially in the CREB signaling and related neurocognitive pathways such as LTP and learning. Importantly, the highest dose used in this study (0.5 Gy) influenced these pathways in an

opposite manner to the lower doses (0.063 Gy, 0.125 Gy), namely by inhibition. In similarly treated B6C3F1 mice, significant behavioral defects were observed 18 m after the radiation exposure in the 0.5 Gy group, whereas no or even opposite effects (increased ASR and rearing) emerged at this age in the lowest-dose group.³⁰

CREB-mediated transcription is essential for synaptic plasticity and neuroprotective response to pathophysiological stressors.^{31,32} The transcriptional activity of CREB is regulated by phosphorylation on Ser133 by several kinases, in the brain mainly by p38 and ERK1/2.^{22–24} At the lower doses (0.063 Gy, 0.125 Gy) we showed an increase in the total and phosphorylated forms of both of these upstream kinases as well as increased phosphorylation (activation) of CREB itself. This was accompanied by upregulation of three downstream targets of CREB, c-FOS, ARC, and PSD-95. In contrast, after the highest exposure (0.5 Gy) the expression of these kinases as well as phospho-CREB was decreased. This, however, was not mirrored by changes in the expression of the three target proteins tested, probably due to other regulatory factors and processes that are known to be required for the transcriptional attenuation of CREB downstream targets.^{33,34}

Several studies have previously investigated radiation-induced changes in the CREB expression in hippocampus. Neonatal C57BL/6 mice were exposed to fractionated (20 × 0.1 Gy) low-dose radiation and the hippocampal proteome was investigated at different time points ranging from 72 h to 6 months.¹⁰ The immunoblot analysis showed a marked upregulation of CREB and phospho-CREB as well as its downstream targets BDNF and ARC at 3 months, while no upregulation of phospho-CREB, BDNF, or ARC was seen at 6 months.¹⁰ In another study using neonatally exposed male NMRI mice the expression of CREB, ARC, and c-FOS was significantly downregulated 7 months after a total body irradiation (1.0 Gy).⁵ These mice showed significant and persistent impairment in spontaneous behavior in a novel home environment already 2 months postradiation. Similarly, total CREB, phospho-CREB, and ARC were downregulated in the hippocampus after irradiating 8-week old female C57BL/6 ApoE^{-/-} mice for 300 days using low-dose-rate exposure with cumulative doses of 0.3 or 6.0 Gy.³⁵ In utero irradiation using X-ray doses of 0.1, 0.5, or 1.0 Gy led to a decrease in the level of phospho-CREB in the male C57Bl/6J offspring 6 months after the exposure.³⁶ Taken together, these data suggest that ionizing radiation may induce or inhibit the CREB expression depending on the dose, dose rate, and age at exposure.

It is widely accepted that high-dose radiation, as used in the therapy of brain tumors, leads to an accumulation of long-lived free radicals in the brain.²⁵ This study shows that a much lower dose than used in radiation therapy (0.5 Gy) is associated with oxidative stress that is indicated by increased levels of oxidized proteins and NRF2. This could be related to the radiation-induced downregulation of active CREB observed here since experiments using a CREB transgenic mouse model³⁷ or siRNA knockdown of CREB in human neuronal cells³⁸ have shown that active CREB is essential in the neuroprotective signaling against ROS-mediated cell toxicity. Consequently, artificial upregulation of CREB signaling could have neuroprotective effects.³⁹ In contrast, inhibition of CREB reduces neuronal plasticity and triggers neuronal cell death via pro-apoptotic processes.^{40,41} In line with this, our proteomics data also indicated ongoing apoptosis at 0.5 Gy that was confirmed using anti- and pro-apoptotic markers.

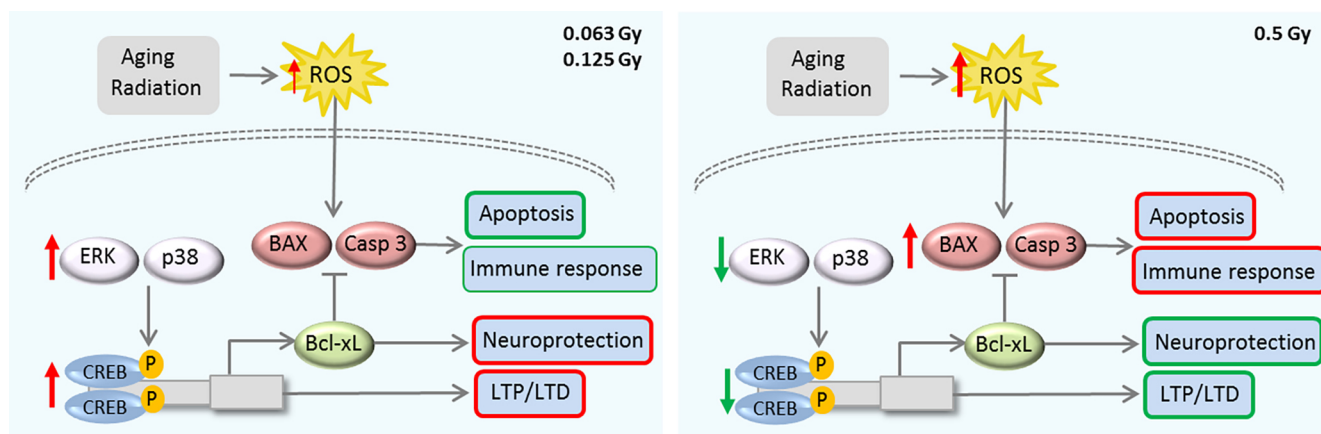


Figure 5. A proposed model for the role of CREB signaling in the long term (24 months) radiation response in the hippocampus based on the study data. The lower doses (0.063 Gy, 0.125 Gy) (shown on the left) have an activating effect on this pathway, while the higher dose (0.5 Gy) functions as deactivating (shown on the right). The radiation-induced changes in the expression of upstream regulators and downstream targets of this pathway are shown with red (up-regulation) or green (down-regulation) arrows.

The low-dose radiation (0.063 Gy) resulted in an anti-inflammatory effect in the hippocampus. This result is in agreement with previous data using mice that were chronically irradiated with a very low dose rate (1 mGy/d) for 300 days resulting in a cumulative dose of 0.3 Gy.³⁵ A reduced number of IBA1-positive microglia was found in the molecular layer of the hippocampus of these mice.³⁵ However, radiation-induced ROS accumulation at high doses has been shown to induce pro-inflammatory reaction via glia activation,^{42–44} especially when old animals were exposed to radiation.⁴⁵ In this study, the group exposed to 0.5 Gy showed increased level of IBA1-positive cells. In addition, an increase in the number of reactive astrocytes was seen in this group further suggesting enhanced inflammatory status of the hippocampus. Persistently activated microglia have been shown to produce ROS that may play a role in the progression of neurodegenerative diseases.⁴⁶ This could partly explain the increase in oxidized protein level seen in this study.

In conclusion, we show that a single exposure to a dose of 0.5 Gy leads to increased oxidative stress, inflammation, and apoptosis in the hippocampus (Figure 5). These impairments resemble those seen in normal brain aging. With increasing age, the ability to adequately respond to oxidative stress reduces.⁴⁷ Consequently, the accumulation of free radicals leads to a higher susceptibility to neurodegenerative diseases.^{48,49} Age-dependent CREB dysregulation has been correlated with neurodegenerative disorders like Alzheimer's disease, Parkinson's disease, and Huntington's disease.^{50–52} Importantly, in this study, radiation effects were first seen when the mice reached an advanced age corresponding that of approximately 70 years in humans.⁵³ This indirectly suggests that moderate radiation doses, comparable to those received from repeated CT scans² and much lower than received in radiation therapy of many cancers,^{54–56} may accelerate the normal aging process in the brain. Previous studies using considerably higher doses (2–10 Gy) than here have indicated radiation-induced aging-like pathology in cerebral cortical cells⁵⁷ and in activated microglia.⁵⁸ The study presented here is to our knowledge the first one suggesting radiation-induced accelerated aging to occur at a much lower radiation dose.

■ ASSOCIATED CONTENT

📄 Supporting Information

The Supporting Information is available free of charge on the ACS Publications website at DOI: 10.1021/acs.jproteome.9b00552.

Table S1: All significantly ($q \leq 0.05$) deregulated (fold-change ± 1.3) proteins for all measurements (4, 12, 18, and 24 months); Table S2: All identified proteins at 24 months; Table S3: All quantified proteins with an identification based on at least two UP for the low-dose (0.063 Gy) group; Table S4: All quantified proteins with an identification based on at least two UP for the medium-dose (0.125 Gy) group; Table S5: All quantified proteins with an identification based on at least two UP for the high-dose (0.5 Gy) group; Table S6: All deregulated proteins in the low-dose (0.063 Gy) group; Table S7: All deregulated proteins in the medium-dose (0.125 Gy) group; Table S8: All deregulated proteins in the high-dose (0.5 Gy) group; Table S9: Raw data of the carbonylation and BCA assay (XLS)

Figure S1: Western blots with corresponding Ponceau-stained gels; Figure S2: Western blots of the downstream targets of CREB (PDF)

■ AUTHOR INFORMATION

Corresponding Author

*Phone: +49 89 3187 3445. E-mail: soile.tapio@helmholtz-muenchen.de.

ORCID

Stefanie M. Hauck: 0000-0002-1630-6827

Omid Azimzadeh: 0000-0001-8984-0388

Soile Tapio: 0000-0001-9860-3683

Notes

The authors declare no competing financial interest.

■ ACKNOWLEDGMENTS

The research leading to these results received funding from the Federal Ministry of Education and Research (BMBF) under the reference numbers 02NUK045A, 02NUK045B, and 02NUK045C (INSTRA). We thank Stefanie Winkler for

excellent technical assistance in experiments and graphics, Dr. Stefan Kempf and Dr. Lillian Garrett for their help in the tissue collection, and Dr. Sabine Hölter-Koch for discussions about the behavioral results.

REFERENCES

- (1) Smith-Bindman, R.; Miglioretti, D. L.; Larson, E. B. Rising use of diagnostic medical imaging in a large integrated health system. *Health Aff (Millwood)* **2008**, *27*, 1491–1502.
- (2) Tonolini, M.; Valconi, E.; Vanzulli, A.; Bianco, R. Radiation overexposure from repeated CT scans in young adults with acute abdominal pain. *Emerg Radiol* **2018**, *25*, 21–27.
- (3) Kempf, S. J.; Azimzadeh, O.; Atkinson, M. J.; Tapio, S. Long-term effects of ionising radiation on the brain: cause for concern? *Radiat. Environ. Biophys.* **2013**, *52*, 5–16.
- (4) Hladik, D.; Tapio, S. Effects of ionizing radiation on the mammalian brain. *Mutat. Res., Rev. Mutat. Res.* **2016**, *770*, 219–230.
- (5) Kempf, S. J.; Casciati, A.; Buratovic, S.; Janik, D.; von Toerne, C.; Ueffing, M.; Neff, F.; Moertl, S.; Stenerlow, B.; Saran, A.; Atkinson, M. J.; Eriksson, P.; Pazzaglia, S.; Tapio, S. The cognitive defects of neonatally irradiated mice are accompanied by changed synaptic plasticity, adult neurogenesis and neuroinflammation. *Mol. Neurodegener.* **2014**, *9*, 57.
- (6) Eriksson, P.; Buratovic, S.; Fredriksson, A.; Stenerlow, B.; Sundell-Bergman, S. Neonatal exposure to whole body ionizing radiation induces adult neurobehavioural defects: Critical period, dose–response effects and strain and sex comparison. *Behav. Brain Res.* **2016**, *304*, 11–19.
- (7) Bliss, T. V.; Collingridge, G. L. A synaptic model of memory: long-term potentiation in the hippocampus. *Nature* **1993**, *361*, 31–39.
- (8) Kempf, S. J.; Sepe, S.; von Toerne, C.; Janik, D.; Neff, F.; Hauck, S. M.; Atkinson, M. J.; Mastroberardino, P. G.; Tapio, S. Neonatal Irradiation Leads to Persistent Proteome Alterations Involved in Synaptic Plasticity in the Mouse Hippocampus and Cortex. *J. Proteome Res.* **2015**, *14*, 4674–4686.
- (9) Casciati, A.; Dobos, K.; Antonelli, F.; Benedek, A.; Kempf, S. J.; Belles, M.; Balogh, A.; Tanori, M.; Heredia, L.; Atkinson, M. J.; von Toerne, C.; Azimzadeh, O.; Saran, A.; Safrany, G.; Benotmane, M. A.; Linares-Vidal, M. V.; Tapio, S.; Lumniczky, K.; Pazzaglia, S. Age-related effects of X-ray irradiation on mouse hippocampus. *Oncotarget* **2016**, *7*, 28040–28058.
- (10) Schmal, Z.; Isermann, A.; Hladik, D.; von Toerne, C.; Tapio, S.; Rube, C. E. DNA damage accumulation during fractionated low-dose radiation compromises hippocampal neurogenesis. *Radiother. Oncol.* **2019**, *137*, 45–54.
- (11) Averbeck, D.; Salomaa, S.; Bouffler, S.; Ottolenghi, A.; Smyth, V.; Sabatier, L. Progress in low dose health risk research: Novel effects and new concepts in low dose radiobiology. *Mutat. Res., Rev. Mutat. Res.* **2018**, *776*, 46–69.
- (12) Mothersill, C.; Seymour, C. Changing paradigms in radiobiology. *Mutat. Res., Rev. Mutat. Res.* **2012**, *750*, 85–95.
- (13) Brooks, A. L. Paradigm shifts in radiation biology: their impact on intervention for radiation-induced disease. *Radiat. Res.* **2005**, *164*, 454–461.
- (14) Tapio, S.; Jacob, V. Radioadaptive response revisited. *Radiat. Environ. Biophys.* **2007**, *46*, 1–12.
- (15) Ebrahimian, T. G.; Beugnieux, L.; Surette, J.; Priest, N.; Gueguen, Y.; Gloaguen, C.; Benderitter, M.; Jourdain, J. R.; Tack, K. Chronic Exposure to External Low-Dose Gamma Radiation Induces an Increase in Anti-inflammatory and Anti-oxidative Parameters Resulting in Atherosclerotic Plaque Size Reduction in ApoE(–/–) Mice. *Radiat. Res.* **2018**, *189*, 187–196.
- (16) Azzam, E. I.; Colangelo, N. W.; Domogauer, J. D.; Sharma, N.; de Toledo, S. M. Is Ionizing Radiation Harmful at any Exposure? An Echo That Continues to Vibrate. *Health Phys.* **2016**, *110*, 249–251.
- (17) Dalke, C.; Neff, F.; Bains, S. K.; Bright, S.; Lord, D.; Reitmeir, P.; Rossler, U.; Samaga, D.; Unger, K.; Braselmann, H.; Wagner, F.; Greiter, M.; Gomolka, M.; Hornhardt, S.; Kunze, S.; Kempf, S. J.; Garrett, L.; Holter, S. M.; Wurst, W.; Rosemann, M.; Azimzadeh, O.; Tapio, S.; Aubele, M.; Theis, F.; Hoeschen, C.; Slijepcevic, P.; Kadhim, M.; Atkinson, M.; Zitzelsberger, H.; Kulka, U.; Graw, J. Lifetime study in mice after acute low-dose ionizing radiation: a multifactorial study with special focus on cataract risk. *Radiat. Environ. Biophys.* **2018**, *57*, 99–113.
- (18) Wisniewski, J. R.; Zougman, A.; Nagaraj, N.; Mann, M. Universal sample preparation method for proteome analysis. *Nat. Methods* **2009**, *6*, 359–362.
- (19) Grosche, A.; Hauser, A.; Lepper, M. F.; Mayo, R.; von Toerne, C.; Merl-Pham, J.; Hauck, S. M. The Proteome of Native Adult Muller Glial Cells From Murine Retina. *Mol. Cell. Proteomics* **2016**, *15*, 462–480.
- (20) Schneider, C. A.; Rasband, W. S.; Eliceiri, K. W. NIH Image to ImageJ: 25 years of image analysis. *Nat. Methods* **2012**, *9*, 671–675.
- (21) Perez-Riverol, Y.; Csordas, A.; Bai, J.; Bernal-Llinares, M.; Hewapathirana, S.; Kundu, D. J.; Inuganti, A.; Griss, J.; Mayer, G.; Eisenacher, M.; Perez, E.; Uszkoreit, J.; Pfeuffer, J.; Sachsenberg, T.; Yilmaz, S.; Tiwary, S.; Cox, J.; Audain, E.; Walzer, M.; Jarnuczak, A. F.; Ternent, T.; Brazma, A.; Vizcaino, J. A. The PRIDE database and related tools and resources in 2019: improving support for quantification data. *Nucleic Acids Res.* **2019**, *47*, D442–d450.
- (22) Gonzalez, G. A.; Montminy, M. R. Cyclic AMP stimulates somatostatin gene transcription by phosphorylation of CREB at serine 133. *Cell* **1989**, *59*, 675–680.
- (23) Zhu, G.; Liu, Y.; Zhi, Y.; Jin, Y.; Li, J.; Shi, W.; Liu, Y.; Han, Y.; Yu, S.; Jiang, J.; Zhao, X. PKA- and Ca(2+)-dependent p38 MAPK/CREB activation protects against manganese-mediated neuronal apoptosis. *Toxicol. Lett.* **2019**, *309*, 10–19.
- (24) Medina, J. H.; Viola, H. ERK1/2: A Key Cellular Component for the Formation, Retrieval, Reconsolidation and Persistence of Memory. *Front. Mol. Neurosci.* **2018**, *11*, 361.
- (25) Kim, J. H.; Brown, S. L.; Jenrow, K. A.; Ryu, S. Mechanisms of radiation-induced brain toxicity and implications for future clinical trials. *J. Neuro-Oncol.* **2008**, *87*, 279–286.
- (26) Stefanatos, R.; Sanz, A. The role of mitochondrial ROS in the aging brain. *FEBS Lett.* **2018**, *592*, 743–758.
- (27) Regen, F.; Hellmann-Regen, J.; Costantini, E.; Reale, M. Neuroinflammation and Alzheimer's Disease: Implications for Microglial Activation. *Curr. Alzheimer Res.* **2017**, *14*, 1140–1148.
- (28) Keller, D.; Ero, C.; Markram, H. Cell Densities in the Mouse Brain: A Systematic Review. *Front. Neuroanat.* **2018**, *12*, 83.
- (29) Oliveira-da-Silva, A.; Vieira, F. B.; Cristina-Rodrigues, F.; Filgueiras, C. C.; Manhaes, A. C.; Abreu-Villaca, Y. Increased apoptosis and reduced neuronal and glial densities in the hippocampus due to nicotine and ethanol exposure in adolescent mice. *Int. J. Dev. Neurosci.* **2009**, *27*, 539–548.
- (30) Ung, M.-C.; Garrett, L.; Dalke, C.; Leitner, V.; Hladik, D.; Neff, F.; Wagner, F.; Zitzelsberger, H.; Miller, G.; Hrabě de Angelis, M.; Rößler, U.; Vogt Weisenhorn, D.; Wurst, W.; Graw, J.; Hölter, S. Long-term effects of a single low-dose radiation event on behavior and microglia. *Mol. Neurobiol.* **2019**, submitted.
- (31) Sakamoto, K.; Karelina, K.; Obrietan, K. CREB: a multifaceted regulator of neuronal plasticity and protection. *J. Neurochem.* **2011**, *116*, 1–9.
- (32) Walton, M. R.; Dragunow, I. Is CREB a key to neuronal survival? *Trends Neurosci.* **2000**, *23*, 48–53.
- (33) Bateman, E. Autoregulation of eukaryotic transcription factors. *Prog. Nucleic Acid Res. Mol. Biol.* **1998**, *60*, 133–168.
- (34) Ortega-Martinez, S. A new perspective on the role of the CREB family of transcription factors in memory consolidation via adult hippocampal neurogenesis. *Front. Mol. Neurosci.* **2015**, *8*, 46.
- (35) Kempf, S. J.; Janik, D.; Barjaktarovic, Z.; Braga-Tanaka, I., 3rd; Tanaka, S.; Neff, F.; Saran, A.; Larsen, M.; Tapio, S. Chronic low-dose-rate ionising radiation affects the hippocampal phosphoproteome in the ApoE(–/–) Alzheimer's mouse model. *Oncotarget* **2016**, *7*, 71817–71832.
- (36) Kempf, S. J.; von Toerne, C.; Hauck, S. M.; Atkinson, M. J.; Benotmane, M. A.; Tapio, S. Long-term consequences of in utero

irradiated mice indicate proteomic changes in synaptic plasticity related signalling. *Proteome Sci.* **2015**, *13*, 26.

(37) Lee, B.; Cao, R.; Choi, Y. S.; Cho, H. Y.; Rhee, A. D.; Hah, C. K.; Hoyt, K. R.; Obrietan, K. The CREB/CRE transcriptional pathway: protection against oxidative stress-mediated neuronal cell death. *J. Neurochem.* **2009**, *108*, 1251–1265.

(38) Pregi, N.; Belluscio, L. M.; Berardino, B. G.; Castillo, D. S.; Canepa, E. T. Oxidative stress-induced CREB upregulation promotes DNA damage repair prior to neuronal cell death protection. *Mol. Cell. Biochem.* **2017**, *425*, 9–24.

(39) Kang, H.; Khang, R.; Ham, S.; Jeong, G. R.; Kim, H.; Jo, M.; Lee, B. D.; Lee, Y. I.; Jo, A.; Park, C.; Kim, H.; Seo, J.; Paek, S. H.; Lee, Y. S.; Choi, J. Y.; Lee, Y.; Shin, J. H. Activation of the ATF2/CREB-PGC-1 α pathway by metformin leads to dopaminergic neuroprotection. *Oncotarget* **2017**, *8*, 48603–48618.

(40) Ao, H.; Ko, S. W.; Zhuo, M. CREB activity maintains the survival of cingulate cortical pyramidal neurons in the adult mouse brain. *Mol. Pain* **2006**, *2*, 15.

(41) Jancic, D.; Lopez de Armentia, M.; Valor, L. M.; Olivares, R.; Barco, A. Inhibition of cAMP response element-binding protein reduces neuronal excitability and plasticity, and triggers neurodegeneration. *Cereb Cortex* **2009**, *19*, 2535–2547.

(42) Lumniczky, K.; Szatmari, T.; Safrany, G. Ionizing Radiation-Induced Immune and Inflammatory Reactions in the Brain. *Front. Immunol.* **2017**, *8*, 517.

(43) Kettenmann, H.; Kirchhoff, F.; Verkhratsky, A. Microglia: new roles for the synaptic stripper. *Neuron* **2013**, *77*, 10–18.

(44) Cucinotta, F. A.; Cacao, E. Risks of cognitive detriments after low dose heavy ion and proton exposures. *Int. J. Radiat. Biol.* **2019**, *95*, 985–998.

(45) Schindler, M. K.; Forbes, M. E.; Robbins, M. E.; Riddle, D. R. Aging-dependent changes in the radiation response of the adult rat brain. *Int. J. Radiat. Oncol., Biol., Phys.* **2008**, *70*, 826–834.

(46) Block, M. L.; Hong, J. S. Microglia and inflammation-mediated neurodegeneration: multiple triggers with a common mechanism. *Prog. Neurobiol.* **2005**, *76*, 77–98.

(47) Khan, S. S.; Singer, B. D.; Vaughan, D. E. Molecular and physiological manifestations and measurement of aging in humans. *Aging Cell* **2017**, *16*, 624–633.

(48) Wang, X.; Wang, W.; Li, L.; Perry, G.; Lee, H. G.; Zhu, X. Oxidative stress and mitochondrial dysfunction in Alzheimer's disease. *Biochim. Biophys. Acta, Mol. Basis Dis.* **2014**, *1842*, 1240–1247.

(49) Blesa, J.; Trigo-Damas, I.; Quiroga-Varela, A.; Jackson-Lewis, V. R. Oxidative stress and Parkinson's disease. *Front. Neuroanat.* **2015**, *9*, 91.

(50) Ma, Q. L.; Harris-White, M. E.; Ubeda, O. J.; Simmons, M.; Beech, W.; Lim, G. P.; Teter, B.; Frautschy, S. A.; Cole, G. M. Evidence of Abeta- and transgene-dependent defects in ERK-CREB signaling in Alzheimer's models. *J. Neurochem.* **2007**, *103*, 1594–1607.

(51) Gil, J. M.; Rego, A. C. Mechanisms of neurodegeneration in Huntington's disease. *Eur. J. Neurosci* **2008**, *27*, 2803–2820.

(52) Mantamadiotis, T.; Lemberger, T.; Bleckmann, S. C.; Kern, H.; Kretz, O.; Villalba, A. M.; Tronche, F.; Kellendonk, C.; Gau, D.; Kapfhammer, J.; Otto, C.; Schmid, W.; Schutz, G. Disruption of CREB function in brain leads to neurodegeneration. *Nat. Genet.* **2002**, *31*, 47–54.

(53) Dutta, S.; Sengupta, P. Men and mice: Relating their ages. *Life Sci.* **2016**, *152*, 244–248.

(54) Scoccianti, S.; Detti, B.; Gadda, D.; Greto, D.; Furfaro, I.; Meacci, F.; Simontacchi, G.; Di Brina, L.; Bonomo, P.; Giacomelli, I.; Meattini, I.; Mangoni, M.; Cappelli, S.; Cassani, S.; Talamonti, C.; Bordi, L.; Livi, L. Organs at risk in the brain and their dose-constraints in adults and in children: a radiation oncologist's guide for delineation in everyday practice. *Radiother. Oncol.* **2015**, *114*, 230–238.

(55) Berrington de Gonzalez, A.; Salotti, J. A.; McHugh, K.; Little, M. P.; Harbron, R. W.; Lee, C.; Ntowe, E.; Braganza, M. Z.; Parker, L.; Rajaraman, P.; Stiller, C.; Stewart, D. R.; Craft, A. W.; Pearce, M. S. Relationship between paediatric CT scans and subsequent risk of

leukaemia and brain tumours: assessment of the impact of underlying conditions. *Br. J. Cancer* **2016**, *114*, 388–394.

(56) Yeh, S. A. Radiotherapy for head and neck cancer. *Semin Plast Surg* **2010**, *24*, 127–136.

(57) Suman, S.; Rodriguez, O. C.; Winters, T. A.; Fornace, A. J., Jr.; Albanese, C.; Datta, K. Therapeutic and space radiation exposure of mouse brain causes impaired DNA repair response and premature senescence by chronic oxidant production. *Aging* **2013**, *5*, 607–622.

(58) Li, M. D.; Burns, T. C.; Kumar, S.; Morgan, A. A.; Sloan, S. A.; Palmer, T. D. Aging-like changes in the transcriptome of irradiated microglia. *Glia* **2015**, *63*, 754–767.

3.2 Combined treatment with low-dose ionizing radiation and ketamine induces adverse changes in CA1 neuronal structure in murine hippocampus

3.2.1 Aim and summary of the study

Ketamine is used as a sedative in paediatric medicine to ensure immobilization during motion-sensitive procedures such as diagnostic imaging and radiotherapy. It has been shown that a combination of ketamine and radiation exposure at clinically relevant doses in neonatal mice leads to cognitive impairment in later life (Buratovic et al., 2018). The aim of this study was to discover the molecular basis for this impairment. Male NMRI mice were treated with a single dose of ketamine (7.5 mg/kg) on PND 10. After one hour, these mice were exposed to low-dose whole body radiation (100 mGy, 200 mGy). For control, mice were included that were treated with either radiation alone, ketamine alone or were sham treated. After six months, hippocampi were harvested, and the proteome profile analysed with label-free LC-MS/MS. In parallel, histological analysis was performed to investigate changes in neuronal morphology. A sustained effect on the structure of CA1 hippocampal neurons, expressed as an increase in both the number of basal dendrites and their branching was discovered. In addition, the mean number of spines of the basal dendrites was decreased. Neither ketamine nor radiation alone induced these changes at the tested doses. Analysis of the proteome showed that pathways involved in learning and memory were impaired after the combined treatment. Central regulators such as brain-derived neurotrophic factor (BDNF), postsynaptic density protein 95 (PSD-95) and activity-regulated cytoskeleton-associated protein (ARC) were altered in the hippocampus of the mice showing structural changes. These proteins are known to regulate neuronal branching and spinogenesis and could therefore their deregulation could be the cause of the observed morphological alterations. The neonatal window of the brain development used in this study corresponds to the developmental period of the human brain that begins approximately in the third trimester of pregnancy and extends over the first two years of life. The results of this study are significant when one considers that the practice of ketamine anaesthesia during procedures necessitating radiation exposure is routinely applied in clinics worldwide and may have unforeseen consequences for brain development and function in children.

3.2.2 Contribution

For this study the treatments with ketamine or/and radiation were performed by Dr. Sonja Buratovic, Prof. Dr. Bo Stenerl w and Prof. Dr. Per Eriksson from the Department of Environmental Toxicology, Uppsala, Sweden. Dr. Christine von T rne (Helmholtz Proteomics Core Facility) performed the label-free LC-MS/MS runs and supported me in the label-free quantification of the peptides. I performed the brain sampling, hippocampal dissection and protein lysis. In addition, I carried out the bioinformatic analysis of the LC-MS/MS data, the Western blotting and the Golgi staining, including all calculations and interpretations. Mr. Jos Philipp assisted with the tissue collection and created the volcano blots. Miss Elenore Samson sectioned the Golgi stained hippocampi and Miss Stefanie Winkler assisted in the reconstruction of the CA1 neurons for structural analysis. I designed all the figures and wrote the manuscript with the help of Dr. Soile Tapio. The co-authors Dr. Omid Azimzadeh, Dr. Prabal Subedi, Dr. Soile Tapio and Prof. Dr. Michael J. Atkinson contributed to the study design, the scientific discussion, the interpretation of the data and in editing the final manuscript.

3.2.3 Publication

The data were presented in an original research paper published on December 3rd, 2019 in "International journal for molecular sciences":

Combined Treatment with Low dose Ionising Radiation and Ketamine Induces Adverse Changes in CA1 Neuronal Structure in Murine Hippocampus.

Daniela Hladik, Sonja Buratovic, Christine von Toerne, Omid Azimzadeh, Prabal Subedi, Jos Philipp, Stefanie Winkler, Annette Feuchtinger, Elenore Samson, Stefanie M. Hauck, Bo Stenerl w, Per Eriksson, Michael J. Atkinson and Soile Tapio

Int J Mol Sci. 2019 Dec 3. doi: 10.3390/ijms20236103 (Hladik et al., 2019)



Article

Combined Treatment with Low-Dose Ionizing Radiation and Ketamine Induces Adverse Changes in CA1 Neuronal Structure in Male Murine Hippocampi

Daniela Hladik ^{1,2}, Sonja Buratovic ³, Christine Von Toerne ⁴ , Omid Azimzadeh ¹, Prabal Subedi ¹, Jos Philipp ¹ , Stefanie Winkler ¹, Annette Feuchtinger ⁵, Elenore Samson ⁵, Stefanie M. Hauck ⁴ , Bo Stenerlöv ⁶, Per Eriksson ³, Michael J. Atkinson ^{1,2} and Soile Tapio ^{1,*}

¹ Institute of Radiation Biology, Helmholtz Zentrum München, German Research Center for Environmental Health GmbH (HMGU), 85764 Neuherberg, Germany; daniela.hladik@helmholtz-muenchen.de (D.H.); omid.azimzadeh@helmholtz-muenchen.de (O.A.); prabal.subedi@helmholtz-muenchen.de (P.S.); jos.philipp@helmholtz-muenchen.de (J.P.); stefanie.winkler@helmholtz-muenchen.de (S.W.); atkinson@helmholtz-muenchen.de (M.J.A.)

² Chair of Radiation Biology, Technical University Munich (TUM), 80333 Munich, Germany

³ Department of Environmental Toxicology, University Uppsala, 75236 Uppsala, Sweden; sonja.buratovic@ebc.uu.se (S.B.); per.eriksson@ebc.uu.se (P.E.)

⁴ Research Unit Protein Science, Helmholtz Zentrum München, German Research Center for Environmental Health GmbH (HMGU), 80939 Munich, Germany; vontoerne@helmholtz-muenchen.de (C.v.T.); hauck@helmholtz-muenchen.de (S.M.H.)

⁵ Research Unit Analytical Pathology, Helmholtz Zentrum München, German Research Center for Environmental Health GmbH (HMGU), 85764 Neuherberg, Germany; annette.feuchtinger@helmholtz-muenchen.de (A.F.); samson@helmholtz-muenchen.de (E.S.)

⁶ Department of Immunology, Genetics and Pathology, Uppsala University, 75185 Uppsala, Sweden; bo.stenerlow@igp.uu.se

* Correspondence: soile.tapio@helmholtz-muenchen.de; Tel.: +49-89-3187-3445

Received: 29 October 2019; Accepted: 2 December 2019; Published: 3 December 2019



Abstract: In children, ketamine sedation is often used during radiological procedures. Combined exposure of ketamine and radiation at doses that alone did not affect learning and memory induced permanent cognitive impairment in mice. The aim of this study was to elucidate the mechanism behind this adverse outcome. Neonatal male NMRI mice were administered ketamine (7.5 mg kg⁻¹) and irradiated (whole-body, 100 mGy or 200 mGy, ¹³⁷Cs) one hour after ketamine exposure on postnatal day 10. The control mice were injected with saline and sham-irradiated. The hippocampi were analyzed using label-free proteomics, immunoblotting, and Golgi staining of CA1 neurons six months after treatment. Mice co-exposed to ketamine and low-dose radiation showed alterations in hippocampal proteins related to neuronal shaping and synaptic plasticity. The expression of brain-derived neurotrophic factor, activity-regulated cytoskeleton-associated protein, and postsynaptic density protein 95 were significantly altered only after the combined treatment (100 mGy or 200 mGy combined with ketamine, respectively). Increased numbers of basal dendrites and branching were observed only after the co-exposure, thereby constituting a possible reason for the displayed alterations in behavior. These data suggest that the risk of radiation-induced neurotoxic effects in the pediatric population may be underestimated if based only on the radiation dose.

Keywords: hippocampus; proteomics; BDNF; CA1 neurons; dendrite abnormality; Golgi staining; irradiation

1. Introduction

Ionizing radiation is an integral part of medical treatment and diagnostics. In radiotherapy, healthy tissues outside the target volume are exposed to low-dose radiation. Therefore, the possibility of radiation-associated risks must be considered. This is especially so for children, since exposure to low doses of ionizing radiation is associated with increased risk of malignancies and cognitive impairment later in life [1–3].

In paediatric radiotherapy and imaging, sedation is often applied during imaging to ensure immobilization [4,5]. Ketamine exerts sedative properties via blockage of the N-methyl-D-aspartate (NMDA) receptors in the brain. These ionotropic glutamate receptors are involved in synaptic plasticity, learning, and memory [6–8]. Ketamine exposure during early brain development has been shown to induce neurodegeneration, followed by cognitive impairment [9–11].

The effects of combined exposure to clinically relevant doses of ketamine (7.5 mg kg⁻¹ body weight) and whole-body low-dose radiation (100 mGy, 200 mGy) during brain development were studied in mice [12]. The co-exposed mice showed lack of habituation, hyperactivity, and reduced learning and memory capabilities, while mice exposed to single agents showed no significant differences in behavior compared to non-exposed controls. A combination of drug and irradiation consistently impaired cognitive function [12].

The aim of this study was to elucidate molecular mechanisms that could be associated with the previously observed cognitive impairment. Therefore, we used mice that were treated identically to the previous experiment [12]. We found that the combination of low-dose radiation and ketamine consistently changed the hippocampal proteome. The combination treatment altered the structure of CA1 neurons, while individual treatments did not display this effect. Neuronal morphology, such as dendrite complexity and spine density, are strongly correlated with neuronal function. Therefore, these observations provide a plausible mechanistic reasoning for the detrimental interaction of ketamine and radiation in the developing brain of newborn mammals.

2. Results

2.1. Analysis of the Hippocampal Proteome after Single or Combined Treatment

The hippocampal proteomes of all of the mice were analyzed using label-free LC/MS-MS. In total, 2668 proteins were identified, of which 1839 were quantified based on at least two unique peptides (UP) (Tables S1–S5). Volcano plots of all quantified proteins showed the distribution of nonregulated and deregulated proteins (Figure 1B). Using the filtering criteria (identification with two UP, $p \leq 0.05$, fold-change ± 1.3) the analysis showed the following numbers of significantly deregulated proteins in comparison to the control group: 103 in the ketamine (Ket) group, 144 in the 100 mGy group, 122 in the 200 mGy group, 164 in the 100 mGy Ket group, and 157 in the 200 mGy Ket group (Figure 1C). Shared deregulated proteins in the different experimental groups are shown in the Venn diagram in Figure 1D. The two co-exposure groups shared 55 deregulated proteins (Figure 1D). These are listed alongside the fold-changes and GO biological functions in Table 1. The majority of these proteins were classified as members of actin cytoskeleton organization or neuronal development.

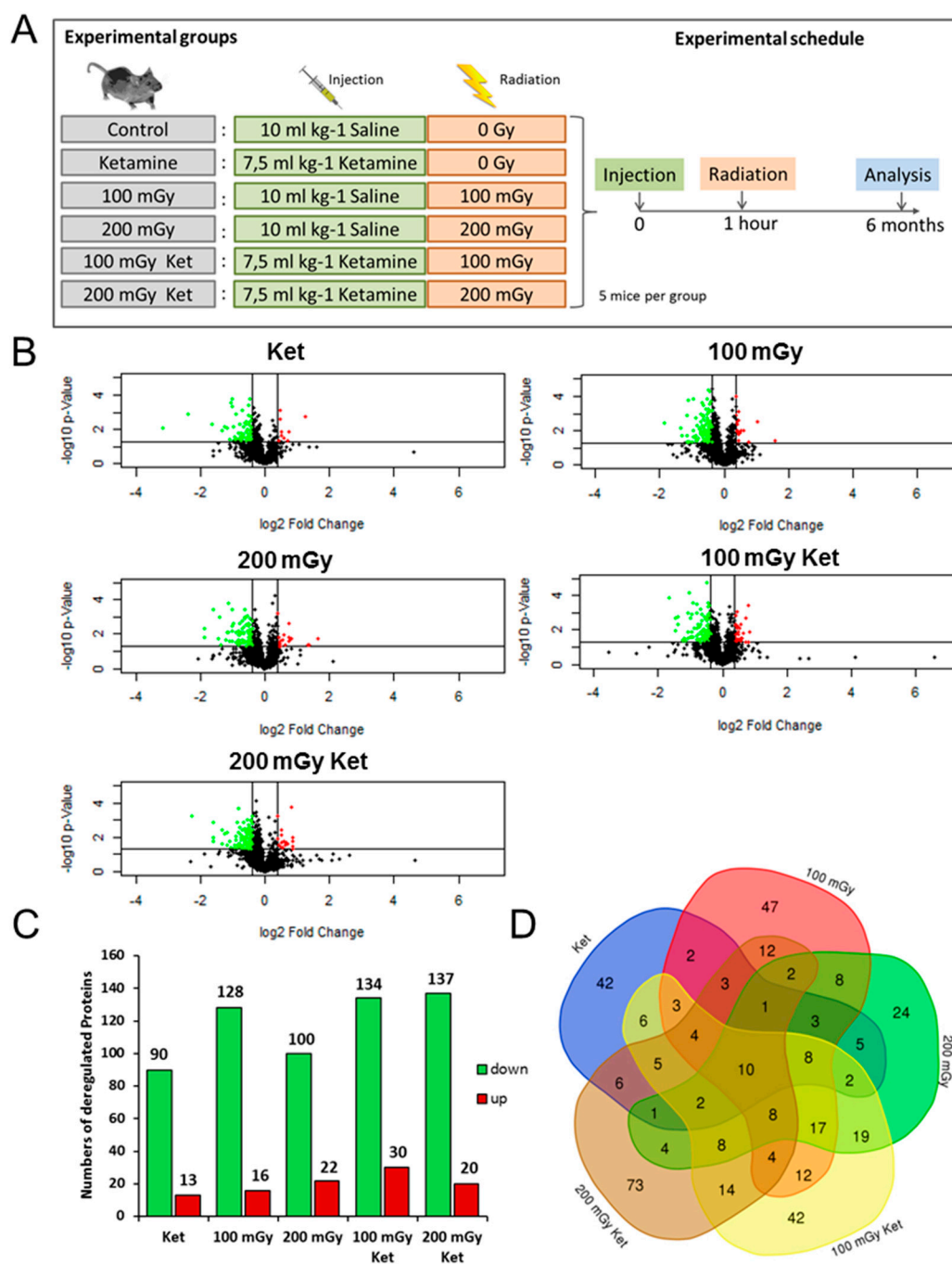


Figure 1. Changes in the hippocampal proteome after single treatment or co-treatment. **(A)** Schematic presentation of the experimental groups and the treatment schedule. **(B)** Volcano plots representing the distribution of all quantified proteins (identification with at least two UP) in hippocampi exposed to single treatment with ketamine (Ket), gamma radiation (100 mGy, 200 mGy), or combined treatment (100 mGy Ket, 200 mGy Ket). Deregulated proteins ($p \leq 0.05$, fold-change ± 1.3) are highlighted in green (downregulated) and red (upregulated). **(C)** Total numbers of significantly downregulated (green) and upregulated (red) proteins are shown for all treatments ($p \leq 0.05$, fold-change ± 1.3). **(D)** Venn diagram illustrating the number of shared deregulated proteins between the five experimental groups.

Table 1. Significantly deregulated proteins shared in the combined treatment groups with ketamine and irradiation.

	Symbol	Entrez Gene Name	Fold-Change		Biological Function	GO Number
			100 mGy Ket	200 mGy Ket		
1	ABHD10	abhydrolase domain containing 10	−2.014	−1.602	glucuronoside catabolic process	GO:0019391
2	ACAN	aggrecan	−2.742	−3.063	negative regulation of cell migration	GO:0030336
3	ADAM11	ADAM metallopeptidase domain 11	−1.344	−1.622	proteolysis	GO:0006508
4	ADAM23	ADAM metallopeptidase domain 23	−1.325	−1.409	proteolysis	GO:0006508
5	ARF6	ADP ribosylation factor 6	−1.432	−1.365	regulation of dendritic spine development	GO:0060998
6	ARMC1	armadillo repeat containing 1	−2.059	−1.752	metal ion transport	GO:0030001
7	ARPC1A	actin related protein 2/3 complex subunit 1A	1.358	1.515	regulation of actin filament polymerization	GO:0030833
8	ASPA	aspartoacylase	1.406	1.575	positive regulation of oligodendrocyte differentiation	GO:0048714
9	BRSK2	BR serine/threonine kinase 2	−1.680	−1.829	neuron differentiation	GO:0030182
10	CBR3	carbonyl reductase 3	−1.478	−1.577	cognition	GO:0050890
11	CDC42	cell division cycle 42	−1.588	−1.474	modification of synaptic structure	GO:0099563
12	CRK	CRK proto-oncogene adaptor protein	−1.948	−2.240	dendrite development	GO:0016358
13	DNAJC6	DnaJ heat shock protein family (Hsp40) member C6	−1.381	−1.484	synaptic vesicle uncoating	GO:0016191
14	DYNLL2	dynein light chain LC8-type 2	−1.316	−1.329	microtubule-based process	GO:0007017
15	ELMO2	engulfment and cell motility 2	−2.612	−2.402	cytoskeleton organization	GO:0007010
16	FBXO2	F-box protein 2	−1.503	−1.307	regulation of protein ubiquitination	GO:0031396
17	GDPD1	glycerophosphodiester phosphodiesterase domain containing 1	−1.286	−1.293	N-acyl ethanolamine metabolic process	GO:0070291
18	GGT7	gamma-glutamyltransferase 7	−2.601	−4.805	regulation of response to oxidative stress	GO:1902883
19	GUK1	guanylate kinase 1	−1.496	−1.412	ATP metabolic process	GO:0046034
20	HIST1H2BD	histone cluster 1 H2B family member d	1.562	1.515	protein ubiquitination	GO:0016567
21	HNRNPUL1	heterogeneous nuclear ribonucleoprotein U like 1	−3.209	−1.488	RNA processing	GO:0006396
22	HTT	huntingtin	−1.862	−1.686	learning or memory	GO:0007611
23	IPO5	importin 5	−1.568	−1.478	protein import into nucleus	GO:0006606
24	MICU3	mitochondrial calcium uptake family member 3	−1.285	−1.484	mitochondrial calcium ion transmembrane transport	GO:0006851
25	NACA	nascent polypeptide associated complex subunit alpha	−1.297	−1.290	positive regulation of nucleic acid-templated transcription	GO:1903508

Table 1. Cont.

	Symbol	Entrez Gene Name	Fold-Change		Biological Function	GO Number
			100 mGy Ket	200 mGy Ket		
26	NDRG2	NDRG family member 2	-1.295	-1.326	nervous system development	GO:0001818
27	NIF3L1	NGG1 interacting factor 3 like 1	-1.649	-1.671	neuron differentiation	GO:0030182
28	NRP1	neuropilin 1	-1.935	-2.487	axon guidance	GO:0007411
29	OCIAD1	OClA domain containing 1	1.529	1.818	regulation of stem cell differentiation	GO:2000736
30	PAK3	p21 (RAC1) activated kinase 3	-2.309	-2.063	dendritic spine development	GO:0060996
31	PCDH1	protocadherin 1	-1.874	-3.052	cell adhesion	GO:0007155
32	PFDN6	prefoldin subunit 6	-2.242	-1.669	protein folding	GO:0006457
33	PIP5K1C	phosphatidylinositol-4-phosphate 5-kinase type 1 gamma	-1.286	-1.306	axonogenesis	GO:0007409
34	PRKAR2A	protein kinase cAMP-dependent type II regulatory subunit alpha	-1.292	-1.351	modulation of chemical synaptic transmission	GO:0050804
35	PTGES3	prostaglandin E synthase 3	-1.543	-1.780	prostaglandin biosynthetic process	GO:0001516
36	PTPRS	protein tyrosine phosphatase, receptor type S	-1.545	-1.301	hippocampus development	GO:0021766
37	RAB1A	RAB1A, member RAS oncogene family	-1.302	-1.374	intracellular protein transport	GO:0006886
38	RAB5C	RAB5C, member RAS oncogene family	-1.323	-1.423	intracellular protein transport	GO:0006886
39	RABL6	RAB, member RAS oncogene family like 6	1.737	1.548	intracellular protein transport	GO:0006886
40	RIMBP2	RIMS binding protein 2	-1.385	-1.856	neuromuscular synaptic transmission	GO:0007274
41	RPLP2	ribosomal protein lateral stalk subunit P2	-1.543	-1.508	translational elongation	GO:0006414
42	SEC24C	SEC24 homolog C, COPII coat complex component	-1.342	-1.390	vesicle-mediated transport	GO:0016192
43	SLC1A4	solute carrier family 1 member 4	-1.414	-1.344	cognition	GO:0050890
44	SNCA	synuclein alpha	-1.432	-1.421	synaptic transmission	GO:0001963
45	STX7	syntaxin 7	-1.324	-1.298	vesicle-mediated transport	GO:0016192
46	SUCLG1	succinate-CoA ligase alpha subunit	1.342	1.356	succinyl-CoA metabolic process	GO:0006104
47	TIMM13	translocase of inner mitochondrial membrane 13	-1.845	-1.487	protein insertion into mitochondrial inner membrane	GO:0045039
48	TPD52	tumor protein D52	-1.468	-1.384	positive regulation of cell population proliferation	GO:0008284
49	TRAPPC10	trafficking protein particle complex 10	-1.392	-1.664	vesicle-mediated transport	GO:0016192
50	TRIO	trio Rho guanine nucleotide exchange factor	-1.562	-1.369	G-protein-coupled receptor signaling pathway	GO:0007186

Table 1. Cont.

	Symbol	Entrez Gene Name	Fold-Change		Biological Function	GO Number
			100 mGy Ket	200 mGy Ket		
51	TUBA8	tubulin alpha 8	-1.472	-1.343	microtubule cytoskeleton organization	GO:0000226
52	UBXN6	UBX domain protein 6	-1.360	-1.419	macroautophagy	GO:0016236
53	UCHL3	ubiquitin C-terminal hydrolase L3	-1.413	-1.427	adult walking behavior	GO:0007628
54	VBP1	VHL binding protein 1	-1.747	-1.809	protein folding	GO:0006457
55	WASF3	WAS protein family member 3	-1.904	-1.429	actin cytoskeleton organization	GO:0030036

2.2. Effects on Neuronal Cytoskeleton and Synaptic Plasticity Following Combined Exposure to Ketamine and Irradiation

To better understand the involvement of biological processes following the combined treatment with ketamine and radiation, the 55 common significantly deregulated proteins from the co-exposure groups were subjected to Ingenuity Pathway Analysis (IPA). In particular, the categories “canonical pathways” and “diseases and biofunctions” were analyzed (Figure 2A). The most enriched canonical pathways were involved either in the organization of the cytoskeleton (signaling by Rho GDI family GTPases, RHOGDI signaling, actin cytoskeleton signaling, Rac signaling, RhoA signaling, regulation of actin-based motility by Rho) or played a role in neuronal transmission (ephrin receptor signaling, cAMP-mediated signaling, integrin signaling). Similarly, the most affected biofunctions were related to reorganization of the neuronal structure (shape change of axons, axonogenesis, growth of neurites, branching of axons) and synaptic transmission (transport of synaptic vesicles, neurotransmission, synaptic depression, long-term potentiation) (Figure 2A).

Activation of the brain-derived neurotrophic factor (BDNF) was predicted based on the deregulation profiles of the co-exposed groups by IPA (Figure 2B). BDNF is one of the key regulators of neuronal morphology and stimulates the growth and differentiation of new neurons and synapses [13]. In good agreement with this, the level of BDNF investigated by immunoblotting showed a significant increase in its expression in the co-exposed groups (upregulation by mean fold-changes of 4.2 ($p < 0.001$) and 3.6 ($p < 0.01$) in the groups “100 mGy Ket” and “200 mGy Ket”, respectively) (Figure 2C).

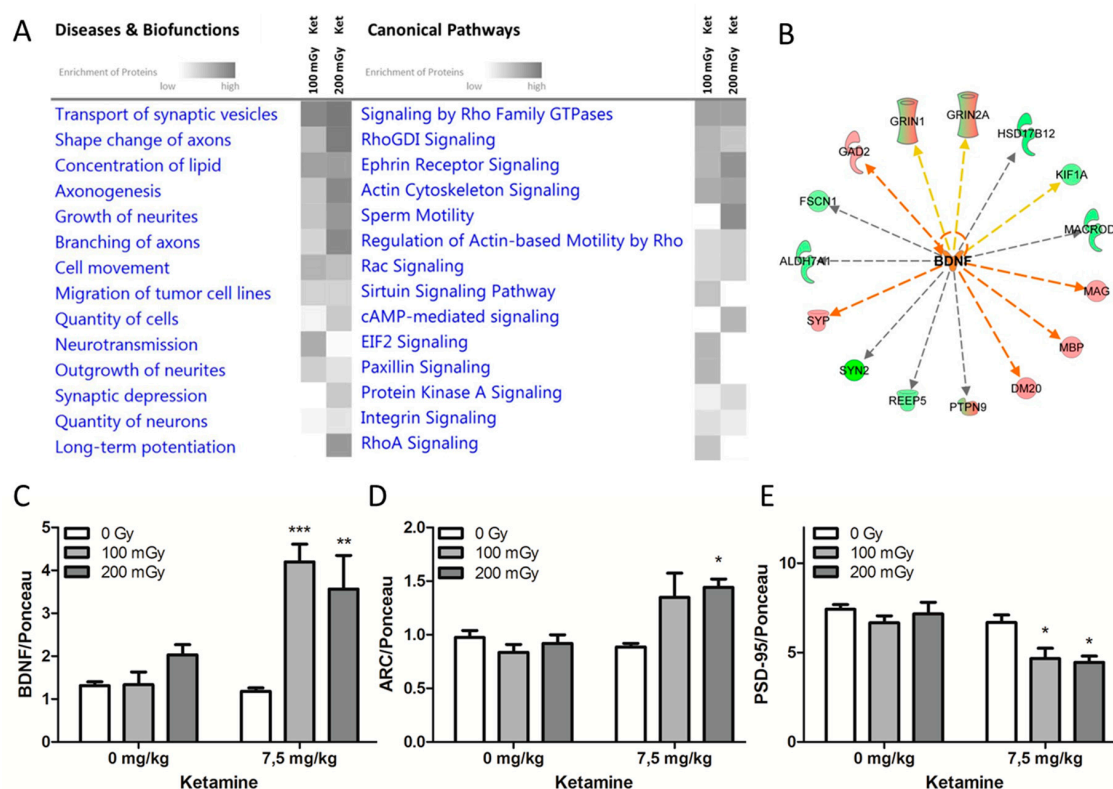


Figure 2. Combined treatment with ketamine radiation affected neuronal morphology and synaptic plasticity. (A) The Ingenuity Pathway Analysis (IPA) of associated signaling pathways based on all significantly deregulated hippocampal proteins in the co-exposure groups is shown. The functions and pathways in the categories “canonical pathways” and “diseases and biofunctions”, respectively, were ranked by their significance and displayed using a gray color gradient (the darker the color, the higher the pathway score). The pathway scores represent the negative log of the p -value derived from the Fisher’s exact test, where all gray boxes have a p -value of ≤ 0.05 ; $n = 5$. (B) Prediction of activation of brain-derived neurotrophic factor (BDNF) (orange color) was based on the deregulated proteins from the co-exposure groups. The upregulated proteins are marked in red and the downregulated proteins are in green. Immunoblot analyses of the relative expression of (C) BDNF, (D) ARC, and (E) PSD-95 in single and combined treatment groups were normalized to the total amount of proteins measured by Ponceau staining (Figure S1). Error bars represent the SEM, $n = 4$, * $p < 0.05$, ** $p < 0.01$, *** $p < 0.001$ (two-way ANOVA with Bonferroni multiple testing).

To further investigate the possible activation of BDNF in the co-exposed groups, the expression of a downstream target of BDNF, the activity-regulated cytoskeleton-associated (ARC) protein, was measured. In agreement with the upregulation of BDNF, the expression level of ARC was significantly increased in the group that received ketamine and gamma radiation (200 mGy, $p < 0.05$) (Figure 2D). In addition to BDNF, postsynaptic density protein 95 (PSD 95) influences both synapses and neuronal branching. [14] Only the combined treatment with ketamine and radiation caused a significant reduction in the level of PSD-95 ($p < 0.05$) (Figure 2E). Ponceau stainings and Western blot bands are shown in Figure S1.

2.3. Morphological Abnormalities of Hippocampal CA1 Neurons only after Combined Treatment with Ketamine and Irradiation

Golgi-Cox staining followed by dendritic reconstruction was performed on tissue sections of the Cornu Ammonis (CA1). Raw images are presented exemplarily for every experimental condition in Figure S2. Representative images of reconstructed neurons are shown in Figure 3A. Apical and basal dendrites were analyzed separately in all experimental groups (Figure 3B). No effect was found on the

structure and number of apical parts of the CA1 neurons (Figure S3A–C). A significant increase ($p < 0.001$) in the total number of basal dendrites was present after the combined treatment with ketamine and radiation (Figure 3B). In the co-treated groups, the total number of nodes was significantly increased (100 mGy Ket: $p < 0.05$, 200 mGy Ket: $p < 0.001$) while there was no difference in the single treatment groups compared to the control (Figure 3C). The number of spines divided by the dendrite length was significantly reduced in the group co-exposed to 200 mGy Ket ($p < 0.05$) (Figure 3D). However, the reduction of spines was not significant in the 100 mGy Ket group and therefore could not explain the observed cognitive impairment. No effect in spine number was detected in the apical dendrites (Figure S3C). This indicated an increase in the complexity of the basal dendrites after co-exposure.

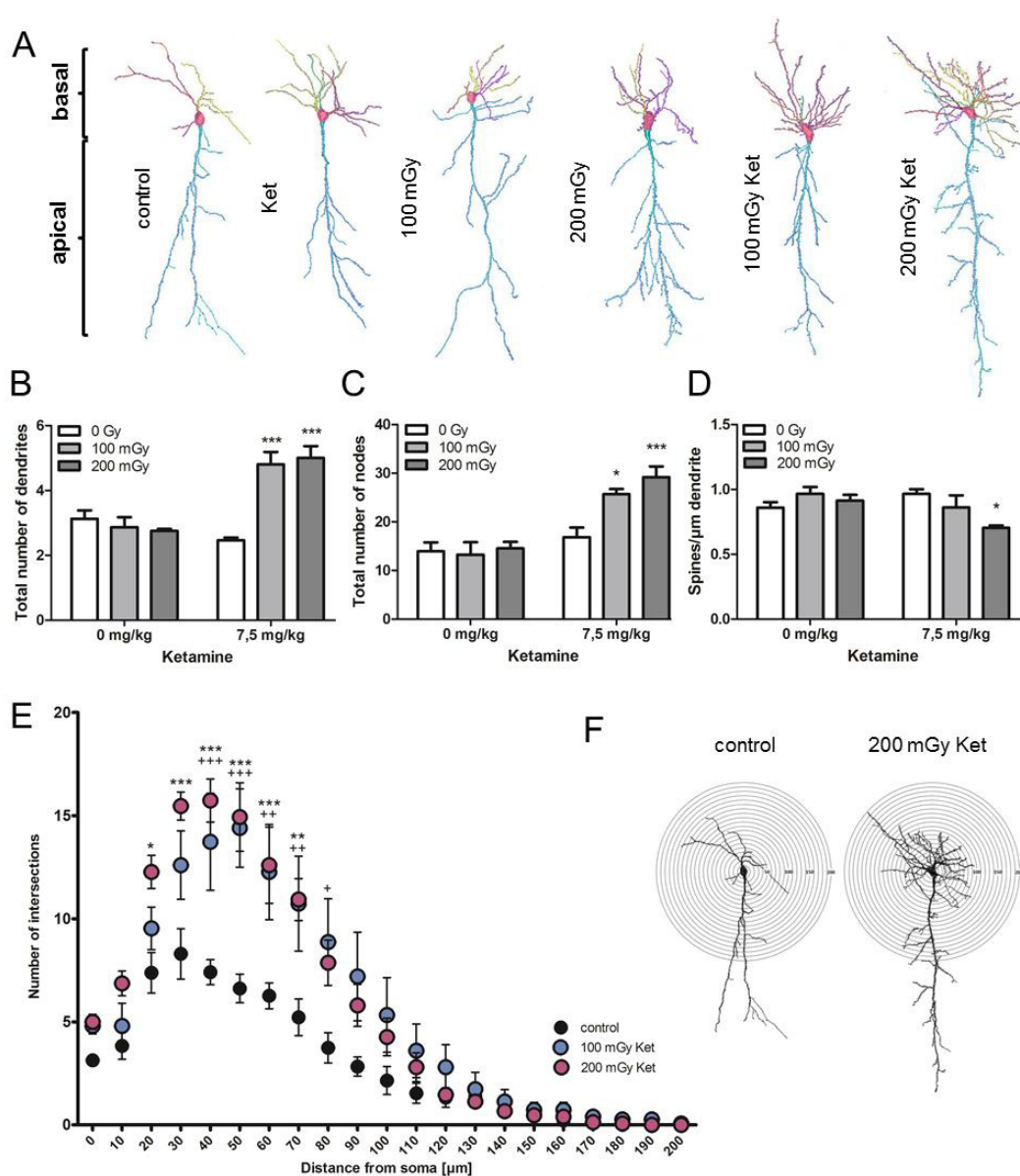


Figure 3. Co-treatment with ketamine and irradiation led to structural changes in hippocampal CA1 neurons. (A) Reconstructed hippocampal CA1 neurons representative for each experimental treatment group are shown. Each individual dendrite is presented in a different color. (B) The number of basal dendrites is shown in all experimental groups. Five neurons per animal with 5 biological replicates were analyzed; *** $p < 0.001$. (C) The number of nodes representing the branching points in basal dendrites is shown. Five neurons per animal with 5 biological replicates were analyzed; * $p < 0.05$, *** $p < 0.001$. (D) The spine densities of the basal dendrites are shown. Five neurons per animal with

5 biological replicates were analyzed; * $p < 0.05$, *** $p < 0.001$. (D) The spine densities of the basal dendrites are shown. Five neurons per animal with 5 biological replicates were analyzed; * $p < 0.05$. (E) A comparison between the total number of dendritic intersections for each circle between the controls (black) and the co-treated neurons (100 mGy Ket: blue; 200 mGy Ket: purple) was performed. The co-treated animals showed significant increase in the number of intersections between 40 and 80 μm (100 mGy ket; + $p < 0.05$, ++ $p < 0.01$, +++ $p < 0.01$) and between 20 and 70 μm (200 mGy Ket; * $p < 0.05$, ** $p < 0.01$, *** $p < 0.001$). At least 5 neurons per animal with 5 biological replicates were analyzed. The first values (2 μm circle) represent the total number of basal dendrites, as shown in (B). (F) Representative CA1 neurons with concentric circles used for the Sholl analysis are shown. The radius interval between the circles was set to 10 μm per step, ranging from 10 to 200 μm from the center of the neuronal soma to the end of the dendrites. The numbers of dendritic intersections per circle were quantified. At least 5 neurons were analyzed per animal. The p values were calculated using a two-way ANOVA with Bonferroni multiple testing.

To investigate this in more detail, Sholl analysis, representing the distribution of dendritic intersections with increasing distance from the cell soma, was performed. A significant shift in the number of intersections in the circle diameter of 20–80 μm was observed in the co-exposed groups compared to the sham-treated controls, thereby confirming a significant increase in the number of basal dendrites and their branching points (Figure 3E,F).

3. Discussion

Pediatric radiotherapy and treatment frequently require ketamine sedation prior to irradiation [15]. Concerns about the long-term safety of this combination have been raised following the report of cognitive impairment in mice co-exposed to clinically relevant doses of ketamine and irradiation [12]. We show here that co-exposure during early brain development results in persistent alterations to both the proteome and structure of hippocampal CA1 neurons. Significant increases in dendrite number and branching were observed when ketamine was given immediately prior to irradiation at 100 or 200 mGy. Neither ketamine nor radiation treatment alone induced the reorganization of dendritic structures.

The structure of dendrites has a profound impact on the processing of neuronal information, including learning and memory. The formation of the dendritic arbour, the sites of synaptic connections from input neurons, is usually completed by adulthood. Aberrations and remodeling of dendritic structures are observed only under pathological conditions [16–18]. Extension of the dendrite length beyond the normal level is related to mental retardation [19,20]. Neuropathic pain linked to depression and cognitive decline is known to be associated with an increase in dendritic length and branching [21].

Interestingly, ketamine (10 μM) was previously shown to promote both the number of dendritic branches and the total length of the arbours in embryonic rat cortical neurons in vitro [22] due to ketamine-induced rapid increase in BDNF secretion [23,24]. Cranial irradiation of adult mice using radiation doses higher than in this study (1 or 10 Gy) resulted in significant reductions in dendritic branching and total length in the hippocampus [25]. Our data showed increased basal branching of CA1 neurons with the combined exposure, therefore suggesting a radiation-enhanced ketamine-like response in the neuronal structure and demonstrating the strong impact of ketamine and irradiation when applied together.

In contrast, the regulation of neuronal structures is dependent upon several factors. Small GTP binding proteins, like Ras-related C3 botulinum toxin substrate 1 (RAC1), Ras homolog gene family member A (RHOA), and cell division control protein 42 homolog (CDC42), are crucial for reorganization of the dendrites and their branching [26–29]. In accordance with this, our proteome analysis showed that most of the significantly deregulated proteins in the co-exposed groups belonged to pathways dependent on the Rho family GTPases. Thus, changes in the neuronal cytoskeleton and associated pathways (shape change of axons, axonogenesis, growth of neurites, and branching of axons) were all predicted from the proteome data and were consistent with the changes in CA1

neuronal morphology. Secreted factors such as neurotrophins are known to play key roles in regulating dendrite outgrowth and branching [30]. BDNF is a well-studied mediator of synaptic plasticity and memory formation [31,32]. Overexpression of BDNF in CA1 neurons was shown to improve fear and object-location memory in mice [33], but was associated with cognitive impairment in MECP2-duplication syndrome [34]. Application of exogenous BDNF was shown to increase the number of dendrites in pyramidal neurons [35]. Ketamine given at doses of 10 or 15 mg kg⁻¹ (but not at 5 mg kg⁻¹) resulted in a rapid and significant increase in the expression of hippocampal BDNF in adult male Wistar rats [36]. In contrast, high-dose cranial irradiation (10 Gy) of adult C57BL/6 mice resulted in a significant decrease in BDNF expression in the hippocampus one month after exposure [37]. In our study, only the co-treatment with ketamine (7.5 mg kg⁻¹) and low-dose radiation (100 mGy or 200 mGy) led to an increase in the total amount of BDNF in the hippocampus. This increase was sustained long after exposure in neonatal mice.

Similar to BDNF, PSD-95 is involved in synaptic functions, especially with regard to NMDA receptors [38,39]. We previously showed that whole-body irradiation of neonatal NMRI or C57BL/6J mice causes increased expression of PSD-95 in the hippocampus six months after exposure [40,41]. This was seen at whole-body doses equal to or higher than 0.5 Gy, but not at lower doses. Similarly, it was shown that high-dose (1 Gy, 10 Gy) cranial gamma-radiation caused increased expression of PSD-95 in the hippocampus of adult mice 30 days after irradiation [25]. Administration of high-dose ketamine (30 mg kg⁻¹ over five consecutive days) was shown to immediately increase the level of PSD-95 in the synaptosomes of adult male Wistar rats [42]. Lower doses of ketamine (10 mg kg⁻¹) did not produce effects on the total level of PSD-95 in the hippocampal membranes of mice immediately (30 min) after administration [43]. In addition to synaptic functions, both BDNF and PSD-95 play a role in regulating dendrite outgrowth and branching [14,35]. In contrast to BDNF, PSD-95 inhibits the branching of dendrites [14]. Contrary to our previous results obtained using a less-sensitive slot blotting method [12], the immunoblotting used here showed reduced expression of PSD-95 after the combined treatment with ketamine and low-dose radiation. No change in the PSD-95 level was detected using single exposure treatments. The persistent upregulation of BDNF and downregulation of PSD-95 after the co-exposure, in addition to the changes in the expression levels of several other proteins responsible for neuronal growth and branching (CDC42, PAK3, ARF6, and others displayed in Table 1), could be the molecular explanation for the observed increase in the number and branching of basal dendrites in the CA1 neurons.

4. Materials and Methods

4.1. Animals

All procedures were in accordance with the European Communities Council Directive of 24 November 1986 (86/609/EEC; approval date: 26 April 2013) after permission by local ethical committees (Uppsala University) and the Swedish Committee for Ethical Experiments on Laboratory Animals. The results were reported in line with relevant aspects of the ARRIVE guidelines [44].

Pregnant Naval Medical Research Institute (NMRI) mice were purchased from Scanbur (Sollentuna, Sweden) and housed in Makrolon[®] III cages. Only the male offspring were used in the experiments to mimic the conditions used for cognitional testing [12].

4.2. Exposure

Neonatal (postnatal day 10) mice were exposed to a single subcutaneous injection of ketamine (7.5 mg kg⁻¹ body weight) or to a low dose of whole-body gamma radiation (¹³⁷Cs; 100 mGy, 200 mGy), or co-exposed. In the co-exposure group, ketamine was administered one hour before irradiation. Control mice were injected with 10 mL kg⁻¹ body weight saline (0.9%) and sham-irradiated. Control mice and mice irradiated only were not given sedatives prior to exposure. The dosages of ketamine and irradiation were determined based on the previous experiments showing no effect of single exposures

on spontaneous behavior, learning and memory, or protein levels [12,45–47]. A schematic presentation of the experimental design is shown in Figure 1A.

4.3. Tissue Collection

The mice were sacrificed with CO₂ 6 months post-treatment. Brains were excised, dissected, and rinsed in cold PBS. The right hemisphere was used for proteome analysis. The hippocampi were microdissected, snap frozen in liquid nitrogen, and stored at –80 °C. The left hemisphere was used for the morphology study.

4.4. Protein Lysis and Determination of Protein Concentration

Frozen hippocampi were pulverized and suspended in RIPA buffer (Thermo Fischer, Darmstadt, Germany) enriched with phosphatase and protease inhibitors (Sigma-Aldrich, Taufkirchen, Germany).

After sonication, lysis, and centrifugation, protein concentrations were measured using BCA Protein Assay Kit (Thermo Fischer) according to the manufacturer's instructions.

4.5. Mass Spectrometry (MS)

Label-free measurements were performed on a QExactive high field mass spectrometer (Thermo Fisher) in data-dependent acquisition mode, as described previously [48,49].

4.6. Protein Identification and Quantification

Spectra were analyzed using Progenesis QI software (Version 3.0, Nonlinear Dynamics) for label-free quantification, as described before [48]. The filtering criteria were as follows: Proteins identified and quantified with two UP and fold-changes of ≤ 0.77 or ≥ 1.3 (*t*-test; $p \leq 0.05$) were considered to be significantly differentially expressed.

4.7. Pathway Analysis

The list of significantly deregulated proteins with their accession numbers, fold-changes and *p*-values were imported into Ingenuity Pathway Analysis (IPA, QIAGEN Redwood City, www.qiagen.com/ingenuity).

4.8. Western Blot Analysis

Western blots were performed according to the protocol described previously [48]. The following antibodies were used: BDNF (abcam, ab203573, Cambridge, UK), ARC (abcam, ab118929, Cambridge, UK) and PSD-95 (abcam, ab18258, Cambridge, UK). Ponceau (Sigma-Aldrich, St. Louis, MO, USA) staining served as an internal loading control (Figure S1).

4.9. Golgi Staining

Staining was performed using the FD Rapid GolgiStain Kit (NeuroTechnologies, Columbia, SC, USA) according to the user manual. Directly after dissection, the hemispheres were put into 5 mL Golgi-Cox solution for fixation and impregnation for one week and then frozen at –20 °C. For imaging, the frozen brain was cut with a cryostat at –20 °C (100 μ m coronal sections), and the sections were mounted on gelatin-coated microscope slides.

4.10. Imaging and Analysis of Dendrites and Spines

CA1 neurons were reconstructed using Neurolucida software (MBF Bioscience, Williston, ND, USA) under 40x magnification (Zeiss AxioPlan 2 microscope) on 100 μ m coronal sections and analyzed with Neurolucida Explorer software (MBF Bioscience). Apical and basal dendrites were separately analyzed. In the Sholl analysis, the radius interval of each section was set to 10 μ m, starting from 10 μ m and ending at a 200 μ m distance from the soma.

4.11. Statistical Analysis

Statistical analysis of the LC-MS/MS data was performed with Excel using a two-sided Student's t-test. The Western blotting and the Golgi-Cox assay were analyzed using Graph Pad prism software (GraphPad Software, San Diego, CA, USA) and a 2-way ANOVA with Bonferroni multiple testing. The error bars were calculated as standard error of the mean (SEM); p -values ≤ 0.05 were defined as significant.

4.12. Data Availability

The raw MS-data are available at <http://dx.doi.org/doi:10.20348/STOREDB/1132/1198>.

5. Conclusions

In conclusion, the data from this study corroborated the results from the previous study regarding behavioral effects [12]. Both studies strongly suggested that a scenario of early postnatal exposure to a combination of ketamine and low-dose radiation, comparable to that found in clinical situations, was able to persistently induce cognitive impairment and changes in the neuronal structure. The neonatal window used in this study corresponded to the human brain developmental period that starts around the third trimester of pregnancy and expands over the first two years of life. Considering that ketamine is one of the most commonly used sedative agents in pediatric emergency departments [50], these results raise concern over the detrimental long-term effects on cognitive function. Whether the combination of ketamine and low-dose radiation is able to induce and exacerbate developmental neurobehavioral and cognitive defects in children should be investigated further, as this may be highly relevant for daily clinical practice.

Supplementary Materials: Supplementary materials can be found at <http://www.mdpi.com/1422-0067/20/23/6103/s1>. Table S1. All quantified proteins with an identification based on at least two UP for the ketamine group. Table S2. All quantified proteins with an identification based on at least two UP for the 100 mGy group. Table S3. All quantified proteins with an identification based on at least two UP for the 200 mGy group. Table S4. All quantified proteins with an identification based on at least two UP for the 100 mGy Ket group. Table S5. All quantified proteins with an identification based on at least two UP for the 200 mGy Ket group. Figure S1. Ponceau staining and western blot bands. Figure S2. Representative hippocampal CA1 neurons for all experimental groups. Figure S3. Co-treatment with ketamine and irradiation does not affect the number of the apical dendrites, their branching or the spine density.

Author Contributions: Data curation, D.H., S.B., B.S., P.E., J.P., S.W., A.F., and E.S.; formal analysis, D.H., O.A., P.S., C.v.T., and S.M.H.; writing—original draft preparation, D.H. and S.T.; writing—review and editing, D.H., S.T., M.J.A., S.B., B.S., P.E., J.P., O.A., C.v.T., S.M.H., and A.F.; supervision, S.T. and M.J.A.; project administration, S.T.

Funding: This research was funded by the Federal Ministry of Education and Research (BMBF) under the grant number 02NUK045C, the EURATOM research and training program 2014–2018 in the framework of CONCERT under the grand number No 662287, and the Swedish Radiation Safety Authority.

Acknowledgments: We thank Vikram Subramanian for his excellent technical support.

Conflicts of Interest: The authors declare no conflict of interest.

References

1. Miglioretti, D.L.; Johnson, E.; Williams, A.; Greenlee, R.T.; Weinmann, S.; Solberg, L.I.; Feigelson, H.S.; Roblin, D.; Flynn, M.J.; Vanneman, N.; et al. The use of computed tomography in pediatrics and the associated radiation exposure and estimated cancer risk. *JAMA Pediatr.* **2013**, *167*, 700–707. [[CrossRef](#)] [[PubMed](#)]
2. Pearce, M.S.; Salotti, J.A.; Little, M.P.; McHugh, K.; Lee, C.; Kim, K.P.; Howe, N.L.; Ronckers, C.M.; Rajaraman, P.; Sir Craft, A.W.; et al. Radiation exposure from CT scans in childhood and subsequent risk of leukaemia and brain tumours: A retrospective cohort study. *Lancet* **2012**, *380*, 499–505. [[CrossRef](#)]
3. Chen, J.X.; Kachniarz, B.; Gilani, S.; Shin, J.J. Risk of malignancy associated with head and neck CT in children: A systematic review. *Otolaryngol. Head Neck Surg.* **2014**, *151*, 554–566. [[CrossRef](#)] [[PubMed](#)]
4. McMullen, K.P.; Hanson, T.; Bratton, J.; Johnstone, P.A. Parameters of anesthesia/sedation in children receiving radiotherapy. *Radiat. Oncol.* **2015**, *10*, 65. [[CrossRef](#)]

5. Green, S.M.; Roback, M.G.; Kennedy, R.M.; Krauss, B. Clinical practice guideline for emergency department ketamine dissociative sedation: 2011 update. *Ann. Emerg. Med.* **2011**, *57*, 449–461. [[CrossRef](#)]
6. Li, F.; Tsien, J.Z. Memory and the NMDA receptors. *N. Engl. J. Med.* **2009**, *361*, 302–303. [[CrossRef](#)]
7. Furukawa, H.; Singh, S.K.; Mancusso, R.; Gouaux, E. Subunit arrangement and function in NMDA receptors. *Nature* **2005**, *438*, 185–192. [[CrossRef](#)]
8. Duchen, M.R.; Burton, N.R.; Biscoe, T.J. An intracellular study of the interactions of N-methyl-DL-aspartate with ketamine in the mouse hippocampal slice. *Brain Res.* **1985**, *342*, 149–153. [[CrossRef](#)]
9. Fredriksson, A.; Archer, T.; Alm, H.; Gordh, T.; Eriksson, P. Neurofunctional deficits and potentiated apoptosis by neonatal NMDA antagonist administration. *Behav. Brain Res.* **2004**, *153*, 367–376. [[CrossRef](#)]
10. Viberg, H.; Ponten, E.; Eriksson, P.; Gordh, T.; Fredriksson, A. Neonatal ketamine exposure results in changes in biochemical substrates of neuronal growth and synaptogenesis, and alters adult behavior irreversibly. *Toxicology* **2008**, *249*, 153–159. [[CrossRef](#)]
11. Fredriksson, A.; Archer, T. Hyperactivity following postnatal NMDA antagonist treatment: Reversal by D-amphetamine. *Neurotox. Res.* **2003**, *5*, 549–564. [[CrossRef](#)] [[PubMed](#)]
12. Buratovic, S.; Stenerlow, B.; Sundell-Bergman, S.; Fredriksson, A.; Viberg, H.; Gordh, T.; Eriksson, P. Effects on adult cognitive function after neonatal exposure to clinically relevant doses of ionising radiation and ketamine in mice. *Br. J. Anaesth.* **2018**, *120*, 546–554. [[CrossRef](#)] [[PubMed](#)]
13. Acheson, A.; Conover, J.C.; Fandl, J.P.; DeChiara, T.M.; Russell, M.; Thadani, A.; Squinto, S.P.; Yancopoulos, G.D.; Lindsay, R.M. A BDNF autocrine loop in adult sensory neurons prevents cell death. *Nature* **1995**, *374*, 450–453. [[CrossRef](#)]
14. Charych, E.I.; Akum, B.F.; Goldberg, J.S.; Jornsten, R.J.; Rongo, C.; Zheng, J.Q.; Firestein, B.L. Activity-independent regulation of dendrite patterning by postsynaptic density protein PSD-95. *J. Neurosci.* **2006**, *26*, 10164–10176. [[CrossRef](#)] [[PubMed](#)]
15. Mahajan, C.; Dash, H.H. Procedural sedation and analgesia in pediatric patients. *J. Pediatr. Neurosci.* **2014**, *9*, 1–6.
16. Penzes, P.; Cahill, M.E.; Jones, K.A.; VanLeeuwen, J.E.; Woolfrey, K.M. Dendritic spine pathology in neuropsychiatric disorders. *Nat. Neurosci.* **2011**, *14*, 285–293. [[CrossRef](#)]
17. Wu, G.Y.; Zou, D.J.; Rajan, I.; Cline, H. Dendritic dynamics in vivo change during neuronal maturation. *J. Neurosci.* **1999**, *19*, 4472–4483. [[CrossRef](#)]
18. McAllister, A.K. Cellular and molecular mechanisms of dendrite growth. *Cereb. Cortex* **2000**, *10*, 963–973. [[CrossRef](#)]
19. Kaufmann, W.E.; Moser, H.W. Dendritic anomalies in disorders associated with mental retardation. *Cereb. Cortex* **2000**, *10*, 981–991. [[CrossRef](#)]
20. Purpura, D.P. Dendritic differentiation in human cerebral cortex: Normal and aberrant developmental patterns. *Adv. Neurol.* **1975**, *12*, 91–134.
21. Metz, A.E.; Yau, H.J.; Centeno, M.V.; Apkarian, A.V.; Martina, M. Morphological and functional reorganization of rat medial prefrontal cortex in neuropathic pain. *Proc. Natl. Acad. Sci. USA* **2009**, *106*, 2423–2428. [[CrossRef](#)] [[PubMed](#)]
22. Ly, C.; Greb, A.C.; Cameron, L.P.; Wong, J.M.; Barragan, E.V.; Wilson, P.C.; Burbach, K.F.; Soltanzadeh Zarandi, S.; Sood, A.; Paddy, M.R.; et al. Psychedelics Promote Structural and Functional Neural Plasticity. *Cell Rep.* **2018**, *23*, 3170–3182. [[CrossRef](#)] [[PubMed](#)]
23. Lepack, A.E.; Fuchikami, M.; Dwyer, J.M.; Banasr, M.; Duman, R.S. BDNF release is required for the behavioral actions of ketamine. *Int. J. Neuropsychopharmacol.* **2014**, *18*. [[CrossRef](#)] [[PubMed](#)]
24. Abdallah, C.G.; Adams, T.G.; Kelmendi, B.; Esterlis, I.; Sanacora, G.; Krystal, J.H. Ketamine's Mechanism of Action: A Path to Rapid-Acting Antidepressants. *Depress. Anxiety* **2016**, *33*, 689–697. [[CrossRef](#)]
25. Parihar, V.K.; Limoli, C.L. Cranial irradiation compromises neuronal architecture in the hippocampus. *Proc. Natl. Acad. Sci. USA* **2013**, *110*, 12822–12827. [[CrossRef](#)]
26. Chen, H.; Firestein, B.L. RhoA regulates dendrite branching in hippocampal neurons by decreasing cypin protein levels. *J. Neurosci.* **2007**, *27*, 8378–8386. [[CrossRef](#)]
27. Arikath, J. Molecular mechanisms of dendrite morphogenesis. *Front. Cell. Neurosci.* **2012**, *6*, 61. [[CrossRef](#)]
28. Leemhuis, J.; Boutillier, S.; Barth, H.; Feuerstein, T.J.; Brock, C.; Nurnberg, B.; Aktories, K.; Meyer, D.K. Rho GTPases and phosphoinositide 3-kinase organize formation of branched dendrites. *J. Biol. Chem.* **2004**, *279*, 585–596. [[CrossRef](#)]

29. Luo, L. Actin cytoskeleton regulation in neuronal morphogenesis and structural plasticity. *Annu. Rev. Cell Dev. Biol.* **2002**, *18*, 601–635. [[CrossRef](#)]
30. McAllister, A.K.; Lo, D.C.; Katz, L.C. Neurotrophins regulate dendritic growth in developing visual cortex. *Neuron* **1995**, *15*, 791–803. [[CrossRef](#)]
31. Bramham, C.R.; Panja, D. BDNF regulation of synaptic structure, function, and plasticity. *Neuropharmacology* **2014**, *76*(Pt. C), 601–602. [[CrossRef](#)]
32. Tongiorgi, E.; Baj, G. Functions and mechanisms of BDNF mRNA trafficking. *Novartis Found. Symp.* **2008**, *289*, 136–147, discussion 147–151, 193–135.
33. Wang, M.; Li, D.; Yun, D.; Zhuang, Y.; Repunte-Canonigo, V.; Sanna, P.P.; Behnisch, T. Translation of BDNF-gene transcripts with short 3' UTR in hippocampal CA1 neurons improves memory formation and enhances synaptic plasticity-relevant signaling pathways. *Neurobiol. Learn. Mem.* **2017**, *138*, 121–134. [[CrossRef](#)] [[PubMed](#)]
34. Jiang, M.; Ash, R.T.; Baker, S.A.; Suter, B.; Ferguson, A.; Park, J.; Rudy, J.; Torsky, S.P.; Chao, H.T.; Zoghbi, H.Y.; et al. Dendritic arborization and spine dynamics are abnormal in the mouse model of MECP2 duplication syndrome. *J. Neurosci.* **2013**, *33*, 19518–19533. [[CrossRef](#)] [[PubMed](#)]
35. Horch, H.W.; Katz, L.C. BDNF release from single cells elicits local dendritic growth in nearby neurons. *Nat. Neurosci.* **2002**, *5*, 1177–1184. [[CrossRef](#)] [[PubMed](#)]
36. Yang, C.; Hu, Y.M.; Zhou, Z.Q.; Zhang, G.F.; Yang, J.J. Acute administration of ketamine in rats increases hippocampal BDNF and mTOR levels during forced swimming test. *Upsala J. Med. Sci.* **2013**, *118*, 3–8. [[CrossRef](#)] [[PubMed](#)]
37. Son, Y.; Yang, M.; Kang, S.; Lee, S.; Kim, J.; Park, S.; Kim, J.S.; Jo, S.K.; Jung, U.; Shin, T.; et al. Cranial irradiation regulates CREB-BDNF signaling and variant BDNF transcript levels in the mouse hippocampus. *Neurobiol. Learn. Mem.* **2015**, *121*, 12–19. [[CrossRef](#)] [[PubMed](#)]
38. Caldeira, M.V.; Melo, C.V.; Pereira, D.B.; Carvalho, R.F.; Carvalho, A.L.; Duarte, C.B. BDNF regulates the expression and traffic of NMDA receptors in cultured hippocampal neurons. *Mol. Cell. Neurosci.* **2007**, *35*, 208–219. [[CrossRef](#)] [[PubMed](#)]
39. Chen, X.; Levy, J.M.; Hou, A.; Winters, C.; Azzam, R.; Sousa, A.A.; Leapman, R.D.; Nicoll, R.A.; Reese, T.S. PSD-95 family MAGUKs are essential for anchoring AMPA and NMDA receptor complexes at the postsynaptic density. *Proc. Natl. Acad. Sci. USA* **2015**, *112*, E6983–E6992. [[CrossRef](#)]
40. Kempf, S.J.; Casciati, A.; Buratovic, S.; Janik, D.; von Toerne, C.; Ueffing, M.; Neff, F.; Moertl, S.; Stenerlow, B.; Saran, A.; et al. The cognitive defects of neonatally irradiated mice are accompanied by changed synaptic plasticity, adult neurogenesis and neuroinflammation. *Mol. Neurodegener.* **2014**, *9*, 57. [[CrossRef](#)]
41. Kempf, S.J.; Sepe, S.; von Toerne, C.; Janik, D.; Neff, F.; Hauck, S.M.; Atkinson, M.J.; Mastroberardino, P.G.; Tapio, S. Neonatal Irradiation Leads to Persistent Proteome Alterations Involved in Synaptic Plasticity in the Mouse Hippocampus and Cortex. *J. Proteome Res.* **2015**. [[CrossRef](#)] [[PubMed](#)]
42. Lisek, M.; Ferenc, B.; Studzian, M.; Pulaski, L.; Guo, F.; Zylinska, L.; Boczek, T. Glutamate Deregulation in Ketamine-Induced Psychosis-A Potential Role of PSD95, NMDA Receptor and PMCA Interaction. *Front. Cell. Neurosci.* **2017**, *11*, 181. [[CrossRef](#)] [[PubMed](#)]
43. Beurel, E.; Grieco, S.F.; Amadei, C.; Downey, K.; Jope, R.S. Ketamine-induced inhibition of glycogen synthase kinase-3 contributes to the augmentation of alpha-amino-3-hydroxy-5-methylisoxazole-4-propionic acid (AMPA) receptor signaling. *Bipolar Disord.* **2016**, *18*, 473–480. [[CrossRef](#)] [[PubMed](#)]
44. Kilkenny, C.; Browne, W.J.; Cuthill, I.C.; Emerson, M.; Altman, D.G. Improving bioscience research reporting: The ARRIVE guidelines for reporting animal research. *PLoS Biol.* **2010**, *8*, e1000412. [[CrossRef](#)]
45. Buratovic, S.; Stenerlow, B.; Fredriksson, A.; Sundell-Bergman, S.; Viberg, H.; Eriksson, P. Neonatal exposure to a moderate dose of ionizing radiation causes behavioural defects and altered levels of tau protein in mice. *Neurotoxicology* **2014**, *45*, 48–55. [[CrossRef](#)]
46. Eriksson, P.; Buratovic, S.; Fredriksson, A.; Stenerlow, B.; Sundell-Bergman, S. Neonatal exposure to whole body ionizing radiation induces adult neurobehavioural defects: Critical period, dose–response effects and strain and sex comparison. *Behav. Brain Res.* **2016**, *304*, 11–19. [[CrossRef](#)]
47. Kempf, S.J.; Buratovic, S.; von Toerne, C.; Moertl, S.; Stenerlow, B.; Hauck, S.M.; Atkinson, M.J.; Eriksson, P.; Tapio, S. Ionising radiation immediately impairs synaptic plasticity-associated cytoskeletal signalling pathways in HT22 cells and in mouse brain: An in vitro/in vivo comparison study. *PLoS ONE* **2014**, *9*, e110464. [[CrossRef](#)]

48. Schmal, Z.; Isermann, A.; Hladik, D.; von Toerne, C.; Tapio, S.; Rube, C.E. DNA damage accumulation during fractionated low-dose radiation compromises hippocampal neurogenesis. *Radiother. Oncol.* **2019**, *137*, 45–54. [[CrossRef](#)]
49. Grosche, A.; Hauser, A.; Lepper, M.F.; Mayo, R.; von Toerne, C.; Merl-Pham, J.; Hauck, S.M. The Proteome of Native Adult Muller Glial Cells from Murine Retina. *Mol. Cell. Proteom.* **2016**, *15*, 462–480. [[CrossRef](#)]
50. Dial, S.; Silver, P.; Bock, K.; Sagy, M. Pediatric sedation for procedures titrated to a desired degree of immobility results in unpredictable depth of sedation. *Pediatr. Emerg. Care* **2001**, *17*, 414–420. [[CrossRef](#)]



© 2019 by the authors. Licensee MDPI, Basel, Switzerland. This article is an open access article distributed under the terms and conditions of the Creative Commons Attribution (CC BY) license (<http://creativecommons.org/licenses/by/4.0/>).

3.3 DNA damage accumulation during fractionated low-dose radiation compromises hippocampal neurogenesis

3.3.1 Aim and summary of the study

Radiotherapy plays an important role in the treatment and diagnostic of paediatric and adult brain tumours. Treatment plans often include fractionated doses of intensity-modulated radiation to better match the dose to the morphology of the tumour, while minimizing exposure to surrounding healthy tissue. Nevertheless, some areas of the brain adjacent to the target area are repeatedly exposed to low doses of radiation. This is particularly critical for very young children, as their developing brains are more sensitive to radiation damage and this may have late effects due to their long-life expectancy. The aim of this study was to investigate the effects of fractionated low-dose radiation on the molecular and cellular dynamics of hippocampal neurogenesis in a mouse model.

The pathophysiology of radiation-induced neurotoxicity after daily exposure (5x - 20x 0.1 Gy) was characterized by immunohistology assays and label-free LC-MS/MS proteomics. It was demonstrated that repeated exposure to 0.1 Gy doses leads to an accumulation of DNA damage, as well as to a progressive decrease in hippocampal neurogenesis. This was associated with a lower number of stem and progenitor cells and less dendritic complexity compared to the non-irradiated controls. The proteome analysis showed that signalling pathways associated with neurotropic regulation exhibited strong downregulation immediately after exposure, followed by a slower compensatory activation indicative of a functional recovery. The main affected pathway was the CREB signalling and the CREB-mediated transcription. The expression of the CREB targets BDNF and ARC was elevated three months after the fractional exposure. BDNF plays an important role in neurogenesis by promoting neuronal maturation, whilst ARC triggers dendritic modelling and supports dendritic plasticity of the spine. The increase in both neurotropic factors indicates a possible compensatory response to the decrease in neurogenesis and dendritic complexity caused by the radiation exposure. These data show the sensitivity of hippocampal neurogenesis, especially in the maturing brain, which can lead to a severe cognitive decline later in life.

3.3.2 Contribution

For this study the radiation, immunofluorescence staining, and microscopy were performed by Miss Zoe Schmal and Miss Anna Isermann. The dissection of the brains, the protein concentration measurements, the protein lysis and the preparation of the samples for LC-MS/MS measurements were performed by me. Dr. Christine von Törne supported the study with the LC-MS/MS runs. I performed the bioinformatic analysis of the proteomic data using IPA analysis as well as the validation by Western blotting. The manuscript was jointly written by Zoe Schmal and me with the help of Dr. Claudia Rube and Dr. Soile Tapio. All co-authors were involved in the scientific discussion and preparation of the manuscript.

3.3.3 Publication

The original data were published in an original research paper on May 4th, 2019 in "Radiotherapy & Oncology":

DNA damage accumulation during fractionated low-dose radiation compromises hippocampal neurogenesis.

Zoe Schmal, Anna Isermann, Daniela Hladik, Christine von Toerne, Soile Tapio, Claudia Rube

Radiother Oncol. 2019 Aug; 137:45-54. doi: 10.1016/j.radonc.2019.04.02 (Schmal et al., 2019)



Original Article

DNA damage accumulation during fractionated low-dose radiation compromises hippocampal neurogenesis

Zoé Schmal^a, Anna Isermann^a, Daniela Hladik^b, Christine von Toerne^c, Soile Tapio^b, Claudia E. Rube^{a,*}^a Department of Radiation Oncology, Saarland University, Homburg/Saar; ^b Institute of Radiation Biology, Helmholtz Zentrum München, German Research Center for Environmental Health GmbH; and ^c Research Unit Protein Science, Helmholtz Zentrum München, German Research Center for Environmental Health GmbH, Neuherberg, Germany

ARTICLE INFO

Article history:

Received 10 January 2019

Received in revised form 22 March 2019

Accepted 18 April 2019

Keywords:

Neurogenesis

Hippocampus

Low-dose radiation

Normal tissue toxicity

DNA double-strand breaks

DNA damage foci

ABSTRACT

Background and purpose: High-precision radiotherapy is an effective treatment modality for tumors. Intensity-modulated radiotherapy techniques permit close shaping of high doses to tumors, however healthy organs outside the target volume are repeatedly exposed to low-dose radiation (LDR). The inherent vulnerability of hippocampal neurogenesis is likely the determining factor in radiation-induced neurocognitive dysfunctions. Using preclinical *in-vivo* models with daily LDR we attempted to precisely define the pathophysiology of radiation-induced neurotoxicity.

Material and methods: Genetically defined mouse strains with varying DNA repair capacities were exposed to fractionated LDR (5×/10×/15×/20×0.1 Gy) and dentate gyri from juvenile and adult mice were analyzed 72 h after last exposure and 1, 3, 6 months after 20 × 0.1 Gy. To examine the impact of LDR on neurogenesis, persistent DNA damage was assessed by quantifying 53BP1-foci within hippocampal neurons. Moreover, subpopulations of neuronal stem/progenitor cells were quantified and dendritic arborization of developing neurons were assessed. To unravel molecular mechanisms involved in radiation-induced neurotoxicity, hippocampi were analyzed using mass spectrometry-based proteomics and affected signaling networks were validated by immunoblotting.

Results: Radiation-induced DNA damage accumulation leads to progressive decline of hippocampal neurogenesis with decreased numbers of stem/progenitor cells and reduced complexities of dendritic architectures, clearly more pronounced in repair-deficient mice. Proteome analysis revealed substantial changes in neurotrophic signaling, with strong suppression directly after LDR and compensatory upregulation later on to promote functional recovery.

Conclusion: Hippocampal neurogenesis is highly sensitive to repetitive LDR. Even low doses affect signaling networks within the neurogenic niche and interrupt the dynamic process of generation and maturation of neuronal stem/progenitor cells.

© 2019 Elsevier B.V. All rights reserved. Radiotherapy and Oncology 137 (2019) 45–54

Radiotherapy is an effective treatment modality for patients of all ages with malignant and benign tumors. With intensity-modulated radiotherapy (IMRT) multiple photon-beams from different directions and with adjusted intensities permit close shaping of radiation dose to target volumes, thereby delivering high doses to tumors while sparing specific risk regions. However, with IMRT large volumes of non-targeted brain regions are exposed to daily low-dose radiation (LDR), which may adversely affect neurocognitive functions. Due to improved treatment techniques, young cancer patients survive longer, and can therefore experience the debilitating late-effects of radiotherapy, including attention deficits and learning difficulties later in life [1].

Accumulating data indicate that ionizing radiation (IR) not only affects mature neuronal networks, but particularly proliferation and differentiation of neuronal stem/progenitor cells [2–7]. The generation of new neurons from largely quiescent neural stem cells occurs throughout life in the subgranular zone (SGZ) of hippocampal dentate gyrus. Neural stem cells give rise to transiently dividing precursor cells, that migrate into the granule cell layer, and differentiate into mature neurons which become functionally integrated into hippocampal circuitry [8]. Specific markers expressed in distinct cell types during different stages of neurogenesis permit to identify subpopulations within the complex hippocampal architecture. Transcription-factor SOX2 (SRY[sex-determining-region-Y]b ox2) plays important roles in maintaining neural stem/progenitor cell properties [9]. DCX (doublecortin) is expressed in migrating neuroblasts and immature neurons [10]. NeuN is used as specific marker for mature post-mitotic neurons [11]. Aging of the brain

* Corresponding author at: Department of Radiation Oncology, Saarland University, Kirrbergerstrasse Building 6.5, 66421 Homburg/Saar, Germany.

E-mail address: claudia.rube@uks.eu (C.E. Rube).

is marked by major decrease in the number of new neurons generated in hippocampal dentate gyrus [12]. This age-dependent decline of neurogenesis leads to reduced regeneration capacity and is caused by cell-intrinsic and cell-extrinsic signals within the neurogenic niche [13]. In hippocampal microenvironment, *cAMP response element-binding* (CREB) protein plays critical roles in proliferation, survival and differentiation of neuronal stem/progenitor cells [14]. In response to genotoxic insults, CREB-activation leads to expression of neuroprotective factors, such as *brain-derived neurotrophic factor* (BDNF) [15] and *activity-regulated cytoskeleton-associated protein* (ARC) [16], and contributes to protection and survival of newborn neurons.

Following exposure to ionizing radiation, cells incur DNA lesions that jeopardize genomic integrity, with double-strand breaks (DSBs) being the most critical DNA lesions. During DNA damage response (DDR) the formation of large aggregates of sensor/mediator proteins at DSB sites can be visualized as nuclear foci by immunofluorescence microscopy (IFM) [17]. Within these foci, activation of mediator proteins, most notably DNA-PK and Ataxia-Telangiectasia-Mutated (ATM), transduce DSB signals to numerous downstream effectors, setting the scene for DSB repair [18]. Mutations in these sensor/mediator proteins have been shown to contribute to pronounced radiosensitivity. Severe combined immunodeficiency (*SCID*) is caused by gene mutations encoding DNA-PKcs, resulting in defective V(D)J-recombination and extreme radiosensitivity [19]. ATM is mutated in the Ataxia-Telangiectasia (AT) syndrome, which is characterized by progressive neurodegeneration, telangiectasia, immunodeficiency, and marked radiosensitivity [18].

Radiation-induced accumulation of DNA damage in neuronal stem/progenitor cells may have profound impact on genomic integrity and may contribute to impairment of stem cell functions, with loss of self-renewal and differentiation capacities [20,21]. In the current experimental study, acute and long-term effects of fractionated LDR on the complex process of adult neurogenesis were characterized to evaluate the impact of genomic damage on neuronal stem cell behaviour.

Materials and methods

Mouse strains

C57BL/6 mice (Charles River Laboratories, Sulzfeld, Germany) were used as DNA repair-proficient wild-type (WT) mice; homozygous *ATM*^{-/-} (129S6/SvEvTac-*Atm*^{tm1Awb}/J; Jackson Laboratory) and *DNA-PKcs*^{-/-} mice (CB17/Icr-Prkdc^{scid}/Rj; Janvier, St. Berthevin Cedex, France.) served as DNA repair-deficient AT and SCID mice. Only male mice were used for these studies and housed in groups in IVC cages under standard laboratory conditions.

Animal irradiation

Whole-body radiation (0.1 Gy) was performed at linear accelerators (Artiste™, Siemens) as described previously [22]. Juvenile and young adult C57BL/6 mice (age P11 or P56 at start of LDR experiments) were daily irradiated from Monday to Friday for 1, 2, 3 or 4 weeks. 72 h after 5×, 10×, 15×, 20× fractions, and 1, 3, 6 months after 20× fractions animals were anesthetized prior to tissue collection. Adult AT and SCID mice received 1×, 10×, or 20× fractions and brain tissue was analyzed 72 h after the last exposure. Brain tissues of ≥3 mice per age, per strain and per time-point were analyzed compared to age-matched, non-irradiated controls. Studies were approved by Medical Sciences Animal Care and Use Committee of Saarland University.

Immunofluorescence microscopy

Formalin-fixed brain tissues were embedded in paraffin and cut into 4-μm coronal sections from Bregma -1.9 mm onwards. Paraffin was removed in xylene and sections were rehydrated in decreasing alcohol concentrations. Tissues were boiled in citrate buffer and pre-incubated with Roti™-Immunoblock (Carl Roth, Karlsruhe, Germany), incubated with primary antibodies (53BP1, Bethyl Laboratories, Montgomery, TX, USA; NeuN, Merck Millipore, Darmstadt, Germany; DCX, SantaCruz, Dallas, TX, USA; SOX2, Abcam, Cambridge, UK) followed by incubation with Alexa-Fluor-488 or Alexa-Fluor-568 secondary antibodies (Invitrogen, Karlsruhe, Germany). Finally, sections were mounted in VECTASHIELD™ with 4',6-diamidino-2-phenylindole (DAPI; Vector Laboratories, Burlingame, CA, USA). Nikon Eclipse Ni-E epifluorescence microscope equipped with charge-coupled-device camera and acquisition software (NIS-Elements, Nikon, Düsseldorf, Germany) was used to capture fluorescence images. 53BP1-foci were quantified in NeuN-positive neurons until at least 40 cells and 40 foci were registered per tissue sample. In DCX-stained sections overview tiles were acquired with ZEISS AxioScan, whereupon detailed 3D-image z-stacks were acquired with higher magnification (60×) using LSM-800-AiryScan. DCX⁺ cells were quantified in entire granule cell layers (GCL), SOX2⁺ cells were captured exclusively in subgranular zones (SGZ). Cell numbers and dendritic arborization (evaluated by measuring DCX⁺ areas) were reported in relation to GCL size, evaluated by NIS-elements software.

Protein isolation

Snap-frozen hippocampi were pulverized and resuspended in RIPA enriched with phosphatase/protease inhibitors. After sonification, suspensions were incubated and centrifugated and protein concentrations were determined using BCA method according to manufacturer's instructions [23].

Mass spectrometry-based proteome analysis:

Measurements were performed on QExactive mass-spectrometer (Thermo Fisher Scientific Inc.) coupled to UltiMate™3000 nano-RSLC (Thermo Fisher Scientific Inc.) as described previously [24].

Label-free proteomic analysis with progenesis QI

MS-spectra were further analyzed with Progenesis QI software (Nonlinear Dynamics, Water, Newcastle upon Tyne, UK) for label-free quantification as described before [24].

Bioinformatics

To identify radiation-affected signaling pathways, differentially regulated proteins were imported into Ingenuity Pathway Analysis (IPA, QIAGEN Redwood City, www.qiagen.com/ingenuity).

Western Blot

Samples were denatured with Laemmli-buffer and proteins were separated using 4–12% gradient gels and blotted onto nitrocellulose membranes. Membranes were blocked and incubated with first antibodies. After washing membranes were incubated with HRP-secondary antibodies and visualized with chemiluminescence detection. Protein bands were quantified with Image-J software. Ponceau staining served as internal loading control.

Statistical analysis

Differences in 53BP1-foci, DCX⁺ and SOX2⁺ cells between irradiated versus non-irradiated hippocampi were assessed using unpaired Student's *t*-test (GraphPad Software, La Jolla, CA, USA). Differences were considered statistically significant at *p*-values ≤ 0.05 . Filtering criteria for proteomics analyses: (i) significance for fold-change (ratio irradiated to non-irradiated) ≥ 1.30 or ≤ 0.770 ; (ii) $p \leq 0.05$; (iii) identification by $\geq 2UP$. For immunoblotting, differences in protein expression were considered to be significant if $p \leq 0.05$ (unpaired Student's *t*-test). Error bars were calculated as standard error of the mean (SEM).

Data availability

Raw MS-data are available in https://www.storedb.org/store_v3/study.jsp?studyId=1107

Results

53BP1-foci accumulation in hippocampal neurons during and after LDR

Double-staining for NeuN and 53BP1 was used to quantify DNA damage foci in mature, post-mitotic neurons located in hippocampal dentate gyrus of WT mice (Fig. 1). Only low 53BP1-foci levels (~ 0.03 foci/cell) were observed in non-irradiated controls (Fig. 1A, left panel). Directly after single-dose exposure to 0.1 Gy, approximately 1 focus/cell was induced at 0.1 h post-IR (Fig. 1A, middle panel). Following fractionated LDR (20×0.1 Gy, 72 h post-IR) the number of persisting foci was higher in hippocampal neurons compared to non-irradiated WT mice (Fig. 1A, right panel). To assess possible accumulation of persisting 53BP1-foci during fractionated LDR, juvenile and adult WT mice were examined 72 h after exposure to $5\times$, $10\times$, $15\times$, or $20\times$ fractions of 0.1 Gy, compared to non-irradiated, age-matched controls (Fig. 1B). The number of persisting 53BP1-foci increased significantly in juvenile and adult WT mice during fractionated LDR, with the maximum at 1 m post-IR (juvenile: 0.092 ± 0.0046 foci/cell; adult: 0.075 ± 0.004 foci/cell; Fig. 1B). Subsequently, numbers of radiation-induced foci decreased gradually, but failed to return to baseline levels observed in non-irradiated controls, even six months after the last exposure (Fig. 1B). Due to the limited numbers of DCX⁺ neuroprogenitors, it was not feasible to perform the quantitative analysis of 53BP1-foci in older mice. However, in the juvenile dentate gyrus we found similar kinetics of 53BP1-foci formation and disappearance in DCX⁺ neuroprogenitors.

Radiation-induced DNA damage usually induces cell-cycle arrest and apoptosis. Ki-67 immunostaining was performed to analyze the proliferative potential of neuronal precursors in the hippocampus (Suppl.1A). In juvenile WT mice the proportion of Ki67⁺ cells in the SGZ of dentate gyrus was significantly decreased 72 h after 20×0.1 Gy and, notably, at all later time-points (Suppl.1A, inset), indicating that proliferation of neurogenic precursors was compromised by repetitive LDR in the long term. In contrast, numbers of Ki67⁺ cells in adult WT mice were not significantly affected by LDR (Fig. 1A). To test whether this moderate DNA damage caused apoptosis in immature DCX⁺ neurons, Caspase-3 expression was analyzed (Suppl.1B). Quantification of Caspase-3 immunostaining showed no significant increase in apoptotic cells in juvenile or adult hippocampi 72 h after 20×0.1 Gy (Suppl.1B). In summary, these results indicate that even low doses of ionizing radiation may negatively influence neuronal proliferation in immature brain.

Cellular response of DCX⁺ neuroprogenitors to fractionated LDR

Using high-resolution imaging we analyzed the morphology of DCX⁺ neuroprogenitors to examine the effects of LDR on the development and maturation of their dendritic tree (Fig. 2A). In hippocampal dentate gyrus of non-irradiated brain, DCX⁺ cell bodies were primarily located in SGZ, while their dendrites extended radially into the molecular layer (Fig. 2A, left panel). Fractionated LDR resulted in distinct reduction in dendritic arborization with diminished branching, total length and dendritic complexity (Fig. 2B, right panel).

Next, the number of DCX⁺ cells was quantified in the SGZ of hippocampal dentate gyrus. In non-irradiated WT mice the physiological age-related decline of hippocampal neurogenesis correlated with decreased levels of DCX⁺ neuroprogenitors (Fig. 2B, upper panels). During and after fractionated LDR, the number of DCX⁺ neuroprogenitors was significantly lower across all time-points compared to non-irradiated, age-matched controls (Fig. 2B, upper panels). In juvenile WT mice, DCX⁺ neuroprogenitors decreased to $\sim 70\%$ during and immediately after fractionated LDR (20×0.1 Gy, 72 h post-IR: 702 ± 26 DCX⁺ cells/mm²; non-IR: 1007 ± 29 DCX⁺ cells/mm²), and stayed at low levels showing $\sim 50\%$ decrease in the long term, compared to non-irradiated aged-matched controls (20×0.1 Gy, 6 m post-IR: 85 ± 4 DCX⁺ cells/mm²; non-IR: 172 ± 11 DCX⁺ cells/mm²). In adult WT mice, radiation-induced decrease in DCX⁺ neuroprogenitors was less prominent, showing $\leq 25\%$ cell loss at early (20×0.1 Gy, 72 h post-IR: 298 ± 11 DCX⁺ cells/mm²; non-IR: 389 ± 8 DCX⁺ cells/mm²) and later time-points (20×0.1 Gy, 3 m post-IR: 147 ± 5 DCX⁺ cells/mm²; non-IR: 189 ± 14 DCX⁺ cells/mm²). Our findings suggest that the high neurogenic potential of developing brain is associated with marked susceptibility to genotoxic stress and may explain age-dependent vulnerability of hippocampal neurogenesis to radiation injury.

Subsequently, DCX⁺ areas were measured in hippocampal regions by 2D-image analysis to quantify radiation effects on arborization densities (Fig. 2B, lower panels). During fractionated LDR the percentage of DCX⁺ area in juvenile hippocampus declined from $\sim 12\%$ (5×0.1 Gy, 72 h post-IR) to $\sim 6\%$ (20×0.1 Gy, 72 h post-IR), and in adult hippocampus from $\sim 5\%$ (5×0.1 Gy, 72 h post-IR) to $\sim 3\%$ (20×0.1 Gy, 72 h post-IR), correlating with radiation-induced decrease of $\leq 50\%$ in juvenile and $\leq 25\%$ in adult hippocampus (Fig. 2B). Following fractionated LDR we observed constant reductions in dendritic arborization with clear decreases of $\leq 50\%$ in juvenile and $\leq 25\%$ in adult hippocampus, compared to non-irradiated controls. In summary, these results indicate significant long-lasting effects of repetitive LDR on the number of differentiating DCX⁺ neurons and the outgrowth and branching of their dendritic arbors. These radiation effects were even more pronounced in maturing brain of juvenile mice, likely reflecting the higher neurogenic potential leading to increased vulnerability to genotoxic stress.

Cellular response of SOX2⁺ stem/progenitor cells to fractionated LDR

Transcription-factor SOX2, expressed by slowly proliferating neuroprogenitors, is important in controlling self-renewal and multipotency. In the hippocampus of juvenile and adult WT mice, SOX2⁺ cells were quantified in the SGZ along the hilus of dentate gyrus (Fig. 3). In juvenile WT mice, numbers of SOX2⁺ precursors remained stable during LDR, but were significantly reduced at all time-points after LDR with 30–40% decreases compared to non-irradiated, age-matched controls (Fig. 3B, left panel). These temporal dynamics of SOX2⁺ cells may reflect that genotoxic insults caused by repetitive LDR result in their premature differentiation to replace damaged cells after radiation injury. In adult WT mice,

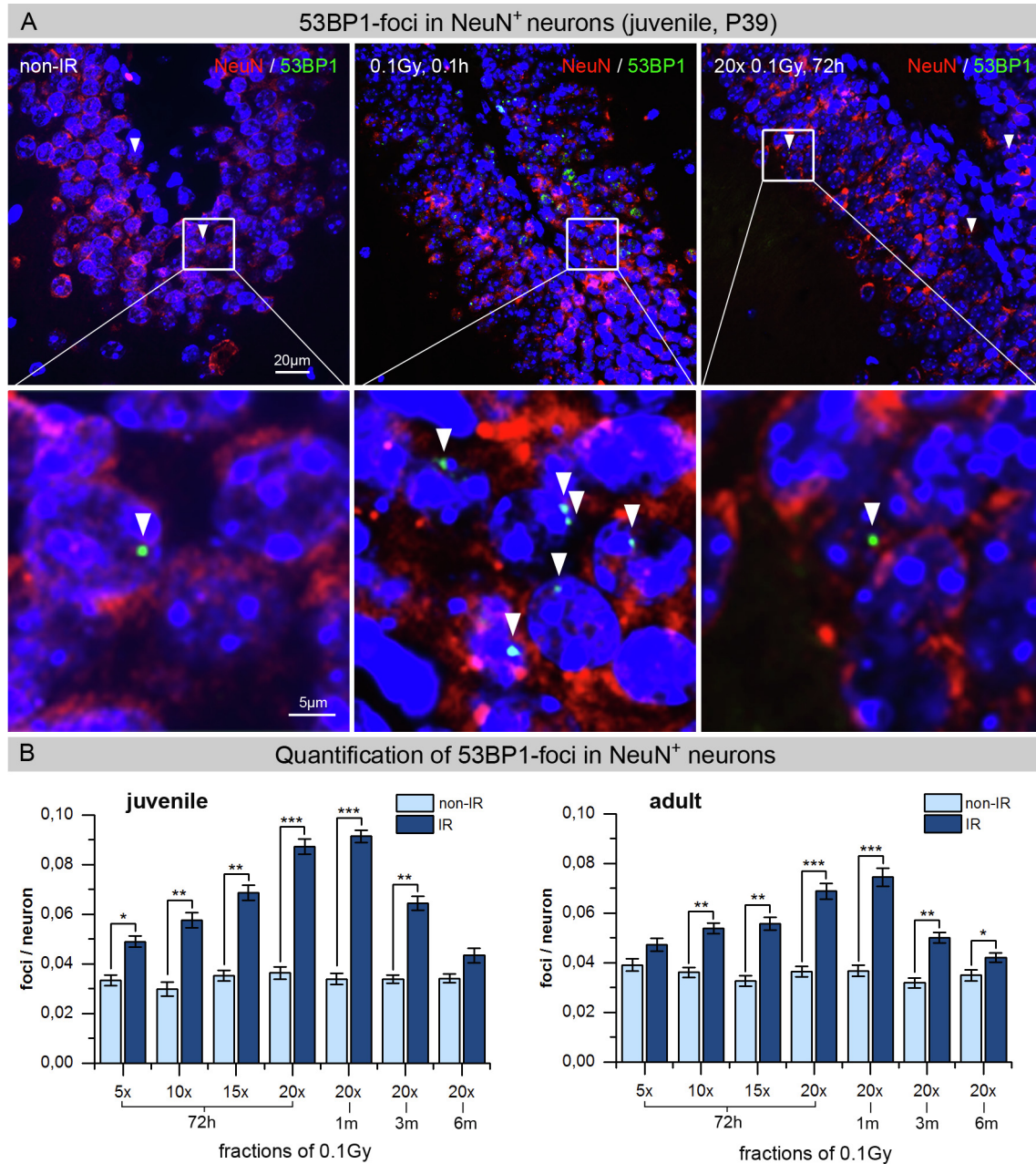


Fig. 1. 53BP1-foci accumulation in neurons during and after fractionated LDR. **A:** Immunofluorescence imaging of 53BP1-foci (green) in NeuN-positive nuclei (red) of non-irradiated and irradiated hippocampus from repair-proficient juvenile WT mice. Hippocampal neurons of control hippocampus show low 53BP1-foci levels (left panel). At 0.1 h after single-dose exposure to 0.1 Gy the number of foci was clearly increased (~1 focus/cell; middle panel). At 72 h after 20 × 0.1 Gy only few neurons showed persistent 53BP1-foci. Framed regions are shown at higher magnification (600×). Arrow heads mark 53BP1-foci. **B:** Quantification of radiation-induced 53BP1-foci in NeuN-positive hippocampal neurons. To analyze persistent DNA damage during and after fractionated LDR, numbers of 53BP1-foci per cell were quantified 72 h after 5×, 10×, 15× or 20× fractions of 0.1 Gy and 1, 3, and 6 months after 20 × 0.1 Gy. 53BP1-foci were quantified in hippocampal neurons of juvenile and young adult WT mice and compared to age-matched, non-irradiated controls. Error bars represent SEM, $n \geq 3$; *denotes statistically significant difference compared to non-irradiated control: $p < 0.05$; ** $p < 0.01$; *** $p < 0.001$.

the number of SOX2⁺ stem/progenitor cells *per se* was clearly lower compared to maturing brain, but was not significantly affected by LDR (Fig. 3B, right panel).

Defective DNA damage signaling determines stem cell functionality

ATM and DNA-PKcs are central DDR regulators, but understanding of their downstream signals determining stem cell functionality remains incomplete. Repair-deficient AT and SCID mice showed significantly increased basal levels of 53BP1-foci in neurons of non-irradiated hippocampi compared to WT mice (AT: 0.13 ± 0.02 foci/

cell; SCID: 0.35 ± 0.04 foci/cell) (Fig. 4A). Following fractionated LDR, repair-deficient AT mice showed significantly increased levels of remaining foci after 10 or 20 fractions, with the maximum of 0.66 ± 0.07 foci/cell (20 × 0.1 Gy). Repair-deficient SCID mice showed most pronounced accumulation of unrepaired DNA damage, with 1.70 ± 0.09 foci/cell after 20 × 0.1 Gy (Fig. 4A). Taken together, these elevated foci numbers after LDR reflect prominent DSB repair deficiency of AT and SCID mice.

As neurogenesis is particularly susceptible to genotoxic stress, neuronal stem/progenitor cells were quantified in SGZ of hippocampal dentate gyrus (Fig. 4B). In AT mice numbers of DCX⁺

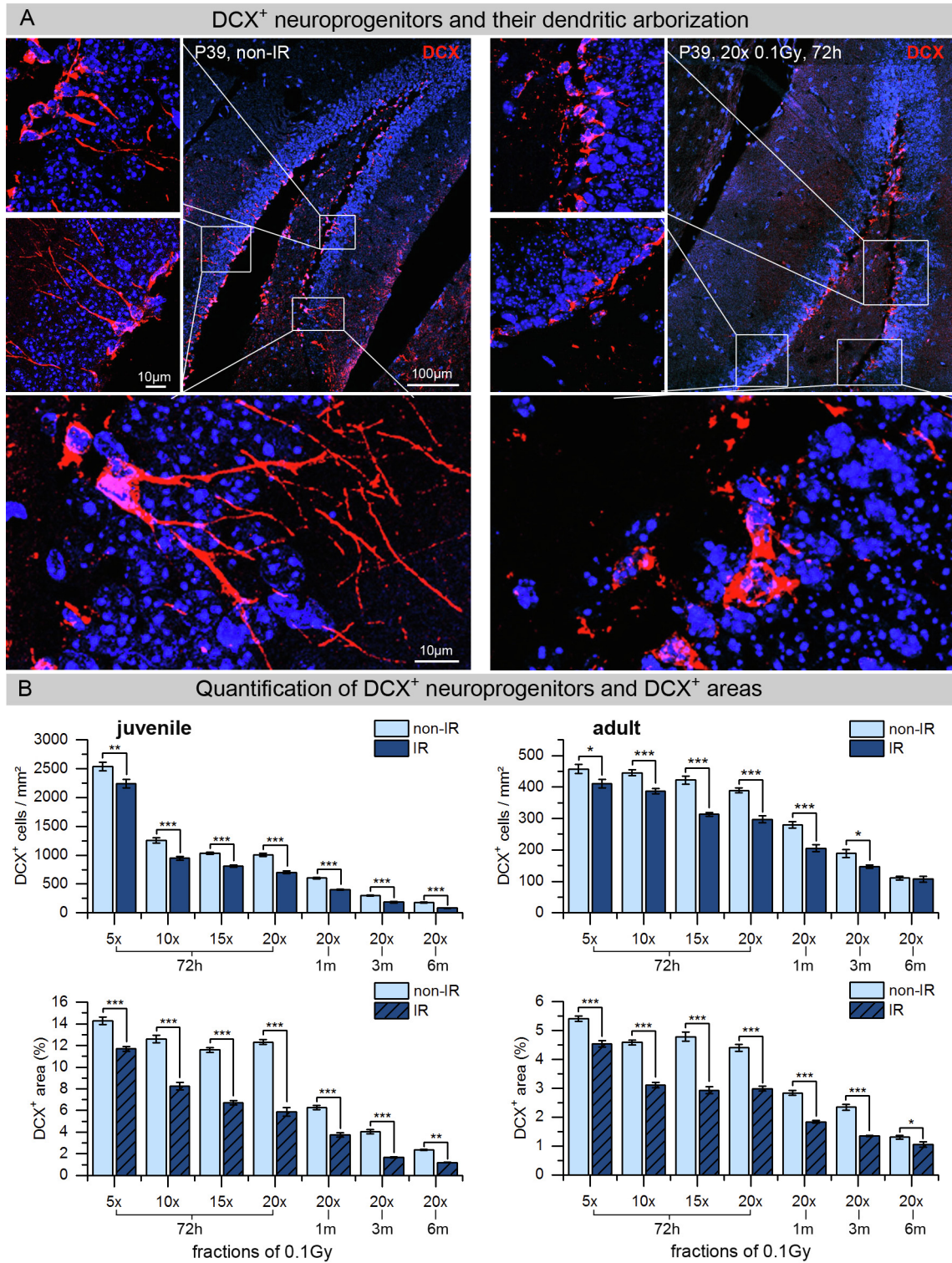


Fig. 2. DCX⁺ neuroprogenitors and their dendritic arborization. A: Immunofluorescence imaging of DCX (red) in the dentate gyrus of non-irradiated (left panel) and irradiated (20 × 0.1 Gy, 72 h) hippocampus (right panel) from juvenile WT mice. DCX⁺ precursor cells are abundant in the SGZ of the dentate gyrus and show intact dendritic arborization. Framed regions are shown at higher magnification (600×). Projections of confocal z-stacks show that DCX⁺ precursors after fractionated LDR are characterized by an impaired maturation of their dendritic tree. B: In the hippocampus of juvenile and adult WT mice the numbers of DCX⁺ cells and DCX⁺ area were quantified 72 h after 5 ×, 10 ×, 15 ×, or 20 × fractions of 0.1 Gy and 1, 3, and 6 months after 20 × 0.1 Gy, in comparison to age-matched, non-irradiated controls. Error bars represent SEM, *n* ≥ 3; *denotes statistically significant difference compared to non-irradiated control: *p* < 0.05; ***p* < 0.01; ****p* < 0.001.

immature neurons were clearly reduced before and after repetitive LDR (AT: 30–55 cells/mm²; WT: 300–450 cells/mm²), suggesting that even low levels of genomic damage result in their apoptotic elimination (Fig. 4B, lower panel). In SCID mice, almost normal

basal levels of DCX⁺ neuroprogenitors were observed in non-irradiated hippocampus (385 ± 6 cells/mm²), while DCX⁺ cell numbers decreased to ~30% after 10 × 0.1 Gy (116 ± 23 cells/mm²) and to ~10% after 20 × 0.1 Gy (39 ± 4 cells/mm²) (Fig. 4B). These

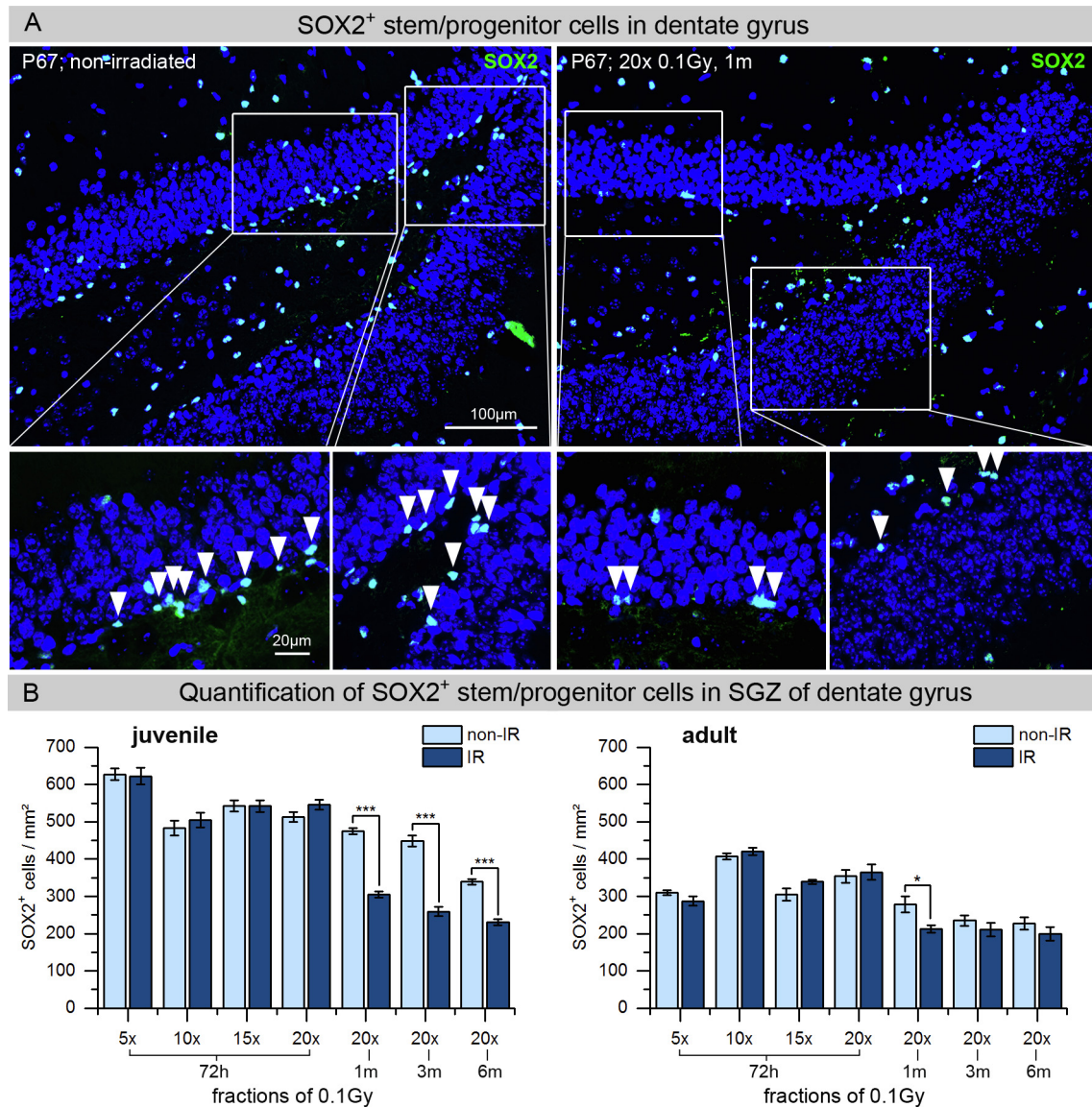


Fig. 3. SOX2⁺ stem/progenitor cells in the SGZ of the dentate gyrus. **A:** Immunofluorescence imaging for SOX2 (green) in the dentate gyrus of non-irradiated (left panel) and irradiated (20 × 0.1 Gy, 1 m) hippocampus (right panel) from adult WT mice (P67). SOX2⁺ cells in the SGZ represent neuronal stem cells. Framed regions are shown at higher magnification. Arrow heads mark SOX2⁺ nuclei in the SGZ. Scale bars represent 100 μm or 20 μm, respectively. Original magnification 600×. **B:** In the hippocampus of juvenile and adult WT mice the numbers of SOX2⁺ cells in the SGZ were quantified 72 h after 5×, 10×, 15×, 20× fractions of 0.1 Gy and 1, 3 and 6 months after 20 × 0.1 Gy, and compared to age-matched, non-irradiated controls. Error bars represent SEM, $n \geq 3$; *denotes statistically significant difference compared to non-irradiated control: * $p < 0.05$; ** $p < 0.01$; *** $p < 0.001$.

findings suggest that excessive DNA damage leads to apoptotic elimination of DCX⁺ neuroprogenitors due to their increased susceptibility. The number of slowly proliferating SOX2⁺ cells, by contrast, remained stable during fractionated LDR throughout the different mouse strains.

Fractionated LDR affects the hippocampal proteome

Analysis of hippocampal proteome of juvenile WT mice was performed 72 h, 1, 3 and 6 months after fractionated LDR (20 × 0.1 Gy). Label-free LC/MS-MS was used for comparison of irradiated hippocampus versus age-matched, non-irradiated controls. Volcano plots of all quantified proteins show the distribution of non-regulated and deregulated proteins (Fig. 5A). Total numbers of significantly down- and up-regulated proteins are shown in Fig. 5B. At 72 h post-IR, most proteins were down-regulated,

whereas at 1 m post-IR most proteins were up-regulated. At later time-points, the distribution of down- and up-regulated proteins was almost equal. Shared proteins are presented in the Venn diagram (Fig. 5C).

Pathway analysis indicates the modulation of CREB signaling

Deregulated proteins were further analyzed using Ingenuity Pathway Analysis (IPA) software. Most affected signaling pathways were synaptic long-term potentiation and CREB signaling, both of which are important in neuronal functioning (Suppl.2). Transcription-factor CREB is activated by phosphorylation of Ser133 via calmodulin kinases (CAMKs). Based on proteomics data, CAMKs were down-regulated at 72 h and 1 m post-IR, but up-regulated at 3 m post-IR (Suppl.2). Predicted changes in CREB-pathway were validated using immunoblotting. Levels of

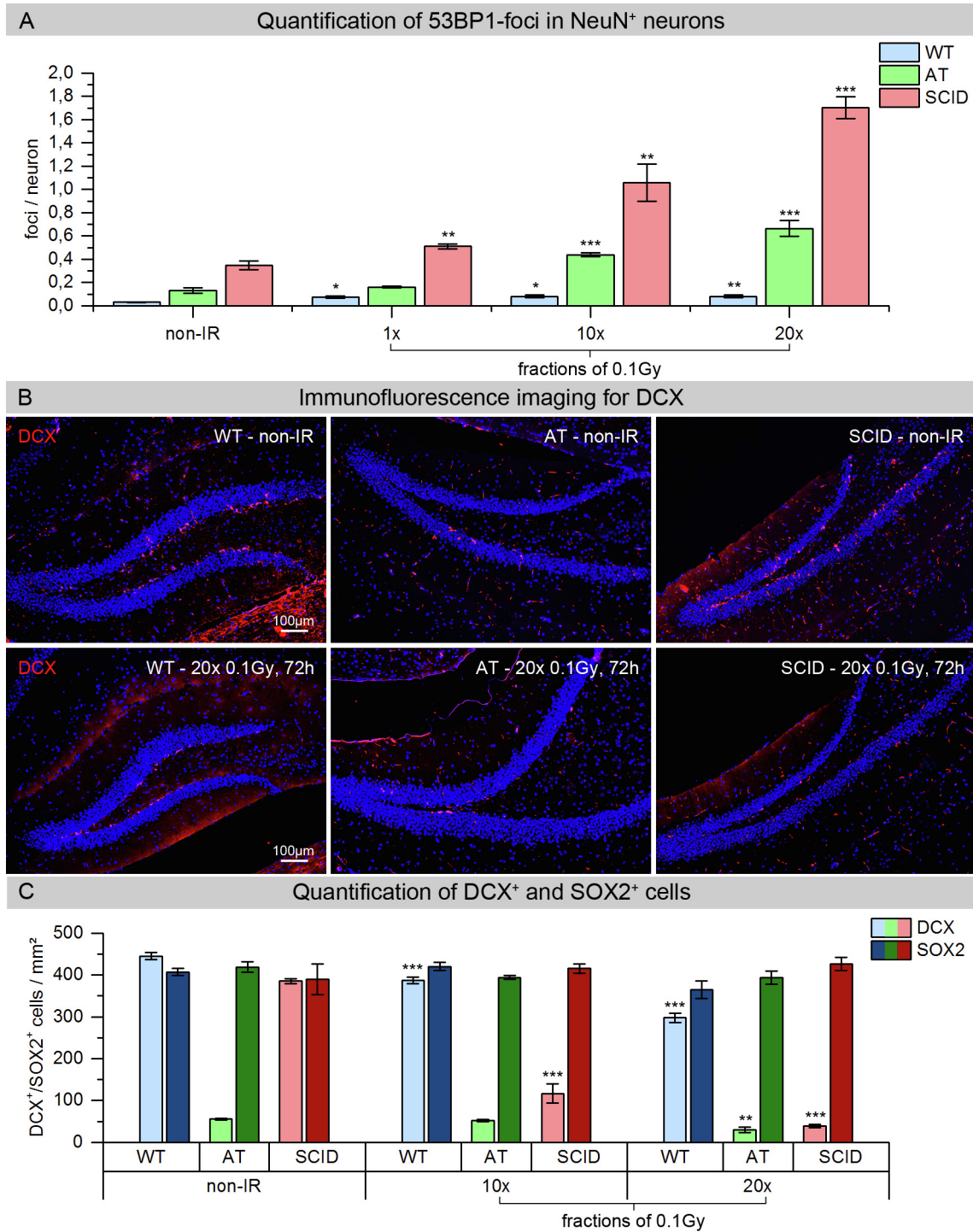


Fig. 4. Effect of DNA damage accumulation on adult neurogenesis A: Quantification of 53BP1-foci in hippocampal neurons 72 h after 1×, 10× and 20× fractions of 0.1 Gy in WT, AT and SCID mice, compared to non-irradiated controls. B: Immunofluorescence imaging for DCX in the dentate gyrus of non-irradiated and irradiated (20 × 0.1 Gy, 72 h) hippocampus from adult WT, AT and SCID mice. C: Quantification of DCX⁺ and SOX2⁺ cells in the SGZ of dentate gyrus of WT, AT and SCID mice performed 72 h after the last exposure of fractionated LDR (10× and 20× fractions of 0.1 Gy). Error bars represent SEM, *n* ≥ 3; * denotes statistically significant difference compared to non-irradiated control: * *p* < 0.05; ** *p* < 0.01; *** *p* < 0.001.

phosphorylated (Ser133) and total-CREB, and the downstream targets BDNF and ARC are shown in Fig. 6. Down-regulation of phospho-CREB (pCREB) at 72 h and 1 m post-IR and up-regulation at 3 m post-IR is in line with simultaneous down- and up-regulation of CAMKs (Suppl.2). In agreement with pCREB deregulation, the downstream targets BDNF and ARC were significantly

downregulated at 1 m post-IR and upregulated at 3 m post-IR (Fig. 6). Down-regulation of CREB-signaling directly after LDR suggests that radiation-induced genotoxic insults suppress hippocampal neurogenesis, whereas late-term CREB-activation may stimulate neuronal cell proliferation/differentiation and promote functional regeneration after genotoxic stress.

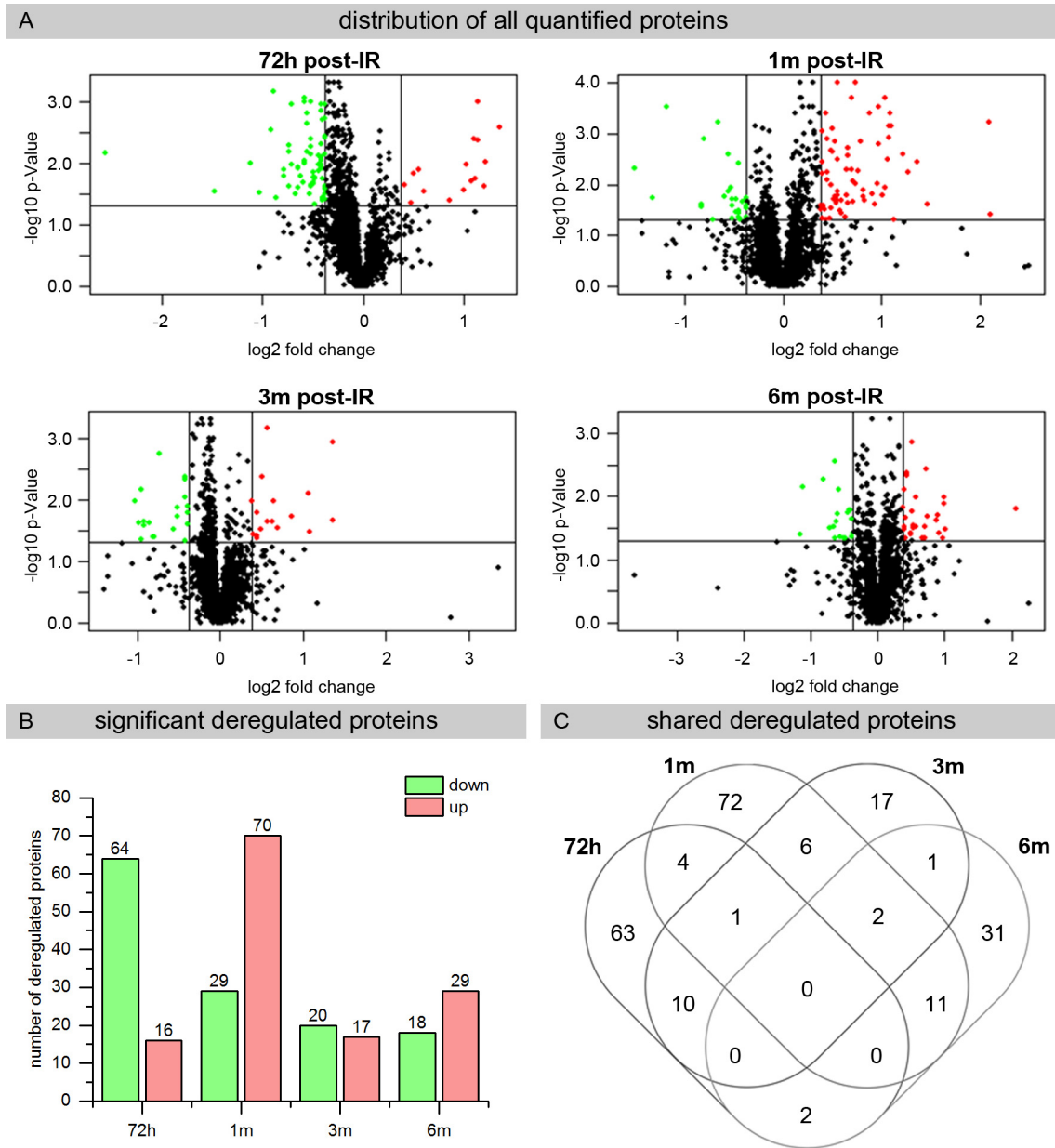


Fig. 5. Analysis of the hippocampal proteome. A: Volcano plots representing the distribution of all quantified proteins (identification with ≥ 2 UP) at 72 h, 1, 3 and 6 months post-IR (20×0.1 Gy). Deregulated proteins ($p \leq 0.05$, fold change ± 1.3) are highlighted in green (down-regulated) and red (up-regulated), respectively. B: Total numbers of significantly down-regulated (green) and up-regulated (red) proteins are shown for all time points ($p \leq 0.05$, fold change ± 1.3). C: Venn diagram illustrates the number of shared deregulated proteins at different time-points.

Discussion

The high hippocampal susceptibility to radiation injury is likely the causal factor of neurocognitive dysfunctions after exposure to ionizing radiation [25]. To analyze the impact of repeated low-dose exposure on hippocampal neurogenesis, we utilized an *in vivo* model, exposing genetically determined mouse strains with different DNA repair capacities to daily LDR. During this LDR regime mice were irradiated with 0.1 Gy every day (except weekends) for up to 4 weeks. Fractionated LDR enclosing only the head of every single animal is very laborious and time-consuming and would require daily narcosis for immobilization. The risks and side effects of daily anesthesia would clearly exceed the benefits of the selective brain irradiation, especially for young animals. Depending on their DNA repair capacity, repeated LDR led to varying levels of persisting DNA damage foci in hippocampal

neurons with increasing cumulative doses [22]. As a result of radiation-induced DNA damage accumulation hippocampal neurogenesis was seriously affected in DNA repair-deficient mice [26]. But even in repair-proficient WT mice, radiation-induced genotoxic stress resulted in progressive reduction in DCX⁺ immature neurons with impairment in their dendritic development. Importantly, following completion of fractionated LDR, DCX⁺ and SOX2⁺ cells exhibited significant long-lasting decline within their neurogenic niche, which was even more pronounced in juvenile brain.

The response of tissue-specific stem/progenitor cells to radiation exposure is an important determinant of overall tissue reaction. During the process of adult neurogenesis, heterogeneous mixtures of neuronal stem/precursors cells undergo numerous proliferation and differentiation stages. Our findings indicate that different subpopulations of neuronal stem/progenitor cells respond differently to fractionated LDR. The number of DCX⁺

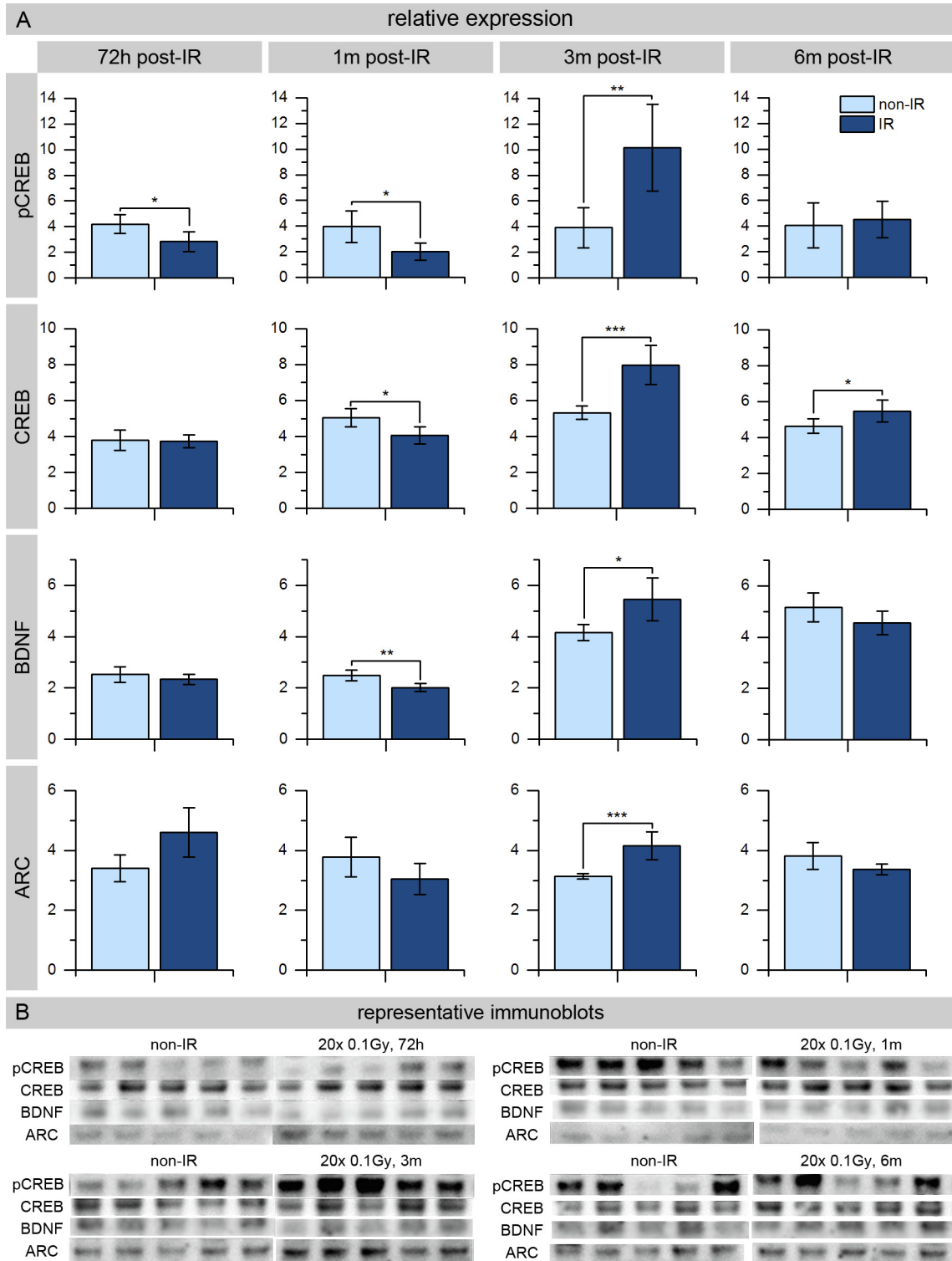


Fig. 6. Immunoblot analysis of phospho- and total-CREB levels and the downstream targets BDNF and ARC. The relative expression of phospho-CREB (Ser133), CREB, BDNF and ARC at 72 h, 1, 3 and 6 months post-IR (20 × 0.1 Gy) compared to non-irradiated, age-matched controls, after background correction and normalization to total amount of protein visualized by Ponceau staining. Error bars represent SEM, n ≥ 3; *denotes statistically significant difference compared to non-irradiated control: *p < 0.05; **p < 0.01; ***p < 0.001.

dividing progenitor cells and the complexity of their dendritic architectures gradually declined during and after LDR, likely due to radiation-induced suppression of proliferation and maturation. The number of SOX2⁺ stem/progenitor cells remained constant during LDR, but decreased significantly within several months after LDR. Regenerative processes necessitate stem cell replication with

enhanced differentiation/maturation to replace damaged cells after radiation injury [27]. Excessive activation of stem/progenitor cells by genotoxic insults may result in premature exhaustion of stem cells [20,28]. Our results suggest that this dynamic balance within the stem cell pool is critically influenced by repeated small doses of ionizing radiation. Higher proportions of proliferating

neuroprogenitors in juvenile hippocampus may explain the increased radiosusceptibility of young organisms [29]. This study provides the basis for future experiments designed to assess neurogenesis and neuroinflammation by the combination of immunocytochemistry with stereological techniques to estimate exactly the numbers of different cell populations in defined brain volumes after radiation-mediated damage.

Label-free quantitative proteomics based on mass spectrometry is an important approach for exploring protein functions and interactions in a large-scale manner. Since the isolation of specific regions is not feasible in unstained tissue, we used the whole hippocampus for proteomics analysis. Label-free LC-MS/MS technology is not sensitive enough to identify very weakly expressed proteins such as transcription factors. Nevertheless, based on protein profiling, the activation status of central transcriptional regulators can be predicted using specific software tools. In this study, the predicted changes in the active form of transcription factor CREB were followed by performing immunoblotting. Our hippocampal proteome analysis revealed the importance of CREB-mediated gene transcription in radiation response, with CREB-target proteins BDNF and ARC promoting neuronal maturation with outgrowth of axons and dendrites [30,31]. Down-regulation of CREB-signaling directly after LDR correlates with suppression of hippocampal neurogenesis. CREB-mediated up-regulation of neurotrophic factors suggest functional recovery of neurogenesis several months after fractionated LDR [32].

In summary, these results enhance our understanding of molecular and cellular dynamics that underlie hippocampal neurogenesis during and after fractionated LDR. Our experimental data indicate that fractionated LDR impairs neurogenesis, and may compromise hippocampus-dependent learning and memory. Markedly, our findings suggest that repeated LDR leads to persistent injury of hippocampal neurogenesis, even more pronounced in young individuals [33]. In future studies, cognitive functioning will be tested in this mouse model of fractionated LDR to assess potential radiation-induced deficits. This experimental study provides a framework for clinical radiotherapy, with recommendation for significant dose reduction in hippocampus regions whenever possible to prevent neuro-cognitive dysfunction.

Conflicts of interest

The authors declare no potential conflicts of interest.

Acknowledgement

The authors acknowledge the technical assistance of Dr. Eric Hummel, Carl Zeiss Microscopy GmbH, for high-resolution imaging and Kathrin Förderer for performing animal experiments.

Research grants

The research leading to these results has received funding from the Federal Ministry of Education and Research (BMBF), Germany under their reference numbers 02NUK035A (Claudia E. Rube) and 02NUK045C (Soile Tapio).

Appendix A. Supplementary data

Supplementary data to this article can be found online at <https://doi.org/10.1016/j.radonc.2019.04.021>.

References

[1] Padovani L, Andre N, Constine LS, Muracciole X. Neurocognitive function after radiotherapy for paediatric brain tumours. *Nat Rev Neurol* 2012;8:578–88.

- [2] Acharya MM, Patel NH, Craver BM, Tran KK, Giedzinski E, Tseng BP, et al. Consequences of low dose ionizing radiation exposure on the hippocampal microenvironment. *PLoS One* 2015;10:e0128316.
- [3] Parihar VK, Limoli CL. Cranial irradiation compromises neuronal architecture in the hippocampus. *Proc Natl Acad Sci USA* 2013;110:12822–7.
- [4] Rao AA, Ye H, Decker PA, Howe CL, Wetmore C. Therapeutic doses of cranial irradiation induce hippocampus-dependent cognitive deficits in young mice. *J Neurooncol* 2011;105:191–8.
- [5] Rola R, Fishman K, Baure J, Rosi S, Lamborn KR, Obenaus A, et al. Hippocampal neurogenesis and neuroinflammation after cranial irradiation with (56)Fe particles. *Radiat Res* 2008;169:626–32.
- [6] Schindler MK, Bourland JD, Forbes ME, Hua K, Riddle DR. Neurobiological responses to stereotactic focal irradiation of the adult rodent hippocampus. *J Neurol Sci* 2011;306:129–37.
- [7] Tang FR, Loke WK, Khoo BC. Postnatal irradiation-induced hippocampal neuropathology, cognitive impairment and aging. *Brain Dev* 2017;39:277–93.
- [8] Kempermann G, Song H, Gage FH. Neurogenesis in the Adult Hippocampus. *Cold Spring Harb Perspect Biol* 2015;7:a018812.
- [9] Amador-Arjona A, Cimadamore F, Huang CT, Wright R, Lewis S, Gage FH, et al. SOX2 primes the epigenetic landscape in neural precursors enabling proper gene activation during hippocampal neurogenesis. *Proc Natl Acad Sci USA* 2015;112:E1936–45.
- [10] von Bohlen Und Halbach O. Immunohistological markers for staging neurogenesis in adult hippocampus. *Cell Tissue Res* 2007;329:409–20.
- [11] Guse'nikova VV, Korzhevskiy DE, NeuN As a Neuronal Nuclear Antigen and Neuron Differentiation Marker. *Acta Naturae* 2015;7:42–7.
- [12] Semple BD, Blomgren K, Gimlin K, Ferriero DM, Noble-Haeusslein LJ. Brain development in rodents and humans: Identifying benchmarks of maturation and vulnerability to injury across species. *Prog Neurobiol* 2013;106–107:1–16.
- [13] Urban N, Guillemot F. Neurogenesis in the embryonic and adult brain: same regulators, different roles. *Front Cell Neurosci* 2014;8:396.
- [14] Merz K, Herold S, Lie DC. CREB in adult neurogenesis—master and partner in the development of adult-born neurons? *Eur J Neurosci* 2011;33:1078–86.
- [15] Panja D, Bramham CR. BDNF mechanisms in late LTP formation: A synthesis and breakdown. *Neuropharmacology* 2014;664–76.
- [16] Li Y, Pehrson AL, Waller JA, Dale E, Sanchez C, Gulino M. A critical evaluation of the activity-regulated cytoskeleton-associated protein (Arc/Arg3.1)'s putative role in regulating dendritic plasticity, cognitive processes, and mood in animal models of depression. *Front Neurosci* 2015;9:279.
- [17] Rothkamm K, Barnard S, Moquet J, Ellender M, Rana Z, Burdak-Rothkamm S. DNA damage foci: Meaning and significance. *Environ Mol Mutagen* 2015;56:491–504.
- [18] Shiloh Y, Ziv Y. The ATM protein kinase: regulating the cellular response to genotoxic stress, and more. *Nat Rev Mol Cell Biol* 2013;14:197–210.
- [19] Chang C, Biedermann KA, Mezzina M, Brown JM. Characterization of the DNA double strand break repair defect in scid mice. *Cancer Res* 1993;53:1244–8.
- [20] Behrens A, van Deursen JM, Rudolph KL, Schumacher B. Impact of genomic damage and ageing on stem cell function. *Nat Cell Biol* 2014;16:201–7.
- [21] Tang FR, Loke WK, Khoo BC. Low-dose or low-dose-rate ionizing radiation-induced bioeffects in animal models. *J Radiat Res* 2017;58:165–82.
- [22] Lorat Y, Schanz S, Rube CE. Ultrastructural insights into the biological significance of persisting DNA Damage foci after low doses of ionizing radiation. *Clin Cancer Res* 2016;22:5300–11.
- [23] Wisniewski JR, Zougman A, Nagaraj N, Mann M. Universal sample preparation method for proteome analysis. *Nat Methods* 2009;6:359–62.
- [24] Grosche A, Hauser A, Lepper MF, Mayo R, von Toerne C, Merl-Pham J, et al. The proteome of native adult muller glial cells from murine retina. *Mol Cell Proteomics* 2016;15:462–80.
- [25] Hladik D, Tapio S. Effects of ionizing radiation on the mammalian brain. *Mutat Res* 2016;770:219–30.
- [26] Enriquez-Rios V, Dumitriche LC, Downing SM, Li Y, Brown EJ, Russell HR, et al. DNA-PKcs, ATM, and ATR interplay maintains genome integrity during neurogenesis. *J Neurosci* 2017;37:893–905.
- [27] Favaro R, Valotta M, Ferri AL, Latorre E, Mariani J, Giachino C, et al. Hippocampal development and neural stem cell maintenance require Sox2-dependent regulation of Shh. *Nat Neurosci* 2009;12:1248–56.
- [28] Schuler N, Timm S, Rube CE. Hair follicle stem cell fate is dependent on chromatin remodeling capacity following low-dose radiation. *Stem Cells* 2018;36:574–88.
- [29] Hudson D, Kovalchuk I, Koturbash I, Kolb B, Martin OA, Kovalchuk O. Induction and persistence of radiation-induced DNA damage is more pronounced in young animals than in old animals. *Aging (Albany NY)* 2011;3:609–20.
- [30] Leal G, Comprido D, Duarte CB. BDNF-induced local protein synthesis and synaptic plasticity. *Neuropharmacology* 2014;639–56.
- [31] Sauvage MM, Nakamura NH, Beer Z. Mapping memory function in the medial temporal lobe with the immediate-early gene Arc. *Behav Brain Res* 2013;254:22–33.
- [32] Hwang IK, Yoo KY, Yoo DY, Choi JW, Lee CH, Choi JH, et al. Time-course of changes in phosphorylated CREB in neuroblasts and BDNF in the mouse dentate gyrus at early postnatal stages. *Cell Mol Neurobiol* 2011;31:669–74.
- [33] Casciati A, Dobos K, Antonelli F, Benedek A, Kempf SJ, Belles M, et al. Age-related effects of X-ray irradiation on mouse hippocampus. *Oncotarget* 2016;7:28.

4 Conclusions

The effects of high doses of ionising radiation on the brain and other tissues have been well studied. In the brain, it is generally accepted that the damage caused by high doses extends over several cell types and affects their proliferation and survival, their connections and their function in networks. The damage may also involve changes in the biochemical environment of the brain. This leads to disturbed neurogenesis and impaired signal transmission, which ultimately leads to cognitive impairment. (Hladik et al., 2016)

In contrast, the number of studies addressing the effects of low-dose radiation is relatively limited. Some epidemiological studies suggest that low-dose radiation, as used in medical procedures, may have adverse effects on neurocognitive processes (Hall et al., 2004; Pearce et al., 2012; Ron et al., 1982). However, the molecular mechanisms that underlie such radiation-induced alterations in normal brain function are not fully understood. The work presented here was performed to analyse how radiation doses relevant in medical procedures affect the brain under different experimental conditions.

4.1 Effect of low-dose IR on the murine hippocampus

4.1.1 Low-dose exposure leads to a long-term increase in oxidative stress and inflammation

As already described in the introduction, the impact of IR on water generates free radicals that, in turn, can damage cellular biomolecules (1.2) and play a major role in causing radiation-induced adverse effects on cells and organs.

In the first study (3.1, (Hladik et al., 2020)), an increased proportion of carbonylated proteins indicated enhanced oxidative stress remains even 24 months after a single radiation dose of 0.125 Gy or 0.5 Gy. It is already known that high doses of IR induce persistent oxidative stress in mice and rats (Cucinotta et al., 2019). However, it has not yet been demonstrated whether low doses that are more relevant in clinical applications, such as the dose to adjacent normal tissues during cancer therapy or from repeated imaging, cause oxidative stress. The present results show that oxidative stress remains even 24 months after a single low-dose (0.5 Gy) exposure. Consequently, radiation effects that occur long after irradiation or increase over time could be caused by a long-lasting increase in oxidative stress in the brain.

Inflammation is known to occur as a delayed response to a chronic increase of free radicals. Microglia and astrocytes are activated at the beginning of an acute inflammatory reaction in the brain (see Figure 6). In the activated state they recognize neuronal damage in their environment (Cucinotta et al., 2019; Kettenmann et al., 2013; Lumniczky et al., 2017). These activated immune cells in turn produce ROS that further activates microglia and astrocytes (Greene-Schloesser et al., 2012), leading to a situation of chronic inflammation and sustained oxidative stress such as seen in our model (Hladik et al., 2020). Mice exposed to a radiation dose of 0.5 Gy showed a sustained increase in the IBA1 protein as a marker for activated microglia and an increase in GFAP as a marker for reactive astrocytes 24 months post-exposure. This is an indicator for the initial inflammation that was induced by a single low-dose exposure turning into a chronic inflammatory state typically characterized by the persistent activation of the immune cells. This could therefore be the explanation for the persistently increased oxidative stress observed 24 months after irradiation.

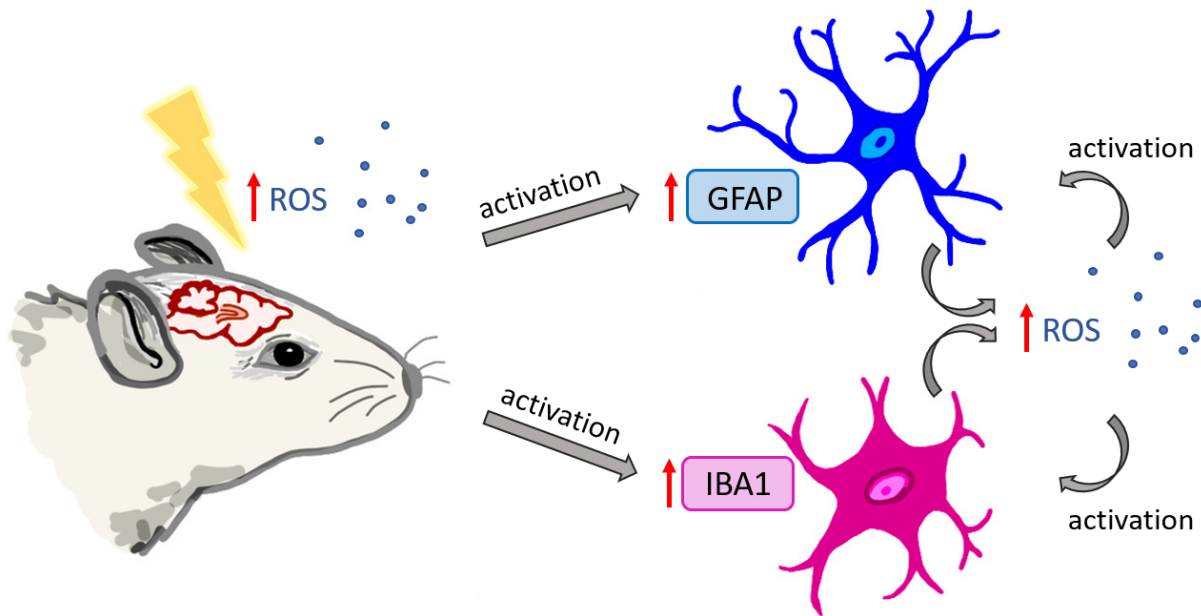


Figure 6: Induction of chronic inflammation by a single low-dose radiation exposure. Radiation exposure leads to the generation of oxidative stress that results in the activation of immune cells in the brain. Consequently, reactive astrocytes (GFAP) and activated microglia (IBA1) produce free radicals. This leads to long-term chronic activation of the immune system and a pro-inflammatory status.

4.1.2 Effect on neuronal structures

In study two of this thesis (3.2, (Hladik et al., 2019)), the proteome analysis of irradiated hippocampal tissue in combination with ketamine showed that many proteins playing an important role in synaptic long-term potentiation (LTP) are altered after irradiation. The LTP describes the enhancement of neuronal synaptic transmission in response to increased action potential frequencies. It is the basis for synaptic plasticity that is defined as the formation and degradation of connections between neurons depending on their use. Precisely this plasticity is essential for learning and memory processes (Bear et al., 1994; Kemp et al., 2007).

The dendritic structures of neurons are the location where the integration of inputs and the propagation of signals take place. Acute and chronic stress was shown to induce changes and remodelling of the dendritic structures that were correlated with neuronal disorders and mental retardation (Kaufmann et al., 2000; McAllister, 2000; Penzes et al., 2011; Purpura, 1975; Wu et al., 1999). For example, depression and cognitive decline are often associated with an increase in dendritic length and branching similar to morphologic changes found in the neuropathic pain disease (Metz et al., 2009).

It could be proven in this doctoral thesis (3.2, (Hladik et al., 2019)) that a combined exposure with low-dose radiation and ketamine had a pronounced effect on the dendritic complexity not present in mice exposed to either ketamine or radiation alone. The dendritic length and number of branching points of the hippocampal CA1 neurons were significantly increased after 100 mGy or 200 mGy in combination with ketamine. Additionally, the relative number of spines was reduced in the same animals. These effects were not present when the mice were sham treated or exposed to ketamine or low-dose radiation alone. We assume that this phenomenon leads to mis-forwarding of neuronal information and could therefore be the molecular explanation for the observed behavioural changes in similarly treated mice (Buratovic et al., 2018; Hladik et al., 2019). At the molecular level, a significant increase in the expression of BDNF, a protein that is known to be an important modulator of synaptic plasticity (Boyce et al., 2012; Gottmann et al., 2009), was detected. Several studies have proven the influence of BDNF on dendritic complexity in the developing, but also in the mature brain, dependent on the neuronal activity (Cohen-Cory, 1999; Kellner et al., 2014). The reduction in BDNF levels during normal brain aging coincided with a reduction in dendritic complexity and spine density in senescent rats

(von Bohlen und Halbach, 2010) and BDNF knockout mice showed strong impairment of the LTP and learning performance (Korte et al., 1995; Psotta et al., 2013). Moreover, patients with depression often show lowered BDNF blood levels (Cunha et al., 2006). Constant ketamine application is known to increase the BDNF level and is therefore considered to be a promising new approach among adult patients with depressive disorder (Allen et al., 2015; Murrough, Iosifescu, et al., 2013; Murrough, Wan, et al., 2013). In the study presented in this thesis (3.2, (Hladik et al., 2019)), the results of combined treatment with radiation are similar to those which were achieved when ketamine was constantly applied (Allen et al., 2015; Murrough, Iosifescu, et al., 2013; Murrough, Wan, et al., 2013). This indicated that a single exposure to the combination ketamine and low-dose radiation induced an effect resembling that of persistent ketamine application without radiation. The mechanistic basis for the BDNF increase is still unclear.

In contrast to the results from the ketamine study (3.2, (Hladik et al., 2019)), the DCX positive neurons of the hippocampus in the third study (3.3, (Schmal et al., 2019)) showed a reduced dendritic complexity after the fractionated radiation exposure of 20 x 100 mGy, with the cumulative dose of 2 Gy. These results are similar to a study by Parihar et al. showing a dose-dependent reduction of dendritic complexity in the hippocampal neurons at doses of 1 Gy or 10 Gy. This suggests that the effect of fractionated low doses resemble those of a single exposure at a similar dose (Parihar et al., 2013), at least in the hippocampus. It could also be shown in this thesis (3.2, (Hladik et al., 2019)) that a single exposure to 100 mGy or 200 mGy had no effect on the neuronal structures.

Figure 7 compares the different effects of a single low-dose irradiation, a single low-dose in combination with ketamine and repeated exposure to low-dose radiation on the structure of hippocampal neurons studied in this work (3.1, 3.2, 3.3).

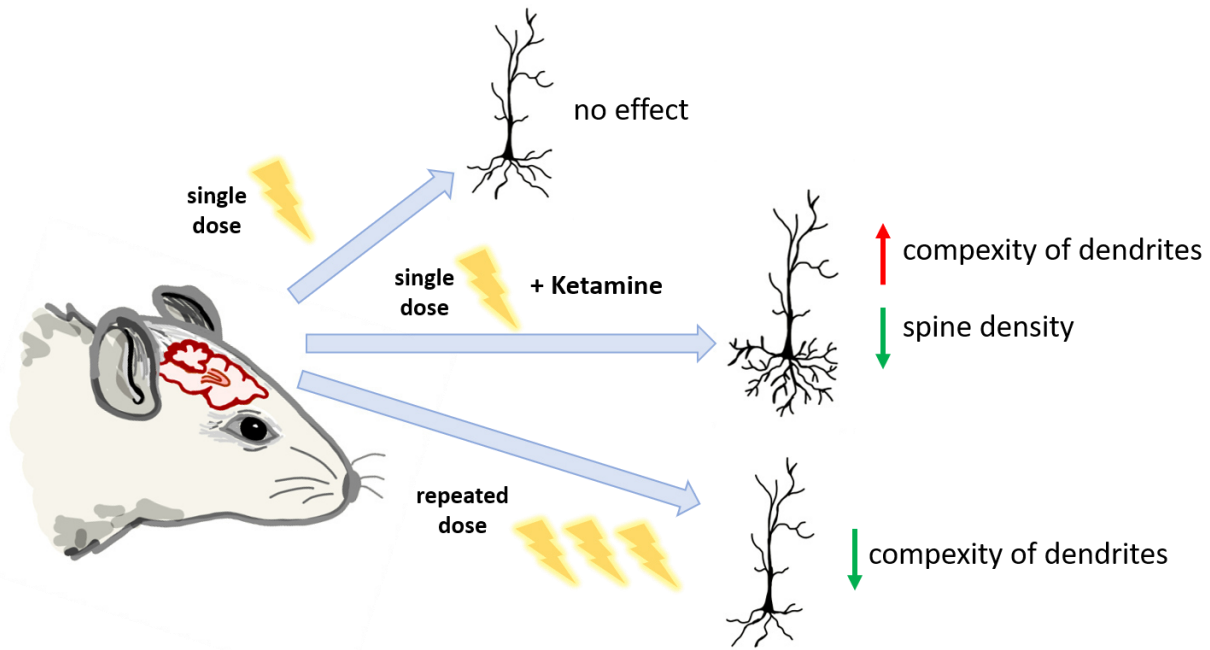


Figure 7: Different impact of low-dose radiation on neuronal structures depending on the experimental set up. It was shown that a single low radiation dose (100 mGy, 200 mGy) had no effect on the basal dendrites of CA1 neurons. Combined to a single injection of ketamine (7,5 mg/kg) the number of dendrites and their branching increased whereas the spine density was lower than in the control animals. In contrast, a fractionated exposure to low radiation dose (20 x 100 mGy) decreased the complexity of DCX positive neurons in the hippocampus. All effects were measured up to six months post-exposure.

4.1.3 Effect on the hippocampal cell composition

The hippocampus is one of the few regions in the adult brain where pools of regenerative neural stem cells remain (1.3). They are located in neurogenic niches, generate mature neurons and appear to be particularly sensitive to the effects of IR (Bellinzona et al., 1996; Mizumatsu et al., 2003; Monje et al., 2002). There are two different ways in which irradiation may act on this group of cells. On the one hand, directly induced cell death of the neurons leads to reduction in the stem cell pool. On the other hand, radiation may cause an indirect change in the tissue microenvironment, also leading to a reduction of proliferation and neurogenesis (Lazarini et al., 2009; Michaelidesova et al., 2019; Mizumatsu et al., 2003).

In the third study of this thesis (3.3, (Schmal et al., 2019)) the effects of fractionated low-dose exposure that is relevant for the healthy surrounding tissue during radiotherapy of

brain tumours was investigated. Therefore, hippocampal tissue of juvenile and adult mice was stained for doublecortin (DCX), as a marker for neural progenitors, and for SRY (sex determining region Y)-box 2 (SOX2) for neuronal stem cells, to analyse the effect of repeated low-dose exposure on the hippocampal cell composition. The results indicate a significant decline in both cell populations already 72 hours post radiation. This effect is still measurable six months later. The decline was present in juvenile and adult mice but more pronounced when mice were irradiated at young age. Reduced proliferation rate and altered neurogenesis are believed to be one of the major causes in the pathogenesis of radiation-induced cognitive decline. These results indicate that even low radiation doses disturb the dynamics of the neural generation. It also emphasizes how sensitive the hippocampal cell composition is even when the irradiation occurs at the adult age. (Schmal et al., 2019)

4.2 The effect of low-dose irradiation on the hippocampal proteome

The data of this work (3.1, 3.2, 3.3) have shown a variety of long-lasting effects following low-dose irradiation of the hippocampus.

Whole hippocampal proteome analysis was performed to determine the effects of low-dose radiation on the composition of the hippocampal proteins at different time points post-irradiation. The label-free LC/MS-MS methodology was applied to gain understanding of the global cellular adaptation to the radiation exposure in order to identify the central affected pathways and key players. The proteome composition after radiation differed depending on the experimental design. The number of deregulated proteins increased after a single exposure to low-dose radiation (0.063 - 0.5 Gy) over time (3.1, (Hladik et al., 2020)). A much higher cumulative dose of 2 Gy given in 0.1 Gy fractions in the third study (3.3, (Schmal et al., 2019)) resulted in an immediate (72 hours) increase in the number of deregulated proteins that declined by six months after irradiation. After fractionated exposure the number of deregulated proteins was the highest after 72 hours and dropped consequently until six months post expose. This shows how different the effects of lower doses are. Repeated exposure leads to an accumulation of radiation, which results in effects similar to them induced by a single high dose exposure.

4.2.1 The central role of the CREB pathway

In the studies of this doctoral thesis, one pathway namely the CREB signalling has been identified as being particularly involved in the radiation response after low-dose exposure. The CREB protein and its associated upstream and downstream targets are involved in a variety of cellular processes in the brain, including neurogenesis, proliferation, synaptic plasticity, and neuronal protection. It has several mediators as illustrated in Figure 8 (Sakamoto et al., 2011; Walton et al., 2000).

In response to external stressors like radiation, the transcriptional activity of CREB is mainly regulated by phosphorylation by kinases including the p38 mitogen-activated protein kinase (p38) and the extracellular signal-regulated kinase 1/2 (ERK1/2) (Gonzalez et al., 1989; Lonze et al., 2002). Through a phosphorylation on Ser133, phospho-CREB forms homodimers and induces the transcription of target genes (Yamamoto et al., 1988). The fact that putative CREB binding sites can be found in the regulatory elements of over 4000 genes (Zhang et al., 2005) underlines the functional diversity and importance of CREB signalling for cellular processes.

All three studies found that either CREB or downstream target genes of CREB respond to low-dose radiation. The regulation of CREB varied depending on the dose and the time after irradiation. In the first study (3.1, (Hladik et al., 2020)) a single exposure of 0.063 or 0.125 Gy caused an increase in the phosphorylation of CREB and the corresponding upstream kinases and downstream targets two years after irradiation. Proteins of the BCL-2 family that inhibit apoptosis-inducing proteins and thus have a neuroprotective effect, were found to be increased. In contrast, irradiation with the dose of 0.5 Gy led to a significant reduction of the CREB protein level and of its phosphorylated Ser133 form. Significantly, the anti-apoptotic CREB target protein b-cell lymphoma-extra large (BCL-xL) was reduced, coinciding with a measurable increase in marker proteins for apoptosis (BAX, CASP3). Importantly, phosphorylated CREB has been proposed to directly inhibit the nuclear factor 'kappa-light-chain-enhancer' of activated B-cells (NF- κ B) activation and thereby inhibit pro-inflammatory responses (Wen et al., 2010). In accordance with the suggested compromised activity of CREB, markers for activated microglia and reactive astrocytes were only detected after the dose of 0.5 Gy (Hladik et al., 2020).

Moreover, the results from the third study (3.3, (Schmal et al., 2019)) also revealed changes of CREB signalling in response to radiation. Protein levels of CREB were significantly downregulated 72 hours after finishing of the fractionated exposure. This correlated with the earlier described (1.4.3, 1.4.4) decrease in neurogenesis and dendritic complexity. After several months, the CREB-mediated transcription was upregulated (Schmal et al., 2019) suggesting the functional recovery of the neuroprotective response.

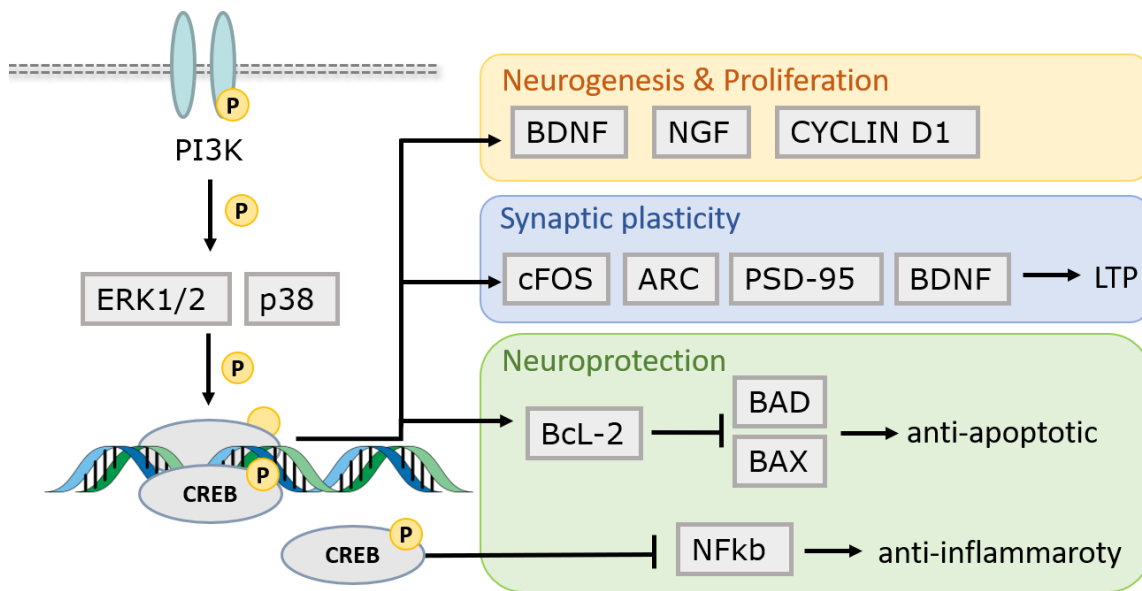


Figure 8: The CREB signalling pathways and its downstream targets. The transcription factor CREB is activated in the brain via kinases that are activated in response to external stressors like radiation exposure. CREB signalling is involved in the maintenance of neurogenesis and proliferation and in the regulation of synaptic plasticity. It is neuroprotective in response to external stimuli.

An especially relevant CREB target is the BDNF protein as it plays a central role in neurogenesis and synaptic plasticity. As already described in 4.1.2, BDNF was significantly upregulated after a combined application of ketamine and low-dose radiation, leading to an increased dendritic complexity. In contrast, BDNF expression was significantly downregulated after fractionated radiation leading to reductions in neurogenesis, dendritic branching and length.

Similar decreases in CREB activity have been found to be present in several neurodegenerative disorders, including Alzheimer’s disease, Parkinson’s disease and Huntington’s disease, as well as during normal brain aging (Gil et al., 2008; Ma et al.,

2007; Mantamadiotis et al., 2002). Knock-out experiments in mice have revealed that the neuroprotective response towards ROS-mediated cell toxicity was abrogated by disruption of the CREB-mediated transcription (B. Lee et al., 2009; Pregi et al., 2017). Therefore, CREB signalling is of importance for the nervous system's response to radiation by adapting its expression and activity to the external stressors. This shows the relevance of CREB for future research in the radiation protection in context of various clinical applications.

4.3 Final Conclusion

The results of this thesis demonstrate that a low-dose of ionising radiation has a strong and sustained effect on the hippocampus of mice irradiated at either a juvenile or adult age. A single radiation dose causes alterations that are suggestive of a potentiation of normal aging processes. The results provide evidence of increased inflammation and cell death at a dose of 0.5 Gy, while lower doses appear to trigger a protective anti-inflammatory effect. In addition, a decrease in neurogenesis was measured when the animals were exposed at a young age. In clinical application, low doses are often used in combination with sedatives to achieve the required immobility of the patient during imaging. Based on observations included in this thesis, the combination of low-dose radiation and ketamine might lead to an enormous increase in complexity of neuronal dendrites as observed in diseases associated with mental retardation.

In conclusion, it is important to consider that possible adverse consequences to the brain may occur following low-dose radiation exposure, especially if children are exposed. Furthermore, the observed activation of neuroprotective mechanisms by very low doses could be a new basis for future strategies to protect the nervous system from higher radiation doses or other harmful stressors.

References

- Allen, A. P., Naughton, M., Dowling, J., Walsh, A., Ismail, F., Shorten, G., Scott, L., McLoughlin, D. M., Cryan, J. F., Dinan, T. G., & Clarke, G. (2015). Serum BDNF as a peripheral biomarker of treatment-resistant depression and the rapid antidepressant response: A comparison of ketamine and ECT. *J Affect Disord*, *186*, 306-311. doi:10.1016/j.jad.2015.06.033
- Anderson, G., & Maes, M. (2017). How Immune-inflammatory Processes Link CNS and Psychiatric Disorders: Classification and Treatment Implications. *CNS Neurol Disord Drug Targets*, *16*(3), 266-278. doi:10.2174/1871527315666161122144659
- Asara, J. M., Christofk, H. R., Freimark, L. M., & Cantley, L. C. (2008). A label-free quantification method by MS/MS TIC compared to SILAC and spectral counting in a proteomics screen. *Proteomics*, *8*(5), 994-999. doi:10.1002/pmic.200700426
- Azimzadeh, O., Atkinson, M. J., & Tapio, S. (2014). Proteomics in radiation research: present status and future perspectives. *Radiat Environ Biophys*, *53*(1), 31-38. doi:10.1007/s00411-013-0495-4
- Baluna, R. G., Eng, T. Y., & Thomas, C. R. (2006). Adhesion molecules in radiotherapy. *Radiat Res*, *166*(6), 819-831. doi:10.1667/RR0380.1
- Bantscheff, M., Schirle, M., Sweetman, G., Rick, J., & Kuster, B. (2007). Quantitative mass spectrometry in proteomics: a critical review. *Anal Bioanal Chem*, *389*(4), 1017-1031. doi:10.1007/s00216-007-1486-6
- Bear, M. F., & Malenka, R. C. (1994). Synaptic plasticity: LTP and LTD. *Curr Opin Neurobiol*, *4*(3), 389-399. doi:10.1016/0959-4388(94)90101-5
- Bellinzona, M., Gobbel, G. T., Shinohara, C., & Fike, J. R. (1996). Apoptosis is induced in the subependyma of young adult rats by ionizing irradiation. *Neurosci Lett*, *208*(3), 163-166.
- Blomstrand, M., Kalm, M., Grander, R., Bjork-Eriksson, T., & Blomgren, K. (2014). Different reactions to irradiation in the juvenile and adult hippocampus. *Int J Radiat Biol*, *90*(9), 807-815. doi:10.3109/09553002.2014.942015
- Boyce, V. S., Park, J., Gage, F. H., & Mendell, L. M. (2012). Differential effects of brain-derived neurotrophic factor and neurotrophin-3 on hindlimb function in paraplegic rats. *Eur J Neurosci*, *35*(2), 221-232. doi:10.1111/j.1460-9568.2011.07950.x
- Brown, W. R., Blair, R. M., Moody, D. M., Thore, C. R., Ahmed, S., Robbins, M. E., & Wheeler, K. T. (2007). Capillary loss precedes the cognitive impairment induced by fractionated whole-brain irradiation: a potential rat model of vascular dementia. *J Neurol Sci*, *257*(1-2), 67-71. doi:10.1016/j.jns.2007.01.014
- Buratovic, S., Stenerlow, B., Sundell-Bergman, S., Fredriksson, A., Viberg, H., Gordh, T., & Eriksson, P. (2018). Effects on adult cognitive function after neonatal exposure to clinically relevant doses of ionising radiation and ketamine in mice. *Br J Anaesth*, *120*(3), 546-554. doi:10.1016/j.bja.2017.11.099
- Casciati, A., Dobos, K., Antonelli, F., Benedek, A., Kempf, S. J., Belles, M., Balogh, A., Tanori, M., Heredia, L., Atkinson, M. J., von Toerne, C., Azimzadeh, O., Saran, A., Safrany, G., Benotmane, M. A., Linares-Vidal, M. V., Tapio, S., Lumniczky, K., & Pazzaglia, S. (2016). Age-related effects of X-ray irradiation on mouse hippocampus. *Oncotarget*, *7*(19), 28040-28058. doi:10.18632/oncotarget.8575
- Chakraborti, A., Allen, A., Allen, B., Rosi, S., & Fike, J. R. (2012). Cranial irradiation alters dendritic spine density and morphology in the hippocampus. *PLoS One*, *7*(7), e40844. doi:10.1371/journal.pone.0040844

- Chang, H. H. Y., Pannunzio, N. R., Adachi, N., & Lieber, M. R. (2017). Non-homologous DNA end joining and alternative pathways to double-strand break repair. *Nat Rev Mol Cell Biol*, *18*(8), 495-506. doi:10.1038/nrm.2017.48
- Chen, H., Yoshioka, H., Kim, G. S., Jung, J. E., Okami, N., Sakata, H., Maier, C. M., Narasimhan, P., Goeders, C. E., & Chan, P. H. (2011). Oxidative stress in ischemic brain damage: mechanisms of cell death and potential molecular targets for neuroprotection. *Antioxid Redox Signal*, *14*(8), 1505-1517. doi:10.1089/ars.2010.3576
- Chiang, C. S., Hong, J. H., Stalder, A., Sun, J. R., Withers, H. R., & McBride, W. H. (1997). Delayed molecular responses to brain irradiation. *Int J Radiat Biol*, *72*(1), 45-53.
- Chiang, C. S., McBride, W. H., & Withers, H. R. (1993). Radiation-induced astrocytic and microglial responses in mouse brain. *Radiother Oncol*, *29*(1), 60-68. doi:10.1016/0167-8140(93)90174-7
- Cohen-Cory, S. (1999). BDNF modulates, but does not mediate, activity-dependent branching and remodeling of optic axon arbors in vivo. *J Neurosci*, *19*(22), 9996-10003.
- Conner, K. R., Forbes, M. E., Lee, W. H., Lee, Y. W., & Riddle, D. R. (2011). AT1 receptor antagonism does not influence early radiation-induced changes in microglial activation or neurogenesis in the normal rat brain. *Radiat Res*, *176*(1), 71-83.
- Cucinotta, F. A., & Cacao, E. (2019). Risks of cognitive detriments after low dose heavy ion and proton exposures. *Int J Radiat Biol*, *95*(7), 985-998. doi:10.1080/09553002.2019.1623427
- Cunha, A. B., Frey, B. N., Andreatza, A. C., Goi, J. D., Rosa, A. R., Goncalves, C. A., Santin, A., & Kapczinski, F. (2006). Serum brain-derived neurotrophic factor is decreased in bipolar disorder during depressive and manic episodes. *Neurosci Lett*, *398*(3), 215-219. doi:10.1016/j.neulet.2005.12.085
- Denham, J. W., & Hauer-Jensen, M. (2002). The radiotherapeutic injury--a complex 'wound'. *Radiother Oncol*, *63*(2), 129-145.
- Desouky, O., Ding, N., & Zhou, G. (2019). Targeted and non-targeted effects of ionizing radiation. *Journal of Radiation Research and Applied Sciences*, *8*(2), 247-254. doi:10.1016/j.jrras.2015.03.003
- Duchen, M. R., Burton, N. R., & Biscoe, T. J. (1985). An intracellular study of the interactions of N-methyl-DL-aspartate with ketamine in the mouse hippocampal slice. *Brain Res*, *342*(1), 149-153.
- Eichenbaum, H. (2001). The hippocampus and declarative memory: cognitive mechanisms and neural codes. *Behav Brain Res*, *127*(1-2), 199-207.
- Eriksson, P. S., Perfilieva, E., Bjork-Eriksson, T., Alborn, A. M., Nordborg, C., Peterson, D. A., & Gage, F. H. (1998). Neurogenesis in the adult human hippocampus. *Nat Med*, *4*(11), 1313-1317. doi:10.1038/3305
- Fike, J. R., Rola, R., & Limoli, C. L. (2007). Radiation response of neural precursor cells. *Neurosurg Clin N Am*, *18*(1), 115-127, x. doi:10.1016/j.nec.2006.10.010
- Fike, J. R., Rosi, S., & Limoli, C. L. (2009). Neural precursor cells and central nervous system radiation sensitivity. *Semin Radiat Oncol*, *19*(2), 122-132. doi:10.1016/j.semradonc.2008.12.003
- Fredriksson, A., & Archer, T. (2003). Hyperactivity following postnatal NMDA antagonist treatment: reversal by D-amphetamine. *Neurotox Res*, *5*(7), 549-564.

- Fredriksson, A., Archer, T., Alm, H., Gordh, T., & Eriksson, P. (2004). Neurofunctional deficits and potentiated apoptosis by neonatal NMDA antagonist administration. *Behav Brain Res*, *153*(2), 367-376. doi:10.1016/j.bbr.2003.12.026
- Furukawa, H., Singh, S. K., Mancusso, R., & Gouaux, E. (2005). Subunit arrangement and function in NMDA receptors. *Nature*, *438*(7065), 185-192. doi:10.1038/nature04089
- Gaber, M. W., Sabek, O. M., Fukatsu, K., Wilcox, H. G., Kiani, M. F., & Merchant, T. E. (2003). Differences in ICAM-1 and TNF-alpha expression between large single fraction and fractionated irradiation in mouse brain. *Int J Radiat Biol*, *79*(5), 359-366.
- Gil, J. M., & Rego, A. C. (2008). Mechanisms of neurodegeneration in Huntington's disease. *Eur J Neurosci*, *27*(11), 2803-2820. doi:10.1111/j.1460-9568.2008.06310.x
- Gonzalez, G. A., & Montminy, M. R. (1989). Cyclic AMP stimulates somatostatin gene transcription by phosphorylation of CREB at serine 133. *Cell*, *59*(4), 675-680.
- Gottmann, K., Mittmann, T., & Lessmann, V. (2009). BDNF signaling in the formation, maturation and plasticity of glutamatergic and GABAergic synapses. *Exp Brain Res*, *199*(3-4), 203-234. doi:10.1007/s00221-009-1994-z
- Grant, G. (2007). How the 1906 Nobel prize in physiology or medicine was shared between Golgi and Cajal. *Brain Res Rev*, *55*(2), 490-498. doi:10.1016/j.brainresrev.2006.11.004
- Green, S. M., Roback, M. G., Kennedy, R. M., & Krauss, B. (2011). Clinical practice guideline for emergency department ketamine dissociative sedation: 2011 update. *Ann Emerg Med*, *57*(5), 449-461. doi:10.1016/j.annemergmed.2010.11.030
- Greene-Schloesser, D., Moore, E., & Robbins, M. E. (2013). Molecular pathways: radiation-induced cognitive impairment. *Clin Cancer Res*, *19*(9), 2294-2300. doi:10.1158/1078-0432.CCR-11-2903
- Greene-Schloesser, D., Robbins, M. E., Peiffer, A. M., Shaw, E. G., Wheeler, K. T., & Chan, M. D. (2012). Radiation-induced brain injury: A review. *Front Oncol*, *2*, 73. doi:10.3389/fonc.2012.00073
- Hall, P., Adami, H. O., Trichopoulos, D., Pedersen, N. L., Laggiou, P., Ekblom, A., Ingvar, M., Lundell, M., & Granath, F. (2004). Effect of low doses of ionising radiation in infancy on cognitive function in adulthood: Swedish population based cohort study. *BMJ*, *328*(7430), 19. doi:10.1136/bmj.328.7430.19
- Hladik, D., Buratovic, S., Von Toerne, C., Azimzadeh, O., Subedi, P., Philipp, J., Winkler, S., Feuchtinger, A., Samson, E., Hauck, S. M., Stenerlow, B., Eriksson, P., Atkinson, M. J., & Tapio, S. (2019). Combined Treatment with Low-Dose Ionizing Radiation and Ketamine Induces Adverse Changes in CA1 Neuronal Structure in Male Murine Hippocampi. *Int J Mol Sci*, *20*(23). doi:10.3390/ijms20236103
- Hladik, D., Dalke, C., von Toerne, C., Hauck, S. M., Azimzadeh, O., Philipp, J., Ung, M. C., Schlattl, H., Rossler, U., Graw, J., Atkinson, M. J., & Tapio, S. (2020). CREB Signaling Mediates Dose-Dependent Radiation Response in the Murine Hippocampus Two Years after Total Body Exposure. *J Proteome Res*, *19*(1), 337-345. doi:10.1021/acs.jproteome.9b00552
- Hladik, D., & Tapio, S. (2016). Effects of ionizing radiation on the mammalian brain. *Mutat Res*, *770*(Pt B), 219-230. doi:10.1016/j.mrrev.2016.08.003

- Hong, J. H., Chiang, C. S., Campbell, I. L., Sun, J. R., Withers, H. R., & McBride, W. H. (1995). Induction of acute phase gene expression by brain irradiation. *Int J Radiat Oncol Biol Phys*, *33*(3), 619-626. doi:10.1016/0360-3016(95)00279-8
- Huang, L., Wickramasekara, S. I., Akinyeke, T., Stewart, B. S., Jiang, Y., Raber, J., & Maier, C. S. (2016). Ion mobility-enhanced MS(E)-based label-free analysis reveals effects of low-dose radiation post contextual fear conditioning training on the mouse hippocampal proteome. *J Proteomics*, *140*, 24-36. doi:10.1016/j.jprot.2016.03.032
- Huang, W. Y., Muo, C. H., Lin, C. Y., Jen, Y. M., Yang, M. H., Lin, J. C., Sung, F. C., & Kao, C. H. (2014). Paediatric head CT scan and subsequent risk of malignancy and benign brain tumour: a nation-wide population-based cohort study. *Br J Cancer*, *110*(9), 2354-2360. doi:10.1038/bjc.2014.103
- Huttenlocher, P. R. (1991). Dendritic and synaptic pathology in mental retardation. *Pediatr Neurol*, *7*(2), 79-85.
- Hwang, S. Y., Jung, J. S., Kim, T. H., Lim, S. J., Oh, E. S., Kim, J. Y., Ji, K. A., Joe, E. H., Cho, K. H., & Han, I. O. (2006). Ionizing radiation induces astrocyte gliosis through microglia activation. *Neurobiol Dis*, *21*(3), 457-467. doi:10.1016/j.nbd.2005.08.006
- James, P. J., Howard, R. F., & Williams, D. G. (2010). The addition of ketamine to a morphine nurse- or patient-controlled analgesia infusion (PCA/NCA) increases analgesic efficacy in children with mucositis pain. *Paediatr Anaesth*, *20*(9), 805-811. doi:10.1111/j.1460-9592.2010.03358.x
- Jenrow, K. A., Brown, S. L., Lapanowski, K., Naei, H., Kolozsvary, A., & Kim, J. H. (2013). Selective inhibition of microglia-mediated neuroinflammation mitigates radiation-induced cognitive impairment. *Radiat Res*, *179*(5), 549-556. doi:10.1667/RR3026.1
- Karen E. Hoffman, T. I. Y. (2009). Radiation Therapy for Pediatric Central Nervous System Tumors.
- Karlsson, P., Holmberg, E., Lundell, M., Mattsson, A., Holm, L. E., & Wallgren, A. (1998). Intracranial tumors after exposure to ionizing radiation during infancy: a pooled analysis of two Swedish cohorts of 28,008 infants with skin hemangioma. *Radiat Res*, *150*(3), 357-364.
- Kaufmann, W. E., & Moser, H. W. (2000). Dendritic anomalies in disorders associated with mental retardation. *Cereb Cortex*, *10*(10), 981-991.
- Kellner, Y., Godecke, N., Dierkes, T., Thieme, N., Zagrebelsky, M., & Korte, M. (2014). The BDNF effects on dendritic spines of mature hippocampal neurons depend on neuronal activity. *Front Synaptic Neurosci*, *6*, 5. doi:10.3389/fnsyn.2014.00005
- Kemp, A., & Manahan-Vaughan, D. (2007). Hippocampal long-term depression: master or minion in declarative memory processes? *Trends Neurosci*, *30*(3), 111-118. doi:10.1016/j.tins.2007.01.002
- Kempf, S. J., Casciati, A., Buratovic, S., Janik, D., von Toerne, C., Ueffing, M., Neff, F., Moertl, S., Stenerlow, B., Saran, A., Atkinson, M. J., Eriksson, P., Pazzaglia, S., & Tapio, S. (2014). The cognitive defects of neonatally irradiated mice are accompanied by changed synaptic plasticity, adult neurogenesis and neuroinflammation. *Mol Neurodegener*, *9*, 57. doi:10.1186/1750-1326-9-57
- Kettenmann, H., Kirchhoff, F., & Verkhratsky, A. (2013). Microglia: new roles for the synaptic stripper. *Neuron*, *77*(1), 10-18. doi:10.1016/j.neuron.2012.12.023
- Kim, J. S., Lee, H. J., Kim, J. C., Kang, S. S., Bae, C. S., Shin, T., Jin, J. K., Kim, S. H., Wang, H., & Moon, C. (2008). Transient impairment of hippocampus-dependent

- learning and memory in relatively low-dose of acute radiation syndrome is associated with inhibition of hippocampal neurogenesis. *J Radiat Res*, 49(5), 517-526.
- Kim, K. P., Berrington de Gonzalez, A., Pearce, M. S., Salotti, J. A., Parker, L., McHugh, K., Craft, A. W., & Lee, C. (2012). Development of a database of organ doses for paediatric and young adult CT scans in the United Kingdom. *Radiat Prot Dosimetry*, 150(4), 415-426. doi:10.1093/rpd/ncr429
- Kim, S. H., Lim, D. J., Chung, Y. G., Cho, T. H., Lim, S. J., Kim, W. J., & Suh, J. K. (2002). Expression of TNF-alpha and TGF-beta 1 in the rat brain after a single high-dose irradiation. *J Korean Med Sci*, 17(2), 242-248. doi:10.3346/jkms.2002.17.2.242
- Kleinerman, R. A. (2006). Cancer risks following diagnostic and therapeutic radiation exposure in children. *Pediatr Radiol*, 36 Suppl 2, 121-125. doi:10.1007/s00247-006-0191-5
- Korte, M., Carroll, P., Wolf, E., Brem, G., Thoenen, H., & Bonhoeffer, T. (1995). Hippocampal long-term potentiation is impaired in mice lacking brain-derived neurotrophic factor. *Proc Natl Acad Sci U S A*, 92(19), 8856-8860. doi:10.1073/pnas.92.19.8856
- Kyrkanides, S., Olschowka, J. A., Williams, J. P., Hansen, J. T., & O'Banion, M. K. (1999). TNF alpha and IL-1beta mediate intercellular adhesion molecule-1 induction via microglia-astrocyte interaction in CNS radiation injury. *J Neuroimmunol*, 95(1-2), 95-106. doi:10.1016/s0165-5728(98)00270-7
- Lamproglou, I., Chen, Q. M., Boisserie, G., Mazon, J. J., Poisson, M., Baillet, F., Le Poncin, M., & Delattre, J. Y. (1995). Radiation-induced cognitive dysfunction: an experimental model in the old rat. *Int J Radiat Oncol Biol Phys*, 31(1), 65-70. doi:10.1016/0360-3016(94)00332-F
- Lazarini, F., Mouthon, M. A., Gheusi, G., de Chaumont, F., Olivo-Marin, J. C., Lamarque, S., Abrous, D. N., Boussin, F. D., & Lledo, P. M. (2009). Cellular and behavioral effects of cranial irradiation of the subventricular zone in adult mice. *PLoS One*, 4(9), e7017. doi:10.1371/journal.pone.0007017
- Lee, B., Cao, R., Choi, Y. S., Cho, H. Y., Rhee, A. D., Hah, C. K., Hoyt, K. R., & Obrietan, K. (2009). The CREB/CRE transcriptional pathway: protection against oxidative stress-mediated neuronal cell death. *J Neurochem*, 108(5), 1251-1265. doi:10.1111/j.1471-4159.2008.05864.x
- Lee, C., Kim, K. P., Long, D. J., & Bolch, W. E. (2012). Organ doses for reference pediatric and adolescent patients undergoing computed tomography estimated by Monte Carlo simulation. *Med Phys*, 39(4), 2129-2146. doi:10.1118/1.3693052
- Lee, W. H., Sonntag, W. E., Mitschelen, M., Yan, H., & Lee, Y. W. (2010). Irradiation induces regionally specific alterations in pro-inflammatory environments in rat brain. *Int J Radiat Biol*, 86(2), 132-144. doi:10.3109/09553000903419346
- Lee, W. H., Warrington, J. P., Sonntag, W. E., & Lee, Y. W. (2012). Irradiation alters MMP-2/TIMP-2 system and collagen type IV degradation in brain. *Int J Radiat Oncol Biol Phys*, 82(5), 1559-1566. doi:10.1016/j.ijrobp.2010.12.032
- Lee, Y. W., Cho, H. J., Lee, W. H., & Sonntag, W. E. (2012). Whole brain radiation-induced cognitive impairment: pathophysiological mechanisms and therapeutic targets. *Biomol Ther (Seoul)*, 20(4), 357-370. doi:10.4062/biomolther.2012.20.4.357
- Leszczynski, D. (2014). Radiation proteomics: a brief overview. *Proteomics*, 14(4-5), 481-488. doi:10.1002/pmic.201300390

- Levine, R. L. (2002). Carbonyl modified proteins in cellular regulation, aging, and disease. *Free Radical Biology and Medicine*, 32(9), 790-796. doi:Pii S0891-5849(02)00765-7
- Levine, R. L., Williams, J. A., Stadtman, E. R., & Shacter, E. (1994). Carbonyl assays for determination of oxidatively modified proteins. *Methods Enzymol*, 233, 346-357. doi:10.1016/s0076-6879(94)33040-9
- Li, F., & Tsien, J. Z. (2009). Memory and the NMDA receptors. *N Engl J Med*, 361(3), 302-303. doi:10.1056/NEJMcibr0902052
- Lieber, M. R. (2010). The mechanism of double-strand DNA break repair by the nonhomologous DNA end-joining pathway. *Annu Rev Biochem*, 79, 181-211. doi:10.1146/annurev.biochem.052308.093131
- Limoli, C. L., Giedzinski, E., Baure, J., Rola, R., & Fike, J. R. (2007). Redox changes induced in hippocampal precursor cells by heavy ion irradiation. *Radiat Environ Biophys*, 46(2), 167-172. doi:10.1007/s00411-006-0077-9
- Lonze, B. E., & Ginty, D. D. (2002). Function and regulation of CREB family transcription factors in the nervous system. *Neuron*, 35(4), 605-623. doi:10.1016/s0896-6273(02)00828-0
- Lumniczky, K., Szatmari, T., & Safrany, G. (2017). Ionizing Radiation-Induced Immune and Inflammatory Reactions in the Brain. *Front Immunol*, 8, 517. doi:10.3389/fimmu.2017.00517
- Ma, Q. L., Harris-White, M. E., Ubeda, O. J., Simmons, M., Beech, W., Lim, G. P., Teter, B., Frautschy, S. A., & Cole, G. M. (2007). Evidence of Abeta- and transgene-dependent defects in ERK-CREB signaling in Alzheimer's models. *J Neurochem*, 103(4), 1594-1607. doi:10.1111/j.1471-4159.2007.04869.x
- Mabuchi, K., Soda, M., Ron, E., Tokunaga, M., Ochikubo, S., Sugimoto, S., Ikeda, T., Terasaki, M., Preston, D. L., & Thompson, D. E. (1994). Cancer incidence in atomic bomb survivors. Part I: Use of the tumor registries in Hiroshima and Nagasaki for incidence studies. *Radiat Res*, 137(2 Suppl), S1-16.
- Madsen, T. M., Kristjansen, P. E., Bolwig, T. G., & Wortwein, G. (2003). Arrested neuronal proliferation and impaired hippocampal function following fractionated brain irradiation in the adult rat. *Neuroscience*, 119(3), 635-642.
- Mantamadiotis, T., Lemberger, T., Bleckmann, S. C., Kern, H., Kretz, O., Martin Villalba, A., Tronche, F., Kellendonk, C., Gau, D., Kapfhammer, J., Otto, C., Schmid, W., & Schutz, G. (2002). Disruption of CREB function in brain leads to neurodegeneration. *Nat Genet*, 31(1), 47-54. doi:10.1038/ng882
- Markesbery, W. R. (1997). Oxidative stress hypothesis in Alzheimer's disease. *Free Radic Biol Med*, 23(1), 134-147.
- Mathews, J. D., Forsythe, A. V., Brady, Z., Butler, M. W., Goergen, S. K., Byrnes, G. B., Giles, G. G., Wallace, A. B., Anderson, P. R., Guiver, T. A., McGale, P., Cain, T. M., Dowty, J. G., Bickerstaffe, A. C., & Darby, S. C. (2013). Cancer risk in 680,000 people exposed to computed tomography scans in childhood or adolescence: data linkage study of 11 million Australians. *BMJ*, 346, f2360. doi:10.1136/bmj.f2360
- McAllister, A. K. (2000). Cellular and molecular mechanisms of dendrite growth. *Cereb Cortex*, 10(10), 963-973.
- McBride, W. H., Pajonk, F., Chiang, C. S., & Sun, J. R. (2002). NF-kappa B, cytokines, proteasomes, and low-dose radiation exposure. *Mil Med*, 167(2 Suppl), 66-67.

- McGeer, P. L., McGeer, E. G., Kawamata, T., Yamada, T., & Akiyama, H. (1991). Reactions of the immune system in chronic degenerative neurological diseases. *Can J Neurol Sci*, *18*(3 Suppl), 376-379. doi:10.1017/s0317167100032479
- McMullen, K. P., Hanson, T., Bratton, J., & Johnstone, P. A. (2015). Parameters of anesthesia/sedation in children receiving radiotherapy. *Radiat Oncol*, *10*, 65. doi:10.1186/s13014-015-0363-2
- Metz, A. E., Yau, H. J., Centeno, M. V., Apkarian, A. V., & Martina, M. (2009). Morphological and functional reorganization of rat medial prefrontal cortex in neuropathic pain. *Proc Natl Acad Sci U S A*, *106*(7), 2423-2428. doi:10.1073/pnas.0809897106
- Michaelidesova, A., Konirova, J., Bartunek, P., & Zikova, M. (2019). Effects of Radiation Therapy on Neural Stem Cells. *Genes (Basel)*, *10*(9). doi:10.3390/genes10090640
- Mizumatsu, S., Monje, M. L., Morhardt, D. R., Rola, R., Palmer, T. D., & Fike, J. R. (2003). Extreme sensitivity of adult neurogenesis to low doses of X-irradiation. *Cancer Res*, *63*(14), 4021-4027.
- Monje, M. L., Mizumatsu, S., Fike, J. R., & Palmer, T. D. (2002). Irradiation induces neural precursor-cell dysfunction. *Nat Med*, *8*(9), 955-962. doi:10.1038/nm749
- Moravan, M. J., Olschowka, J. A., Williams, J. P., & O'Banion, M. K. (2011). Cranial irradiation leads to acute and persistent neuroinflammation with delayed increases in T-cell infiltration and CD11c expression in C57BL/6 mouse brain. *Radiat Res*, *176*(4), 459-473.
- Murrough, J. W., Iosifescu, D. V., Chang, L. C., Al Jurdi, R. K., Green, C. E., Perez, A. M., Iqbal, S., Pillemer, S., Foulkes, A., Shah, A., Charney, D. S., & Mathew, S. J. (2013). Antidepressant efficacy of ketamine in treatment-resistant major depression: a two-site randomized controlled trial. *Am J Psychiatry*, *170*(10), 1134-1142. doi:10.1176/appi.ajp.2013.13030392
- Murrough, J. W., Wan, L. B., Iacoviello, B., Collins, K. A., Solon, C., Glicksberg, B., Perez, A. M., Mathew, S. J., Charney, D. S., Iosifescu, D. V., & Burdick, K. E. (2013). Neurocognitive effects of ketamine in treatment-resistant major depression: association with antidepressant response. *Psychopharmacology (Berl)*. doi:10.1007/s00213-013-3255-x
- Olschowka, J. A., Kyrkanides, S., Harvey, B. K., O'Banion, M. K., Williams, J. P., Rubin, P., & Hansen, J. T. (1997). ICAM-1 induction in the mouse CNS following irradiation. *Brain Behav Immun*, *11*(4), 273-285. doi:10.1006/brbi.1997.0506
- Omran, A. R., Shore, R. E., Markoff, R. A., Friedhoff, A., Albert, R. E., Barr, H., Dahlstrom, W. G., & Pasternack, B. S. (1978). Follow-up study of patients treated by X-ray epilation for tinea capitis: psychiatric and psychometric evaluation. *Am J Public Health*, *68*(6), 561-567. doi:10.2105/ajph.68.6.561
- Otake, M., & Schull, W. J. (1984). In utero exposure to A-bomb radiation and mental retardation; a reassessment. *Br J Radiol*, *57*(677), 409-414. doi:10.1259/0007-1285-57-677-409
- Ozasa, K., Shimizu, Y., Suyama, A., Kasagi, F., Soda, M., Grant, E. J., Sakata, R., Sugiyama, H., & Kodama, K. (2012). Studies of the mortality of atomic bomb survivors, Report 14, 1950-2003: an overview of cancer and noncancer diseases. *Radiat Res*, *177*(3), 229-243.
- Parent, J. M., Yu, T. W., Leibowitz, R. T., Geschwind, D. H., Sloviter, R. S., & Lowenstein, D. H. (1997). Dentate granule cell neurogenesis is increased by seizures and

- contributes to aberrant network reorganization in the adult rat hippocampus. *J Neurosci*, 17(10), 3727-3738.
- Parihar, V. K., Acharya, M. M., Roa, D. E., Bosch, O., Christie, L. A., & Limoli, C. L. (2014). Defining functional changes in the brain caused by targeted stereotaxic radiosurgery. *Transl Cancer Res*, 3(2), 124-137. doi:10.3978/j.issn.2218-676X.2013.06.02
- Parihar, V. K., & Limoli, C. L. (2013). Cranial irradiation compromises neuronal architecture in the hippocampus. *Proc Natl Acad Sci U S A*, 110(31), 12822-12827. doi:10.1073/pnas.1307301110
- Parihar, V. K., Pasha, J., Tran, K. K., Craver, B. M., Acharya, M. M., & Limoli, C. L. (2015). Persistent changes in neuronal structure and synaptic plasticity caused by proton irradiation. *Brain Struct Funct*, 220(2), 1161-1171. doi:10.1007/s00429-014-0709-9
- Patel, V. J., Thalassinou, K., Slade, S. E., Connolly, J. B., Crombie, A., Murrell, J. C., & Scrivens, J. H. (2009). A comparison of labeling and label-free mass spectrometry-based proteomics approaches. *J Proteome Res*, 8(7), 3752-3759. doi:10.1021/pr900080y
- Pearce, M. S., Salotti, J. A., Little, M. P., McHugh, K., Lee, C., Kim, K. P., Howe, N. L., Ronckers, C. M., Rajaraman, P., Sir Craft, A. W., Parker, L., & Berrington de Gonzalez, A. (2012). Radiation exposure from CT scans in childhood and subsequent risk of leukaemia and brain tumours: a retrospective cohort study. *Lancet*, 380(9840), 499-505. doi:10.1016/S0140-6736(12)60815-0
- Peissner, W., Kocher, M., Treuer, H., & Gillardon, F. (1999). Ionizing radiation-induced apoptosis of proliferating stem cells in the dentate gyrus of the adult rat hippocampus. *Brain Res Mol Brain Res*, 71(1), 61-68.
- Penzes, P., Cahill, M. E., Jones, K. A., VanLeeuwen, J. E., & Woolfrey, K. M. (2011). Dendritic spine pathology in neuropsychiatric disorders. *Nat Neurosci*, 14(3), 285-293. doi:10.1038/nn.2741
- Pregi, N., Belluscio, L. M., Berardino, B. G., Castillo, D. S., & Canepa, E. T. (2017). Oxidative stress-induced CREB upregulation promotes DNA damage repair prior to neuronal cell death protection. *Mol Cell Biochem*, 425(1-2), 9-24. doi:10.1007/s11010-016-2858-z
- Preston, D. L., Kusumi, S., Tomonaga, M., Izumi, S., Ron, E., Kuramoto, A., Kamada, N., Dohy, H., Matsuo, T., Matsui, T., & et al. (1994). Cancer incidence in atomic bomb survivors. Part III. Leukemia, lymphoma and multiple myeloma, 1950-1987. *Radiat Res*, 137(2 Suppl), S68-97.
- Preston, D. L., Ron, E., Tokuoka, S., Funamoto, S., Nishi, N., Soda, M., Mabuchi, K., & Kodama, K. (2007). Solid cancer incidence in atomic bomb survivors: 1958-1998. *Radiat Res*, 168(1), 1-64. doi:10.1667/RR0763.1
- Preston, D. L., Shimizu, Y., Pierce, D. A., Suyama, A., & Mabuchi, K. (2003). Studies of mortality of atomic bomb survivors. Report 13: Solid cancer and noncancer disease mortality: 1950-1997. *Radiat Res*, 160(4), 381-407.
- Prise, K. M., & Saran, A. (2011). Concise review: stem cell effects in radiation risk. *Stem Cells*, 29(9), 1315-1321. doi:10.1002/stem.690
- Psotta, L., Lessmann, V., & Endres, T. (2013). Impaired fear extinction learning in adult heterozygous BDNF knock-out mice. *Neurobiol Learn Mem*, 103, 34-38. doi:10.1016/j.nlm.2013.03.003

- Purpura, D. P. (1975). Dendritic differentiation in human cerebral cortex: normal and aberrant developmental patterns. *Adv Neurol*, 12, 91-134.
- Raber, J., Rola, R., LeFevour, A., Morhardt, D., Curley, J., Mizumatsu, S., VandenBerg, S. R., & Fike, J. R. (2004). Radiation-induced cognitive impairments are associated with changes in indicators of hippocampal neurogenesis. *Radiat Res*, 162(1), 39-47. doi:10.1667/rr3206
- Robbins, M. E., Bourland, J. D., Cline, J. M., Wheeler, K. T., & Deadwyler, S. A. (2011). A model for assessing cognitive impairment after fractionated whole-brain irradiation in nonhuman primates. *Radiat Res*, 175(4), 519-525. doi:10.1667/RR2497.1
- Rola, R., Otsuka, S., Obenaus, A., Nelson, G. A., Limoli, C. L., VandenBerg, S. R., & Fike, J. R. (2004). Indicators of hippocampal neurogenesis are altered by 56Fe-particle irradiation in a dose-dependent manner. *Radiat Res*, 162(4), 442-446. doi:10.1667/rr3234
- Rola, R., Raber, J., Rizk, A., Otsuka, S., VandenBerg, S. R., Morhardt, D. R., & Fike, J. R. (2004). Radiation-induced impairment of hippocampal neurogenesis is associated with cognitive deficits in young mice. *Exp Neurol*, 188(2), 316-330. doi:10.1016/j.expneurol.2004.05.005
- Ron, E., Modan, B., Boice, J. D., Jr., Alfandary, E., Stovall, M., Chetrit, A., & Katz, L. (1988). Tumors of the brain and nervous system after radiotherapy in childhood. *N Engl J Med*, 319(16), 1033-1039. doi:10.1056/NEJM198810203191601
- Ron, E., Modan, B., Floro, S., Harkedar, I., & Gurewitz, R. (1982). Mental function following scalp irradiation during childhood. *Am J Epidemiol*, 116(1), 149-160. doi:10.1093/oxfordjournals.aje.a113389
- Ron, E., Preston, D. L., Mabuchi, K., Thompson, D. E., & Soda, M. (1994). Cancer incidence in atomic bomb survivors. Part IV: Comparison of cancer incidence and mortality. *Radiat Res*, 137(2 Suppl), S98-112.
- Sadetzki, S., Chetrit, A., Freedman, L., Stovall, M., Modan, B., & Novikov, I. (2005). Long-term follow-up for brain tumor development after childhood exposure to ionizing radiation for tinea capitis. *Radiat Res*, 163(4), 424-432.
- Saha, G. B. (2013). *Radiation biology in physics and radiobiology of nuclear medicine*: Springer Science + Business Media.
- Sakamoto, K., Karelina, K., & Obrietan, K. (2011). CREB: a multifaceted regulator of neuronal plasticity and protection. *J Neurochem*, 116(1), 1-9. doi:10.1111/j.1471-4159.2010.07080.x
- Schmal, Z., Isermann, A., Hladik, D., von Toerne, C., Tapio, S., & Rube, C. E. (2019). DNA damage accumulation during fractionated low-dose radiation compromises hippocampal neurogenesis. *Radiother Oncol*, 137, 45-54. doi:10.1016/j.radonc.2019.04.021
- Shen, K., & Cowan, C. W. (2010). Guidance molecules in synapse formation and plasticity. *Cold Spring Harb Perspect Biol*, 2(4), a001842. doi:10.1101/cshperspect.a001842
- Shi, L., Adams, M. M., Long, A., Carter, C. C., Bennett, C., Sonntag, W. E., Nicolle, M. M., Robbins, M., D'Agostino, R., & Brunso-Bechtold, J. K. (2006). Spatial learning and memory deficits after whole-brain irradiation are associated with changes in NMDA receptor subunits in the hippocampus. *Radiat Res*, 166(6), 892-899. doi:10.1667/RR0588.1

- Smoll, N. R., Brady, Z., Scurrah, K., & Mathews, J. D. (2016). Exposure to ionizing radiation and brain cancer incidence: The Life Span Study cohort. *Cancer Epidemiol*, *42*, 60-65. doi:10.1016/j.canep.2016.03.006
- Snyder, J. S., Hong, N. S., McDonald, R. J., & Wojtowicz, J. M. (2005). A role for adult neurogenesis in spatial long-term memory. *Neuroscience*, *130*(4), 843-852. doi:10.1016/j.neuroscience.2004.10.009
- Sohal, R. S., Ku, H. H., Agarwal, S., Forster, M. J., & Lal, H. (1994). Oxidative damage, mitochondrial oxidant generation and antioxidant defenses during aging and in response to food restriction in the mouse. *Mech Ageing Dev*, *74*(1-2), 121-133. doi:10.1016/0047-6374(94)90104-x
- Spiegler, B. J., Bouffet, E., Greenberg, M. L., Rutka, J. T., & Mabbott, D. J. (2004). Change in neurocognitive functioning after treatment with cranial radiation in childhood. *J Clin Oncol*, *22*(4), 706-713. doi:10.1200/JCO.2004.05.186
- Spleiss, O., Appel, K., Boddeke, H. W., Berger, M., & Gebicke-Haerter, P. J. (1998). Molecular biology of microglia cytokine and chemokine receptors and microglial activation. *Life Sci*, *62*(17-18), 1707-1710. doi:10.1016/s0024-3205(98)00132-5
- Talamini, L. M., & Gorree, E. (2012). Aging memories: differential decay of episodic memory components. *Learn Mem*, *19*(6), 239-246. doi:10.1101/lm.024281.111
- Terry, R. D., Peck, A., DeTeresa, R., Schechter, R., & Horoupian, D. S. (1981). Some morphometric aspects of the brain in senile dementia of the Alzheimer type. *Ann Neurol*, *10*(2), 184-192. doi:10.1002/ana.410100209
- Thompson, D. E., Mabuchi, K., Ron, E., Soda, M., Tokunaga, M., Ochikubo, S., Sugimoto, S., Ikeda, T., Terasaki, M., Izumi, S., & et al. (1994). Cancer incidence in atomic bomb survivors. Part II: Solid tumors, 1958-1987. *Radiat Res*, *137*(2 Suppl), S17-67.
- Tronel, S., Fabre, A., Charrier, V., Olier, S. H., Gage, F. H., & Abrous, D. N. (2010). Spatial learning sculpts the dendritic arbor of adult-born hippocampal neurons. *Proc Natl Acad Sci U S A*, *107*(17), 7963-7968. doi:10.1073/pnas.0914613107
- Tseng, B. P., Giedzinski, E., Izadi, A., Suarez, T., Lan, M. L., Tran, K. K., Acharya, M. M., Nelson, G. A., Raber, J., Parihar, V. K., & Limoli, C. L. (2014). Functional consequences of radiation-induced oxidative stress in cultured neural stem cells and the brain exposed to charged particle irradiation. *Antioxid Redox Signal*, *20*(9), 1410-1422. doi:10.1089/ars.2012.5134
- Verheyde, J., & Benotmane, M. A. (2007). Unraveling the fundamental molecular mechanisms of morphological and cognitive defects in the irradiated brain. *Brain Res Rev*, *53*(2), 312-320. doi:10.1016/j.brainresrev.2006.09.004
- Viberg, H., Ponten, E., Eriksson, P., Gordh, T., & Fredriksson, A. (2008). Neonatal ketamine exposure results in changes in biochemical substrates of neuronal growth and synaptogenesis, and alters adult behavior irreversibly. *Toxicology*, *249*(2-3), 153-159. doi:10.1016/j.tox.2008.04.019
- von Bohlen und Halbach, O. (2010). Involvement of BDNF in age-dependent alterations in the hippocampus. *Front Aging Neurosci*, *2*. doi:10.3389/fnagi.2010.00036
- Walton, M. R., & Dragunow, I. (2000). Is CREB a key to neuronal survival? *Trends Neurosci*, *23*(2), 48-53. doi:10.1016/s0166-2236(99)01500-3
- Wardman, P. (2009). The importance of radiation chemistry to radiation and free radical biology (The 2008 Silvanus Thompson Memorial Lecture). *Br J Radiol*, *82*(974), 89-104. doi:10.1259/bjr/60186130

- Warrington, J. P., Csiszar, A., Mitschelen, M., Lee, Y. W., & Sonntag, W. E. (2012). Whole brain radiation-induced impairments in learning and memory are time-sensitive and reversible by systemic hypoxia. *PLoS One*, *7*(1), e30444. doi:10.1371/journal.pone.0030444
- Wen, A. Y., Sakamoto, K. M., & Miller, L. S. (2010). The role of the transcription factor CREB in immune function. *J Immunol*, *185*(11), 6413-6419. doi:10.4049/jimmunol.1001829
- Wu, G. Y., Zou, D. J., Rajan, I., & Cline, H. (1999). Dendritic dynamics in vivo change during neuronal maturation. *J Neurosci*, *19*(11), 4472-4483.
- Yamamoto, K. K., Gonzalez, G. A., Biggs, W. H., 3rd, & Montminy, M. R. (1988). Phosphorylation-induced binding and transcriptional efficacy of nuclear factor CREB. *Nature*, *334*(6182), 494-498. doi:10.1038/334494a0
- Yang, M., Kim, H., Kim, J., Kim, S. H., Kim, J. C., Bae, C. S., Kim, J. S., Shin, T., & Moon, C. (2012). Fast neutron irradiation deteriorates hippocampus-related memory ability in adult mice. *J Vet Sci*, *13*(1), 1-6.
- Yoneoka, Y., Satoh, M., Akiyama, K., Sano, K., Fujii, Y., & Tanaka, R. (1999). An experimental study of radiation-induced cognitive dysfunction in an adult rat model. *Br J Radiol*, *72*(864), 1196-1201. doi:10.1259/bjr.72.864.10703477
- Zhang, X., Odom, D. T., Koo, S. H., Conkright, M. D., Canettieri, G., Best, J., Chen, H., Jenner, R., Herbolsheimer, E., Jacobsen, E., Kadam, S., Ecker, J. R., Emerson, B., Hogenesch, J. B., Unterman, T., Young, R. A., & Montminy, M. (2005). Genome-wide analysis of cAMP-response element binding protein occupancy, phosphorylation, and target gene activation in human tissues. *Proc Natl Acad Sci U S A*, *102*(12), 4459-4464. doi:10.1073/pnas.0501076102
- Zhou, C., Huang, Y., & Przedborski, S. (2008). Oxidative stress in Parkinson's disease: a mechanism of pathogenic and therapeutic significance. *Ann N Y Acad Sci*, *1147*, 93-104. doi:10.1196/annals.1427.023

List of figures and table

Figure 1: The direct and indirect effect of IR. IR produces free electrons that either hit DNA molecules directly disrupting their molecular structure or the water molecules generating free radicals that then may further damage DNA molecules..... 10

Figure 2: Adult neurogenesis in the mouse brain. Mid-sagittal view of the mouse brain with the three main regions of adult neurogenesis: dentate gyrus (DG) of the hippocampus, sub ventricular zone (SVZ) and the olfactory bulb (OB)..... 14

Figure 3: Overview of label-free proteomics workflow. Mice were either irradiated or sham-irradiated and the proteins were isolated from the areas of interest after harvesting the brains. The protein solutions were digested and run on a QExactive. The acquired MS-spectra were analysed for label-free quantification and pathway analysis.....22

Figure 4: Detection of radiation-induced free carbonyl groups representative for oxidative stress. Reactive oxygen species (ROS) generate persistent carbonyl groups on proteins by oxidation. The reactive agent DNPH is tagged on the carbonyl groups forming DNP hydrazones that are detectably at 375 nm.....26

Figure 5: Experimental schedule of the structural analysis of CA1 neurons. Mice were treated or sham-treated and the harvested brains were stained, cut and analysed using microscopy. The neurons in the CA1 area of the hippocampus were reconstructed with the NeuroLucida software and analysed with the NeuroLucida Explorer software.....27

Figure 6: Induction of chronic inflammation by a single low-dose radiation exposure. Radiation exposure leads to the generation of oxidative stress that results in the activation of immune cells in the brain. Consequently, reactive astrocytes (GFAP) and activated microglia (IBA1) produce free radicals. This leads to long-term chronic activation of the immune system and a pro-inflammatory status.....69

Figure 7: Different impact of low-dose radiation on neuronal structures depending on the experimental set up. It was shown that a single low radiation dose (100 mGy, 200 mGy) had no effect on the basal dendrites of CA1 neurons. Combined to a single injection of ketamine (7,5 mg/kg) the number of dendrites and their branching increased whereas the spine density was lower than in the control animals. In contrast, a fractionated exposure to low radiation dose (20 x 100 mGy) decreased the complexity of DCX positive

neurons in the hippocampus. All effects were measured up to six months post-exposure.....72

Figure 8: The CREB signalling pathways and its downstream targets. The transcription factor CREB is activated in the brain via kinases that are activated in response to external stressors like radiation exposure. CREB signalling is involved in the maintenance of neurogenesis and proliferation and in the regulation of synaptic plasticity. It is neuroprotective in response to external stimuli.....75

Table 1: Summary of the experimental design.....21

Abbreviations

AGC	Automatic gain control
AMPARs	α -amino-3-hydroxy-5-methyl-4-isoxazolepropionic acid receptors
ARC	Activity-regulated cytoskeleton-associated protein
BAX	Bcl-2-associated x protein
BCA	Bicinchoninic acid
BCL-xL	B-cell lymphoma-extra large
BDNF	Brain-derived neurotrophic factor
CA1	Cornu Ammonis 1
CASP-3	Caspase-3
CD11	Clusters of differentiation 11
CREB	CAMP response element-binding protein
CT	Computer tomography
DCX	Doublecortin
DDA	Data-dependent acquisition
DG	Dentate gyrus
DNA	Deoxyribonucleic acid
DNP	2, 4- Dinitrophenylhydrazine
DSB	DNA double-strand breaks
ERK1/2	Extracellular signal-regulated kinase 1/2
FASP	Filter-aided sample preparation
FDR	False discovery rate
GFAP	Glial fibrillary acidic protein
Gy	Gray
HF	High field
HRP	Horseradish peroxidase
IBA-1	Ionized calcium-binding adapter molecule 1
IPA	Ingenuity Pathway Analysis
IR	Ionising radiation
LC-MS/MS	Liquid chromatography-tandem mass spectrometry

LET	Linear energy transfer
LSS	Life span study
LTP	Synaptic long-term potentiation
MHC	Major histocompatibility complex
MS	Mass spectrometry
NFDM	Non-fat dry milk powder
NF-κB	Nuclear factor 'kappa-light-chain-enhancer' of activated B-cells
NHP	Non-human primates
NMDA	N-methyl-d-aspartate
NMRI	Naval Medical Research Institute
NSC	Neuronal stem cells
OB	Olfactory bulbs
p38	P38 mitogen-activated protein kinase
PBS	Phosphate-buffered saline
PND	Post-natal day
PSD-95	Postsynaptic density protein 95
ROS	Reactive oxygen species
Ser133	Serine 133
SRY	Sex determining region Y
SOX2	SRY- box 2
SVZ	Sub ventricular zone
TBST	Tris-buffered saline with tween20
TCA	Trichloroacetic acid
TNF-α	Necrosis factor- α
UP	Unique peptides

Acknowledgement

First of all, I would like to express my deepest gratitude to my PhD supervisor Prof. Michael J. Atkinson for his professional advice, his mental support and the many scientifically and humanly exciting moments I experienced through the opportunity to do my doctoral thesis at the Institute of Radiation Biology.

My special thanks go to my supervisor and mentor Dr. Soile Tapio, who supported me both scientifically and personally throughout the entire PhD time. Her constant advice helped me to further improve my scientific skills and enabled exciting projects with international experts from different fields.

I would like to thank Dr. Omid Azimzadeh, who was the greatest support for me in carrying out the experiments and evaluating the results. Many thanks for the numerous practical as well as theoretical advice and the moral support.

I would also like to specially thank my second supervisor Prof. Dr. Jochen Graw for his great advice and feedback during the thesis committee meetings.

Moreover, I would also like to thank Dr. Michael Rosemann, Dr. Natasha Anastasov, Dr. Simone Mörtl, Dr. Juliane Merl-Pham, Dr. Christine von Törne, Stephanie Winkler, Claudia Winkler, Rosi Kell and Silvia Köhn and all past and present members of the Institute of Radiation Biology for their collaboration, help and scientific discussion.

My special thank goes to Martina Matjanovski, Jos Philipp, Prabal Subedi and Michael Schneider for the fun times spent together and all the wonderful memories.

Most of all, I would like to thank my family and Marbod for their love and unconditional support.